From the

Physiological Genomics - Biomedical Center (BMC)

of the Ludwig-Maximilians-Universität München

Director: Prof. Dr. Magdalena Götz

The Role of Transmembrane-Agrin and its Receptor Complex during Dendritic Arborization and Synaptogenesis

Dissertation

zum Erwerb des Doctor of Philosophy (Ph.D.)

an der Medizinischen Fakultät der

Ludwig-Maximilians-Universität München

Submitted by:

Gerry Handara

From:

Jakarta, Indonesia

On:

March 25th 2019

Supervisor	: Prof. Dr. Stephan Kröger
Second evaluator	: Prof. Dr. Magdalena Götz
Dean	: Prof. Dr. med. dent. Reinhard Hickel
Date of oral defense	: 16.10.2019

Eidesstattliche Versicherung / Affidavit

I hereby declare, that the submitted thesis entitled “The Role of Transmembrane-Agrin and its Receptor Complex during Dendritic Arborization and Synaptogenesis” is my own work. I have only used the sources indicated and have not made unauthorized use of services of a third party. Where the work of others has been quoted or reproduced, the source is always given.

I further declare that the submitted thesis or parts thereof have not been presented as part of an examination degree to any other university.

Munich, 16.10.2019

Gerry Handara

Confirmation of congruency between printed and electronic version of the doctoral thesis

I hereby declare that the electronic version of the submitted thesis, entitled "The Role of Transmembrane-Agrin and its Receptor Complex during Dendritic Arborization and Synaptogenesis" is congruent with the printed version both in content and format.

Munich, 16.10.2019

Gerry Handara

Parts of this work have been published and submitted.

Handara, G., Hetsch, F.J.A., Juttner, R., Schick, A., Haupt, C., Rathjen, F.G., Kröger, S., (2019). The role of agrin, Lrp4 and MuSK during dendritic arborization and synaptogenesis in cultured embryonic CNS neurons. *Dev Biol.* ;445(1):54-67

Handara G and Kröger S., (2019). Alternative splicing and the intracellular domain mediate TM-agrin's ability to differentially regulate the density of excitatory and inhibitory synapse-like specializations in developing CNS neurons. *Neuroscience,* in press.

Summary

Agrin and its receptors complex, consisting of Lrp4 and MuSK are key regulators during formation, maintenance and regeneration of the neuromuscular junction. Their expression and localization in the CNS are less studied and their functions are unclear. The aim of my thesis was to investigate the role of agrin, MuSK and Lrp4 in the central nervous system during development, in particular during dendritogenesis and synaptogenesis, *in vitro* and *in vivo*.

Analysis of dendritic arborization in primary cortical neurons of WT, Lrp4-knockout (Lrp4-KO) and MuSK-knockout (MuSK-KO) embryos revealed that Lrp4- and MuSK-KO neurons display fewer but longer primary dendrites and a less complex dendritic arborization pattern. Transfection of these neurons with full-length TM-agrin cDNA restored the dendritic arborization deficit in Lrp4-KO neurons, but not in MuSK-KO neurons. The C-terminal half of TM-agrin was sufficient for the restoration. These results show that Lrp4 and MuSK, along with TM-agrin, are required for the normal dendritic arborization.

TM-agrin overexpression in WT neurons increased dendritic spine density. Therefore, I investigated the role of TM-agrin, Lrp4 and MuSK during synaptogenesis. Lrp4-KO neurons, but not MuSK-KO neurons, displayed a lower density of excitatory synapses. TM-agrin overexpression increased the density of excitatory synapses in Lrp4-heterozygous and WT neurons, but not in Lrp4-KO neurons. The TM-agrin-mediated increase of excitatory synapses required the presence of an insert containing four amino acids at the y-splice site (y4), but not the presence of the Lrp4-binding domain within TM-agrin. These results suggest an indirect interaction of TM-agrin with Lrp4 during formation or maintenance of excitatory synapses.

Analysis on the inhibitory synapses revealed that Lrp4-KO neurons, but not MuSK-KO neurons, displayed a lower density of inhibitory synapses. Furthermore, TM-agrin overexpression reduced the density of inhibitory synapses in Lrp4-heterozygous and WT neurons. The TM-agrin-induced reduction of inhibitory synapses depended on the presence of a highly conserved serine-residue (S17) in the intracellular region of TM-agrin. In summary, TM-agrin overexpression upregulates excitatory synapses and downregulates inhibitory synapses requiring two different regions within the TM-agrin protein.

Finally, I investigated the effect of TM-agrin overexpression of the adult neocortex *in vivo* using a mouse line, which conditionally expresses full-length TM-agrin in adult glutamatergic neurons. I observed an increase of transcript levels encoding excitatory synaptic proteins, as well as an increase of excitatory synapses density. Consistent with my *in vitro* data, the transcript levels of inhibitory synaptic proteins, as well as the inhibitory synapses density were significantly reduced in TM-agrin-overexpressing brains. Collectively, these results

suggest an important role of TM-agrin in regulating cortical excitatory-inhibitory balance *in vivo*.

In conclusion, TM-agrin, Lrp4 and MuSK are essential for the formation or maintenance of the dendritic arborization complexity and for excitatory and inhibitory synapses during synaptogenesis as well as their maintenance in adult neurons, both *in vitro* and *in vivo*. My results also demonstrate that synaptogenesis at the NMJ and in the CNS might share common molecular determinants.

Table of contents

List of figures

List of tables

Introduction

Neurons and synapses as a core functional unit in central nervous system

The brain is the most complex of all biological systems. The human brain consists of more than 10^{11} neurons plus an additional 5-10 times the number of glial cells (Herculano-Houzel, 2009). The function of this enormous number of individual cells in the brain requires precise and effective ways of communication. This complex communication is an essential component for all living organism, in particular for processing external and internal information. The most important communication site that distinguishes nervous system from other tissues in the body is a specialized functional connection, which is called synapse. The term synapse (from the Greek synapsis: junction point/conjunction) was coined by Sir Charles Scott Sherrington in 1897 to define the contact zones implicated in the transmission of information. Neurons communicate through chemical synapses, which are formed and maintained by bi-directional transfer of information between the prospective pre- and postsynaptic specializations required for successful synaptic transmission (Tintignac et al., 2015; Waites et al., 2005).

The view of synapses as intercellular communication sites was part of the so-called 'neuron theory' proposed in 1888 by Santiago Ramon y Cajal. This theory suggested a non-continuity of cells in the CNS. The cells were thought to form a functional network by generating communication sites among them, which allowed unidirectional relay of information – but without a continuous cell membrane between the cells. Evidences supporting this theory had overcome the 'reticular theory' of the nervous system. In addition, Charles Sherrington showed that this specialization between nerve cells is a communication site, which subsequently develop into the concept of neurotransmission. This view of synapse-mediated communication is still accepted today, and its function, development and plasticity have become one of the main research fields in modern neuroscience.

Cellular and molecular components of synapses

In general, synapses are grouped into electrical and chemical synapses. Electrical synapses were first observed in crayfish by Edwin Furshpan and David Potter and consist of two membranes continuously connected by an apparatus, termed gap-junction, which allows ions to pass between cells through 1.2 to 2.0 nm pores (Furshpan and Potter, 1957). This type of synapse can be observed in retinal neurons (Hormuzdi et al., 2004). On the other hand, chemical synapses are structurally composed of two elements, a presynaptic membrane bearing an electron-dense structure named active zone and an electro-dense region of the postsynaptic

membrane. The pre- and postsynaptic membranes are separated by an extracellular space, called synaptic cleft, demonstrating the absence of a physical continuity between the cells.

Based on electron microscopic observations, Edward George Gray classified synapses as a Gray's type 1 or an excitatory synapse and as a Gray's type 2 or an inhibitory synapse (Gray, 1959). The type 1 synapse is characterized by an asymmetric thickness of the pre- and postsynaptic membranes with glutamate being the main neurotransmitter. In contrast, the type 2 synapse is characterized by a symmetric thickness of the pre- and postsynaptic membranes with γ-aminobutyric acid (GABA) and glycine being the main neurotransmitters (Colonnier, 1968).

The type 1 synapses represent approximately 80 % of all cortical synapses. They consist of a presynaptic axonal bouton containing vesicles filled with the neurotransmitter glutamate, a 20 nm wide synaptic cleft and an electron-dense thickening of the postsynaptic membrane containing the corresponding neurotransmitter receptors. Type 2 synapses have flattened presynaptic boutons containing GABA-filled vesicles, a synaptic cleft and an electron-dense postsynaptic membrane, which has approximately the same thickness as the active zone and is therefore called "symmetric".

The presynaptic boutons are swellings on the axon terminations containing the neurotransmitter-filled vesicles and the cellular machinery for the calcium-dependent release of the neurotransmitter. On these boutons, the postsynaptic-facing site is called an active zone, a term coined in 1970 by Couteaux and Pecot-Dechavassine while observing the neuromuscular junction of partially contracted frog muscles by electron microscopy (Couteaux and Pecot-Dechavassine, 1970). On the dendrites opposing the respective presynaptic boutons at glutamatergic type I synapses, a specialized structure was observed and named dendritic spine.

The morphology of dendritic spines is plastic, and the transformations correlate to their degree of maturation (De Roo et al., 2008a; De Roo et al., 2008b; De Roo et al., 2008c; Ethell and Pasquale, 2005; Kasai et al., 2003). In the electron microscope, the mature dendritic spines appear as a dark line due to it's high electron density. This electron-dense structure contains a meshwork of proteins which is named postsynaptic density (PSD). The PSD was firstly observed at glutamatergic synapses, as an electron-dense band with 30-60 nm thickness and 300-400 nm diameter (Carlin et al., 1980; Harris et al., 1992). Embedded in this dense specialization are several other molecules which are required for synaptic transmission, such as cytoplasmic signaling enzymes (Kennedy, 2000), cytoskeletal components and other membrane-associated proteins. It has been previously shown that the area of the PSD correlates with the number of presynaptic vesicles (Nusser et al., 1998).

Subcellularly, dendritic spines host a number of membrane-bound organelles. The rough endoplasmic reticulum for example is primarily located in the cell body and proximal dendrites, but the smooth endoplasmic reticulum is predominantly located in distal dendrites and dendritic spines (Spacek and Harris, 1997). Moreover, the dendrites contain polyribosomes, which have the capacity for local proteins synthesis (Gardiol et al., 1999; Ostroff et al., 2002; Pierce et al., 2000). In addition, mitochondria are also localized in dendritic shafts and in some of the dendritic spines in which they assist the transport of ATP into dendritic spines (Li et al., 2004).

Two major families of scaffolding proteins are concentrated in the postsynaptic density. They both anchor the neurotransmitter receptors to the cytoskeleton: Shank proteins and the membrane-associated guanylate kinases (MAGUKs). The Shank family consists of large scaffolding proteins with a multidomain consisting of ankyrin repeats close to the N-terminus, followed by a SH3, a PDZ domain, a long proline-rich region and a sterile alpha motif domain (SAM) at the C-terminal which interact with NMDARs and metabotropic glutamate receptors (Tiffany et al., 2000). The MAGUKs are defined by a SH3- (Src-homology-3) and WW (two conserved TrP residues)-flanked 300 amino acid region with homology to the yeast kinase which catalyzes the ATP-dependent phosphorylation of GMP to GDP. In MAGUKs, this homology region is catalytically inactive but bears the PDZ (PSD-95/Dlg/ZO-1) domain which represents the binding site for many other proteins, which need to be anchored to the PSD (Funke et al., 2005).

The most important member of the MAGUKs are PSD-95-related proteins. This family is encoded by four genes, which encode PSD-95/SAP90 (synapse-associated protein 90), PSD-93/chapsyn110, SAP102 and SAP97. All of these proteins contain three PDZ domains, which consist of postsynaptic density protein-95 (PSD-95), Drosophila disc large tumor suppressor (DlgA) and Zonula occludens-1 protein (Zo-1). It has been shown that the PDZ domains of the PSD-95 bind directly to the NR2-subunit of the NMDAR (Dong et al., 2004; Kornau et al., 1995) and also with the α-amino-3-hydroxy-5-methyl-4-isoxazolepropionic acid receptor (AMPAR)-associated protein stargazin (Schnell et al., 2002). The interaction between PSD-95 and AMPAR is required for the AMPAR targeting to synapses during synaptogenesis and during synaptic plasticity (Chen et al., 2000; Ehrlich et al., 2007; Schnell et al., 2002). Mice with a targeted deletion of PSD-95 showed an impairment of AMPAR-mediated synaptic transmission and of the maintenance of dendritic spines (Béïque et al., 2006; El-Husseini et al., 2000). Moreover, the downregulation of PSD-95 arrests the development of dendritic spines (Ehrlich et al., 2007), whereas the overexpression of PSD-95 leads to multi-innervated spines

(Nikonenko et al., 2008). Therefore, PSD-95 is essential for the formation and maintenance of excitatory glutamatergic synapses.

In terms of functions, the scaffolding proteins play important roles during different stages of synapse development. During early phases of synapse development, the SAP-102 is required for the clustering of NMDA and AMPA receptors. Whereas during the later stages, PSD-95 regulates the clustering of AMPAR and the switching of NMDAR's subunit composition from NR2B to NR2A (Elias et al., 2008; Petralia et al., 2005; van Zundert et al., 2004). Thus, different scaffolding proteins regulate the clustering and composition of the neurotransmitter receptors depending on the stage of synapse development stages.

Postsynaptic scaffolding molecules at inhibitory synapses consist of different molecules compared to the excitatory synapses. One of the most extensively studied proteins at inhibitory synapses is gephyrin. Originally, gephyrin, a 93-kDa protein, was purified directly and in stoichiometric amounts together with glycine receptors (GlyRs) from rat spinal cord (Pfeiffer et al., 1982). In addition, gephyrin also copurified with polymerized tubulin (Prior et al., 1992). Additional studies demonstrated that gephyrin is essential for the clustering of synaptic inhibitory neurotransmitter receptors, such as glycine and γ-aminobutyric acid type A ($GABA_A$) receptors (Petrini et al., 2014; Pfeiffer et al., 1982; Tretter et al., 2008).

Structurally, gephyrin consists of three major domains: G, C and E domains. The E domain mediates the interaction between gephyrin and glycine receptors (GlyRs) by binding to the β-loop of the β-subunit of the GlyRs (Meyer et al., 1995; Schrader et al., 2004). Several serine residues within this domain control the binding affinity between both gephyrin and GlyRs (Bedet et al., 2006; Kim et al., 2006). Moreover, these residues regulate the cytosolic aggregation and clustering of gephyrin in the postsynaptic membrane (Lardi-Studler et al., 2007). Accordingly, knockdown of gephyrin with antisense oligonucleotides in spinal neurons reduced the density of GlyR clusters in the membrane, suggesting a requirement of gephyrin for the GlyR anchorage at the inhibitory postsynaptic specializations *in vitro* (Kirsch et al., 1993; Levi et al., 2004). Similar changes have been also reported *in vivo* in gephyrin-null mice (Feng et al., 1998; Fischer et al., 2000). Apparently, the E-domain within the gephyrin protein is responsible for the interaction between gephyrin and glycine receptors.

In addition to GlyRs, an interaction of gephyrin with $GABA_AR$ has been previously described. The α2-subunit of the $GABA_AR$ interacts directly with gephyrin via a 10-amino-acid hydrophobic motif within the intracellular domain of gephyrin (Tretter et al., 2008). This binding is required for the $GABA_AR$ concentration at inhibitory synapses (Tretter et al., 2008). Furthermore, several studies have shown that the E domain of gephyrin is important for its

binding to other subunits of the GABAAR, such as the α1-subunit (Mukherjee et al., 2011), α3-subunit (Tretter et al., 2011) and γ2-subunit (Alldred et al., 2005). Therefore, gephyrin is important for the clustering of several subunits of the GABAAR and of the GlyR in the PSD of inhibitory synapses.

Gephyrin is a phosphoprotein with 22 phosphorylation sites (in mouse and rat brains), which are located mostly within the C domain (Kuhse et al., 2012; Langosch et al., 1992). The C domain contains several residues that are modified post-translationally and has a capability to regulate the phosphorylation status of the gephyrin (Fuhrmann et al., 2002; Kneussel et al., 2000). The phosphorylation of gephyrin is important for its clustering, its association with postsynaptic membrane and the regulation of miniature inhibitory postsynaptic currents (mIPSCs; Dejanovic et al., 2014). Altogether, the post-translational modification of the C domain of gephyrin is essential for the normal aggregation and normal function of the inhibitory synapses.

The anchoring of gephyrin in the neuronal postsynaptic membrane requires an essential interacting-protein, the neuron-specific dbl-like GDP/GTP exchange factor, named collybistin (Kins et al., 2000). Collybistin binds to the C-terminal domain of gephyrin and this binding is important for the aggregation of gephyrin on the membrane (Kins et al., 2000). Collybistin-deficient mice exhibited a reduction of gephyrin and of the γ2-subunit of the GABAAR clustering, impairment of GABAergic synaptic transmission and also of spatial learning (Jedlicka et al., 2009; Papadopoulos et al., 2008). The interaction of gephyrin with other proteins is required for the aggregation and the function of the inhibitory synapses.

Synaptogenesis in the CNS

The formation of the complex molecular specializations mentioned in the paragraphs above are required for the establishment of synaptic connectivity. It is therefore conceivable that the formation and maintenance of these synaptic specialization is a key step during embryonic and postnatal development. Therefore, these processes must be very precisely controlled. Since in my thesis I analyzed the molecular machinery that regulates synapse formation, I want to introduce this process in the following paragraphs.

Synapses in the nervous system undergo several changes during the life of a mammalian organism. They are formed during embryonic and early postnatal development, maintained into the adult, shaped during synaptic plasticity and reformed during regeneration after damage or under pathological conditions. The proper formation of synaptic specializations during development and during synapse-related plasticity is crucial for a normal function of the adult

CNS. Disturbances of synapse development can lead to several neurological disorders including autism spectrum disorder, mental retardation, and schizophrenia – all of which have been collectively named "synaptopathies" (Lepeta et al., 2016).

The formation, organization and maintenance of synapses during development involve a complex, yet highly orchestrated interaction of proteins, including trans-synaptic adhesion molecules (CAM) between the presumptive presynaptic and postsynaptic cells (Sudhof, 2018). The contact of the highly motile growth cone with the presumptive postsynaptic membrane leads to a cessation of growth and the subsequent differentiation of an 'active zone', which is characterized by docked and primed synaptic vesicles filled with the neurotransmitters and the molecular machinery for the calcium-mediated vesicular release. At the same time, the postsynaptic compartment specializes. The hallmark of this differentiation is the formation of aggregates containing the neurotransmitter receptors, associated or adapter proteins and synaptic signaling molecules. The contact sites between the active zone and postsynaptic density on the pre- and postsynaptic membranes are precisely aligned (Biederer et al., 2017).

At the molecular level, the formation of synapses requires cell adhesion molecules (CAM), such as the cadherins, the neuroligin-neurexin complex and ephrin/Eph receptors (Graf et al., 2004; Inoue and Sanes, 1997; Paradis et al., 2007; Sudhof, 2018). The type 1 synapses are formed by the extension of a filopodia-like protrusions from the dendrite which will bind to the axon and transform into a postsynapse. These newly-formed synapses undergo several type of changes. Most of them will undergo retractions and only small portion of them will be maintained as functional synapses (Lohmann and Bonhoeffer, 2008). On the other hand, the development of inhibitory synapses is different. Here synapse formation is triggered by direct cell surface contact without involvement of the extension of a filopodia-like processes from the dendrite (Wierenga et al., 2008; Wierenga, 2017). Thus, different types of synapses undergo different structural and molecular changes during development and maturation.

The clustering of receptors during synaptogenesis at type 1 synapses requires trans-synaptic signaling, from the pre-synaptic to the post-synaptic compartment that leads to the activation of NMDA receptors. The activation of NMDARs alters the phosphorylation status more than 100 PSD proteins (Coba et al., 2009). In the case of glutamatergic synapses, it is known that the trans-synaptic complex between the presynaptic neurexins and postsynaptic neuroligin 1, neuroligin 3 and neuroligin 4 is bound to PSD-95 via the COOH-termini of neuroligins (Irie et al., 1997). In the case of GABAergic synapses, the interaction between neurexins and postsynaptic neuroligin 2 is essential (Graf et al., 2004). Thus, the trans-synaptic

interaction between neurexins and neuroligins is indispensable for the induction and/or maintenance of the excitatory and also the inhibitory synapses.

In order to form a functional synapse, many molecular components need to be assembled at the site where the synaptic communication will be established. There are two possible scenarios of how synaptic components are assembled. Firstly, the synaptic proteins are synthesized in the cell body in a random and independent manner, independent of the axodendritic contact. Alternatively, the synaptic proteins are assembled as a complex in the cell body, which is subsequently transported to the contact sites. The realization of both scenarios seems to be true (Craig et al., 2006; Waites et al., 2005; Ziv and Garner, 2001).

The assembly of the presynaptic specialization has been reported to be dependent on vesicular intermediates that will deliver most of the synaptic vesicle proteins to nascent synapses (Bauerfeind and Huttner, 1993). The presynaptic protein piccolo, for example, is transported into the active zone of the nascent synapse together with other presynaptic proteins, such as bassoon, syntaxin, SNAP-25 and N-cadherin, in specialized 80 nm granulated vesicles (Shapira et al., 2003; Zhai et al., 2001).

The postsynaptic specializations, on the other hand, develop more gradually with postsynaptic proteins being individually recruited to the synaptic membrane (Sudhof, 2018). As mentioned previously, dendrites contain the molecular machinery for protein synthesis, including the endoplasmic reticulum (ER) and Golgi membranes, as well as vesicle pools which are filled with AMPA or NMDAR receptor subunits (Kennedy and Ehlers, 2006). This specialized structure opens the possibility that both cytosolic and integral membrane proteins can be locally synthesized, processed and inserted into nascent and mature synapses (Ju et al., 2004; Miyata et al., 2005; Steward and Schuman, 2001; Sutton and Schuman, 2006).

PSD-95, GAKP and Shank proteins are transported in an actin-dependent manner in non-synaptic clusters (Setou et al., 2000) to the postsynaptic membrane and become incorporated at the contact sites close to the presynaptic active zones (Gerrow et al., 2006). The formation and maturation of postsynaptic specializations begin with the formation of a cluster of PSD proteins that aggregate other proteins, such as neurologin/SynCAM capable of inducing presynaptic formation. Additional proteins will be added to the contact site which will trigger the growth and maturation of synapse (Bresler et al., 2004; Gerrow and El-Husseini, 2006; Marrs et al., 2001; Prange and Murphy, 2001; Washbourne et al., 2002). Collectively, the formation and the development of the synapses require both, the pre- and the postsynaptic sides.

The establishment of the contact between the pre- and postsynaptic membrane undergoes several alterations to modify and stabilize the respective compartments. This

transforms an instable structure with immature function into a stable adult synapse. In contrast to nascent immature synapses, mature synapses are characterized morphologically by an increase of clustered synaptic vesicles on the presynaptic side, pronounced postsynaptic densities and a shift from unstable highly motile nascent spines to stable less or non-motile stubby- and mushroom-type spines (Yuste and Bonhoeffer, 2004; Takeichi and Abe, 2005).

Both newly formed and mature spines require a set of molecules that are essential for their normal function. These set of molecules consist of receptors, which are important for the neurotransmission. Two main groups of receptors are responsible for neurotransmission to occur at synaptic level: ionotropic receptors, which are ion channels and metabotropic receptors which are coupled with a G-protein pathway. Depending on the neurotransmitter released and, on the receptors, synapses can be further classified as excitatory or inhibitory. A synapse is classified as excitatory when an excitatory postsynaptic potentials (EPSPs) occurs. The EPSP is usually elicited by a depolarizing cation influx through the membrane in response to the binding of neurotransmitters to the corresponding receptors. On the other hand, a synapse is defined as inhibitory when the binding of neurotransmitter to the postsynaptic receptors elicits a hyperpolarization, usually via an influx of anions through the membrane, generating inhibitory postsynaptic potentials (IPSPs).

Newly formed synapses need to be maintained in the adult nervous system. *In vivo* imaging of mature somatosensory cortex, visual cortex and organotypic hippocampal slice cultures demonstrated, that synapses undergo a turnover, meaning that they remain stable only for variable periods of time (De Roo et al., 2008a; De Roo et al., 2008c; Holtmaat et al., 2005; Trachtenberg et al., 2002; Zuo et al., 2005). Mature dendritic spines are dynamic structures whose stability depends on neuronal activity, Hebbian-type of plasticity and homeostatic processes (Sjostrom et al., 2008). Spines undergo plastic changes depending on their intra- and extracellular conditions and on the neuronal network activity (Holtmaat et al., 2008; Holtmaat et al., 2005; Luscher et al., 2000; Sjostrom et al., 2008; Yuste and Bonhoeffer, 2004). Chronic changes of neuronal activity affect the turnover rate of synaptic proteins at mature synapses (Grutzendler et al., 2002; Trachtenberg et al., 2002). Higher neuronal activity reduces the half-life from 5h to 2h, whereas lower neuronal activity increases the half-life from 5h to 20h-30h (Ehlers, 2003). In addition, many postsynaptic proteins undergo a great volume and exchange rate occurring at presumable stable synaptic structures, such as SAP90/PSD-95, SAP97, actin, the NR1-subunit of the NMDAR, and the GluR1-subunit of the AMPAR (Bresler et al., 2004; Iki et al., 2005; Nakagawa et al., 2004; Okabe et al., 2001; Sharma et al., 2006; Yao et al., 2003). Moreover, the overall stability of dendritic spines differs throughout cortical areas and

experimental conditions (Grutzendler et al., 2002; Holtmaat et al., 2005; Trachtenberg et al., 2002; Xu et al., 2007). Altogether, after being formed, synapses undergo several changes throughout the life, and this depends on the intra- and extracellular conditions as well as on the neuronal network activity. This plasticity of the synapses is essential for higher cognitive functions, including learning and memory.

Synaptogenesis at the neuromuscular junction

The molecular basis of synaptogenesis in the developing CNS is not entirely clear. In contrast, much more is known about the development of a specialized synapse outside the brain, the neuromuscular junction (Tintignac et al., 2015). Our laboratory and others have raised the hypothesis, that synaptogenesis in the CNS might share molecular determinants with synaptogenesis at the NMJ (Kröger and Pfister, 2009). My thesis is based on this hypothesis. In the following paragraphs, I will therefore introduce the NMJ and its development including its key determinants. Afterwards, I will summarize the current knowledge of the functions of these molecules in the CNS.

The NMJ is one of the best-characterized synapses in the entire nervous system. NMJs are communication sites between axons of α-motoneurons and skeletal muscle fibers (Tintignac et al., 2015). The formation, maintenance and regeneration of the NMJ require several key regulatory molecules. The master organizer of synaptogenesis at the NMJ is agrin. Agrin's biological activity requires the binding to a receptor complex, consisting of the low-density lipoprotein receptor-related proteins 4 (Lrp4; Weatherbee et al., 2006; Zhang et al., 2008; Kim et al., 2008) and the muscle-specific kinase (MuSK; Zhang et al., 2008)

Agrin is a large multidomain protein that belongs to the family of heparan sulfate proteoglycans (HSPG) because of its post-translational modification with one or more covalently attached heparan sulfate (HS) chains. Agrin was initially purified and cloned from the electric organ of the marine ray *Torpedo californica* (Nitkin et al., 1987; Smith et al., 1992). The cDNA sequence of agrin is highly conserved in many species including chick, mouse, rat and human (Burgess et al., 2000; Rupp et al., 1992; Rupp et al., 1991; Tsen et al., 1995; Tsim et al., 1992). Agrin is expressed in neuronal and non-neuronal tissues, such as endothelial cells of the blood-brain-barrier, astrocytes (Barber and Lieth, 1997; Kröger and Pfister, 2009; Steiner et al., 2014) and lymphocytes (Khan et al., 2001).

The transcription product of the *Agrn* gene is an approximately 9500-nucleotide-long mRNA that is translated into a large multidomain protein with a molecular mass of 220 kDa. As mentioned above, agrin is also subject to extensive modifications, such as the attachment of

glycosaminoglycan side chains to the central part of agrin. These posttranslational modifications increase the molecular mass of native agrin to more than 500 kDa (Tsen et al., 1995; Winzen et al., 2003).

According to the 'agrin hypothesis' (McMahan, 1990), agrin is synthesized by motoneurons and transported along their axons to the nerve terminal at the NMJ. It is secreted at the contact site between axonal growth cone and target myofiber and then stably incorporated into the basal lamina. Accordingly, agrin immunoreactivity is highly concentrated in the synaptic cleft of the NMJ (Reist et al., 1987). Basal lamina-bound agrin interacts with its tetrameric receptor complex, which is located on the surface of the myofiber (Glass et al., 1996a; Glass et al., 1996b). The binding of agrin to Lrp4 (Kim et al., 2008; Zhang et al., 2008; Zong et al., 2012) leads to the activation of the muscle-specific kinase (MuSK) in the skeletal muscle fiber plasma membrane. MuSK activation initiates an intracellular signaling cascade, which is characterized by the phosphorylation of nicotinic acetylcholine receptors (nAChRs) by the downstream kinase of MuSK, the downstream of tyrosine kinase 7 (Dok-7) and a 43-kDa receptor-associated protein rapsyn (Huganir et al., 1986; Huganir and Greengard, 1983; Huganir and Miles, 1989; Qu et al., 1996; Qu and Huganir, 1994; Wallace et al., 1991). This phosphorylation leads to the aggregation of these molecules at the NMJ, most likely by a diffusion-trap mechanism (Ferns et al., 1996; Glass et al., 1996a; Glass et al., 1996b).

Agrin-induced signaling is also required for the formation of structural specializations of the NMJ, including junctional folds (Marques et al., 2000; Meier et al., 1997) as well as for the synapse-specific gene expression, such as utrophin (Grady et al., 2000; Gramolini et al., 1998), acetylcholine-esterase (AChE) (Bezakova et al., 2001; Matthews-Bellinger and Salpeter, 1983) as well as the expression of the ε-subunit of the nAChRs (Meier et al., 1997). The establishment of these structural and molecular specializations together with synapse-specific gene expression are a prerequisite for the establishment of successful synaptic transmission at the NMJ.

The agrin cDNA predicts a number of structural domains within the agrin protein, including domains similar to EGF, follistatin and the globular domain of the laminin α chain (Denzer et al., 1998). The function of these domains is mostly unknown, but the C-terminal of agrin regulates agrin's synaptogenic activity at the NMJ. In particular, alternative splicing generates a number of agrin isoforms which differ dramatically in their synaptogenic activity at the NMJ. Alternative splicing occurs at several splicing sites within agrin, including two named "y" and "z" in mammals and "A" and "B" in chicken (Fig. 1). Alternative splicing within both sites theoretically generates eight isoforms, but only five of them are realized *in vivo*

(Ruegg et al., 1992). Interestingly, alternative splicing at the z site generates several isoforms that differ in their biological activity (Burgess et al., 1999; Gesemann et al., 1995). Only the isoforms with an insert of 8, 11 or 19 (8 plus 11) amino acids are able to bind to Lrp4, activate MuSK and induce aggregation of nAChRs (Kim et al., 2008; Zhang et al., 2008). Agrin isoforms without any insert at the z/B site have no synaptogenic activity at the NMJ. The function of these B0/z0 isoforms is unknown. The ability of these splice variants to interact with Lrp4 is due to conformational change that forms a tetramer between agrin and Lrp4 (Zong et al., 2012).

Splicing at the y/A site in the LG2-domain generates agrin isoforms which contain or lack an insert of 4 amino acids. This splice site itself does not regulate agrin's synaptogenic activity at the NMJ, but the insertion of an exon coding for 4 amino acids (KSRK) increases the affinity of agrin to heparin/heparan sulfate (Gesemann et al., 1995). One binding partner affected by the splicing at the y/A site is α-dystroglycan (Gesemann et al., 1998; Hopf and Hoch, 1996; Scotton et al., 2006), one of the components of the dystroglycan glycoprotein complex (DGC). Of note, the binding of agrin to dystroglycan does not correlate with agrin's binding to heparin/heparan sulfate (Gesemann et al., 1996). However, the function of this interaction is not known.

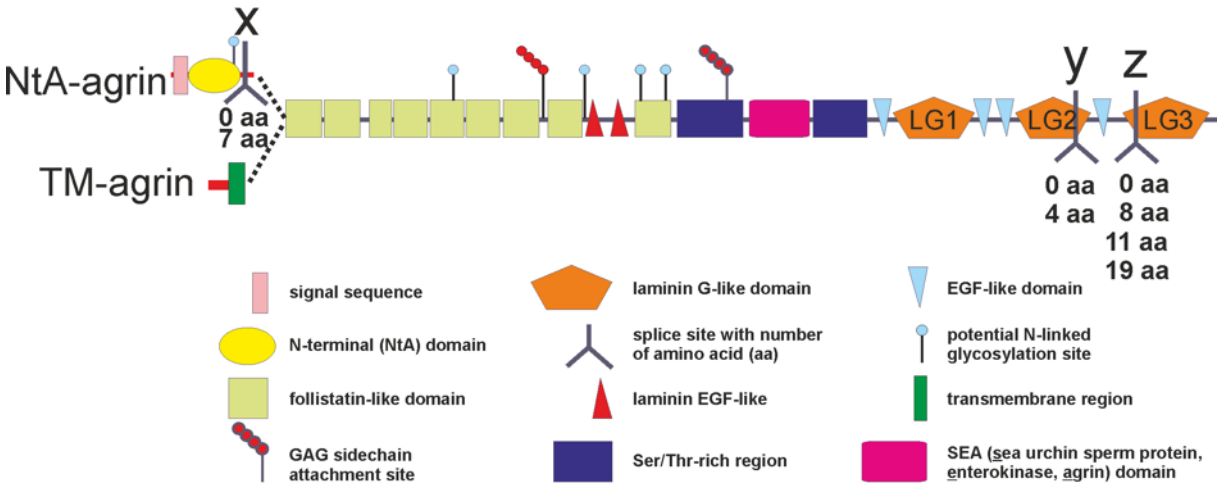

Figure 1. **Domain structure of agrin**. Alternative first exon usage generates two isoforms of agrin, the soluble, secreted-form of agrin (NtA-agrin) and membrane-anchored-form of agrin (TM-agrin). At the C-terminus, agrin contains two splice sites, named y and z. The presence of an insert of 8, 11 or 19 (8+11) amino acid at the z-site is required for the binding of agrin to Lrp4 (adopted from Handara and Kröger, submitted).

As mentioned above, agrin and its receptor complex consisting of the low-density lipoprotein receptor-related proteins-4 (Lrp4) and the muscle-specific kinase (MuSK) are the master organizers for the NMJ formation and maintenance. Null-mutations of any of these proteins exhibit perinatal lethality, i.e. these mice die during or shortly after birth (DeChiara et

al., 1996; Gautam et al., 1996; Weatherbee et al., 2006). In all cases, homozygous mice have no functional NMJs and are, therefore, not able to use their respiratory muscles. Furthermore, the aggregation of nAChRs *in vitro* after agrin incubation on myotubes from Lrp4-KO or MuSK-KO mice was not observed, suggesting that Lrp4 and MuSK are required for agrin's effect on the nAChRs aggregation (Glass et al., 1996; Weatherbee et al., 2006).

Several lines of evidences suggest that agrin is sufficient for NMJ development *in vivo*. Injection of agrin-secreting cells or agrin cDNA into myotubes from skeletal muscle fibers results in the extracellular deposition of agrin in the basal lamina at extrasynaptic sites (Cohen et al., 1997; Jones et al., 1997; Meier et al., 1997; Bezakova et al., 2001). This ectopically deposited agrin induces the formation of the postsynaptic specializations, including the aggregation of nAChRs, rapsyn, acetylcholine esterase (AChE), MuSK and also the aggregation of myonuclei, expression of the AChR ε-subunit and formation of junctional folds. Thus, agrin is not only necessary but also sufficient for the postsynaptic specialization formation at the NMJ.

Agrin and its receptor complex in the central nervous system

Agrin, Lrp4 and MuSK are expressed by neurons and glial cells in the embryonic and adult CNS (Burgess et al., 2000; Garcia-Osta et al., 2006; Karakatsani et al., 2017; Lein et al., 2006). However, their functions in the CNS are still only poorly understood.

While agrin at the NMJ is synthesized as a secreted laminin-binding and basal-lamina-associated form (NtA-agrin; Denzer et al., 1997), the majority of agrin in the CNS is the membrane-anchored isoform, named transmembrane-agrin (TM-agrin; Burgess et al., 2000; Neumann et al., 2002). Both isoforms are transcribed from the same gene, however, alternative first exon usage replaces the N-terminal laminin-binding domain by a single transmembrane region and a 28 amino acids (mouse) intracellular domain (Burgess et al., 2000; Neumann et al., 2002. TM-agrin is a type 2 transmembrane protein and is anchored to the plasma membrane of the CNS neurons (Burgess et al., 2002; Neumann et al., 2001). Subcellularly, TM-agrin is concentrated at synapses (Koulen et al., 1999; Ksiazek et al., 2007) and antibodies against the C-terminal portion of TM-agrin could be detected in the synaptic cleft. However, it is unknown if this agrin is anchored in the pre- or postsynaptic membrane.

The expression pattern and the concentration of agrin at synapses has led to the hypothesis, that agrin might contribute to synapse development in the CNS in a similar way as it does at the NMJ (Daniels, 2012; Kröger and Pfister, 2009). The following observation supports this hypothesis: agrin is highly expressed during the period of synapse formation and

remains expressed (although at a reduced levels) in the adult CNS, particularly in regions with increased synaptic plasticity (Burgess et al., 2000; Li et al., 1997; O'Connor et al., 1994). In the brain of E14 mouse, agrin is expressed in the ventricular, intermediate zone, cortical plate and in the cerebral vasculature. In the adult brain, the expression of agrin is restricted to brain regions with a high degree of synaptic plasticity (Burk et al., 2012). Seizures increase agrin expression level in a rapid, a region-specific and prolonged-manner (O'Connor et al., 1995). Likewise, after traumatic brain injury, agrin expression is increased within 7 days after the insult and reduced to normal levels thereafter (Falo et al., 2008). Thus, agrin is expressed in the developing CNS and during periods of synaptic plasticity.

Interestingly, the absence of agrin in the CNS lead to subtle morphological abnormality at synapses *in vitro* (Gautam et al., 1999; Li et al., 1999; Serpinskaya et al., 1999). *In vitro*, CNS neurons in which the expression of TM-agrin was reduced using siRNA showed a reduction of excitatory synapses density compared to control (McCroskery et al., 2006). Moreover, agrin-deficient neuronal precursors that were transplanted into the subventricular zone of WT mice have the capacity to migrate along the rostral migratory stream (RMS) into the olfactory bulb. However, they fail to integrate correctly into the neuronal network and do not form synapses. Accordingly, these cells display a reduced viability (Burk et al., 2012). This demonstrates the requirement of agrin expression for synapse formation and, as a consequence for the normal integration of neurons into an existing network.

The role of TM-agrin in the CNS has been shown by taking advantage of gain-of-function paradigms. Overexpression of the TM-agrin, but not of NtA-agrin isoform, increases the number of filopodia extended from axons and dendrites of cultured cortical neurons (Annies et al., 2006; McCroskery et al., 2006; Ramseger et al., 2009). The formation of filopodia in neurons after TM-agrin overexpression involves a specific signaling cascade via lipid rafts. The generation of these lipid rafts is required for the activation of mitogen-activated protein kinases (MAPKs). It has been shown that MAPKs activation leads to the Cdc42-mediated actin filament reorganization (McCroskery et al., 2006; Ramseger et al., 2009). Thus, TM-agrin overexpression leads to an increased density of dendritic filopodia via activation of the specific signaling cascade. Since filopodia-like processes have been shown to be precursors of dendritic spines (Ziv & Smith 1996), these results suggested that TM-agrin might affect synaptogenesis by regulating the number of these filopodia (Annies et al., 2006; McCroskery et al., 2006; Ramseger et al., 2009).

Mice in which the perinatal lethality caused by agrin deficiency was rescued by re-expression of agrin cDNA exclusively in motoneurons, display morphological and functional

changes at synapses in the CNS, such as a reduction of spine density and of miniature excitatory postsynaptic currents (mEPSCs) frequency in the adult cortex (Ksiazek et al., 2007). However, agrin-deficient brains have no change of IPSCs amplitude and frequency. Moreover, agrin colocalized only with PSD-95, but not with the α2-subunit of the $GABA_AR$. Collectively, these results demonstrate that agrin is required for the formation of a normal density of excitatory synapses and their maintenance in the CNS. These results also support the hypothesis that agrin might play a role in the developing CNS similar to its role at the NMJ.

Lrp4 in the central nervous system

Lrp4 is a type 1 transmembrane protein that is not only expressed by muscle fibers and aggregated at the NMJ but also expressed in the CNS, including the neocortex, hippocampus, cerebellum and olfactory bulb (Karakatsani et al., 2017; Lein et al., 2007; Sun et al., 2016; Tian et al., 2006). Lrp4 is concentrated at synapses and can be extracted from highly-purified postsynaptic membrane fractions from murine forebrain (Tian et al., 2006). Lrp4 belongs to the low-density lipoprotein receptor (LDLR) family. All proteins from this family carry a common structure that includes ligand binding domains, epidermal growth factor (EGF) domains, a membrane anchoring domain, and a cytoplasmic tail containing the NPxY motif which allows the direct binding of Lrp4 to PSD-95. The structure of Lrp4 itself consists of an extracellular region comprising eight cysteine-rich repeats (LDLa repeats), six epidermal growth factor (EGF)-like domains, four β-propeller domains, a hydrophobic transmembrane region, and a cytoplasmic tail (consisting of 160 amino acids containing the NPxY motif and a PDZ domain-binding consensus sequence, -ESQV; Chen et al., 1990; Tian et al., 2006). The NPxY motif facilitates signal transduction and endocytic trafficking (Gotthardt et al., 2000). Interestingly, Lrp4 has been shown to directly interact with the postsynaptic scaffold protein PSD-95 via the PDZ domain-binding consensus sequence (Tian et al., 2006; Gomez et al., 2014). In addition, Lrp4 binds directly to the LG3 domain of agrin via its LDLa repeats domain, the first two EGF-like domains, and the first β-propeller (Zhang et al., 2011; Zong et al., 2012).

A mouse line with a null mutation of Lrp4 was generated by chemical mutagenesis using N-ethyl-N-nitrosourea (Weatherbee et al., 2006). This chemically-induced mutation generated an early stop codon C terminal to the LA domains and also an alternative splice variant containing another premature stop codon. Mice with the Lrp4 mutation have no structural and functional NMJs. Moreover, the motor nerve axon from this mutant line fail to stop in the central region of muscle fibers, never transform into a presynaptic terminal and instead continue

to grow and arborize extensively (Weatherbee et al., 2006). Therefore, the mutant mice die perinatally due to respiratory muscle failure.

The absence of Lrp4 in the CNS lead to normal architecture of the cortex and hippocampus and no obvious change in the dendritic morphology. However, spine density on primary apical dendrites was reduced causing a disturbance in long-term potentiation in the hippocampus and in cognitive performance, such as memory deficits in the Morris water maze (Gomez et al., 2014; Pohlkamp et al., 2015). In addition, a reduced level of Lrp4 in hippocampal and cortical neurons, *in vitro* and *in vivo*, caused a less complex dendritic arborization and a lower density of spines and synapses (Karakatsani et al., 2017). Altogether, Lrp4 in the CNS is essential for the synapse formation, synapse maintenance and for normal memory functions.

MuSK in the central nervous system

MuSK is a type I transmembrane protein that is expressed not only in skeletal muscles, but also in CNS neurons (Garcia-Osta et al., 2006). It belongs to a member of the large receptor tyrosine kinases (RTKs) family. It was initially discovered in a search for tyrosine kinases from the electric organ of *Torpedo californica* (Jennings et al., 1993), a tissue that resembles innervated skeletal muscle. The extracellular region of MuSK consists of several domains, such as a glycosylated extracellular domain, a single transmembrane helix, and a cytoplasmic region. Furthermore, the extracellular domain consists of three immunoglobulin-like domains (Ig1, Ig2, and Ig3) and a cysteine-rich domain (CRD). This CRD domain shares structural similarities to the CRD domain of Frizzled proteins of the Wnt receptors (Jing et al., 2009).

Functionally, on myotube the Ig1 domain of MuSK binds to Lrp4 in an agrin-dependent manner (Kim et al., 2008; Zhang et al., 2011). This binding leads to an autophosphorylation of MuSK in the cytoplasmic region, due to a presence of a tyrosine kinase domain (Till et al., 2002). The activation of the tyrosine kinase domain activates an intracellular signaling cascade which eventually leads to the formation of the postsynaptic apparatus at the NMJ, including the aggregation of nAChRs. The presence of the cytoplasmic adaptor protein Dok7 is essential for the MuSK-mediated nAChRs aggregation (Okada et al., 2006).

The function of MuSK in the developing and adult CNS is mostly unknown. The presence of MuSK in hippocampus had been shown to be important for memory consolidation, and for the induction and maintenance of LTP (Garcia-Osta et al., 2006). Additional evidence for a role of MuSK in the CNS was provided by an animal model for autoimmune myasthenia gravis (Sabre et al., 2019). Passive immunization of mice with IgG MuSK-positive from patients with myasthenia gravis showed not only an impairment of the neuromuscular integrity

and function, but also an impairment in spatial and recognition memories (Sabre et al., 2019). These evidences support a role for MuSK not only in the NMJ formation and maintenance, but also in the CNS.

Aims of study

In my thesis, I investigated the functions of agrin, Lrp4 and MuSK during synapse formation and synaptic plasticity. Particularly, I analyzed if agrin and its receptor complex influence neuronal morphology and synaptogenesis in developing cortical neurons *in vitro* and in adult mice *in vivo*.

Specifically, I investigated the following questions:

1. Do TM-agrin, Lrp4 and MuSK play a role in dendritic arborization in cultured cortical neurons?
2. Does TM-agrin overexpression affect dendritic development and synapse formation?
3. Does the effect of TM-agrin overexpression on dendritic branching and synapse formation depend on the expression of Lrp4 and MuSK?
4. Which region of TM-agrin is involved in CNS development?
5. Does TM-agrin overexpression affect synapse development and/or maintenance in adult murine cortex?

Materials

Animals

Use and care of animals were approved by German authorities according to the national law (TierSch§7). For this study, C57BL/6J wild-type (Charles River GmbH, Germany), CamKIIa-Cre$_{ERT2}$ and TM-agrin knock-in (TM-agrin KI) were bred in the Core Facility Animal Models of the Biomedical Center of the LMU Munich. The Lrp4$_{mitt}$ or Lrp4-KO mice (Weatherbee et al., 2006) and MuSK$_{tm1gdy}$ or MuSK-KO mice (DeChiara et al., 1996) were bred in the animal facility of the Max-Delbrück-Center in Berlin. Animals were housed in a cage with maximal 5 animals on a 12/12 h light/dark cycle with access to food and water *ad libitum*.

The animal procedures were performed according to the guidelines from Directive 2010/63/EU of the European Parliament on the protection of animals used for scientific purposes. All experimental procedures were approved by the local authorities of Bavaria (Az.: ROB-55.2-2532.Vet_02-17-82. 55.2-1-54-2532.8-160-13 and 55.1-8791-14.587) and of Berlin (LaGeSO; numbers T0313/97 and X9014/15). The day of the vaginal plug was considered as embryonic day 0.5 (E 0.5). Male and female mice were used in all of the experiments. The heterozygous littermates of Lrp4$_{mitt}$ and MuSK$_{tm1gd}$ mice were used as controls.

The CamKIIa-CreER$_{T2}$ line (Erdmann et al., 2007) was maintained on C57BL/6J background. In this line, the fusion protein containing Cre recombinase and human estrogen receptor (CreER$_{T2}$) was expressed under the CamKIIa promoter that shows high expression in excitatory neurons in the forebrain (Erdmann et al., 2007). The fusion protein is located in the cytoplasm and only translocated into the nucleus upon tamoxifen administration (Erdmann et al., 2007). In the nucleus, the Cre recombinase excises the loxP-flanked stop cassette. This excision will disinhibit the expression of knock-in TM-agrin in excitatory neurons, yielding an overexpression of TM-agrin. The homozygosity of CamKIIa-CreER$_{T2}$ was generated and was subject to cross-breeding with the TM-agrin KI line to generate Cre+/Agrin KI and Cre+/Agrin WT as a control.

TM-agrin knock-in (TM-agrin KI) line was generated by taking advantage of the yeast (*Saccharomyces cerevisiae*) homologous recombination system (Schick, 2018). The mouse full-length TM-agrin-y4z0 cDNA was incorporated into a targeting backbone of the pMES vector and inserted in the ROSA26 locus by homologous recombination. This locus was chosen because it shows high efficiency for homologous recombination and mice with homozygous knockout of ROSA26 do not show any obvious phenotype (Zambrowicz et al., 1997). To investigate the effect of TM-agrin overexpression during phase of synaptic plasticity, the TM-

agrin KI line was cross-bred with the CamKIIa-CreER$_{T2}$ line and tamoxifen was applied to animals at 5-weeks of age. The cross-bred line was maintained on C57BL/6J background.

Embryos from Lrp4$_{mitt}$ (termed Lrp4-KO mice; MGI ID: 3707955) were prepared at E15. This line carries two chemically induced mutations, that lead to an early stop of translation at from the C-terminal to the LA domain and a splice site mutation that lead to another early stop codon (Weatherbee et al., 2006). The Lrp4-KO mice were a generous gift from Prof. Dr. Fritz Rathjen (Max-Delbrück-Center Berlin). This line was maintained on C57BL/6N background.

Embryos from MuSK$_{tm1Gdy}$-mice (termed MuSK-KO mice; MGI ID:1929066) were prepared at E15. The MuSK$_{tm1Gdy}$ mice lack the exon coding for the intracellular tyrosine kinase domain which was replaced by a neomycin cassette (DeChiara et al., 1996). These mice also were a generous gift from Prof. Dr. Fritz Rathjen. The MuSK-KO line was maintained on C57BL/6N background.

Generation of antiserum against TM-agrin

Antibodies specifically against murine TM-agrin are not commercially available. In order to investigate the specific localization of TM-agrin, we generated monoclonal and polyclonal antibodies against a peptide from the intracellular region of mouse TM-agrin. The selected sequence was LPLEHRPRQQPGASVC. This sequence of the intracellular region was selected and analyzed *in silico* by basic local alignment search tool for protein (BLASTp) for its specificity and for its potential immunogenicity. The BLASTp analysis showed that the peptide was specific and did not share any similarities with other proteins. In addition, the secondary structure of the selected region was analyzed to select the best epitope using the Welling antigenicity scale (Janin, 1979; Parker et al., 1986). Altogether, the analyses showed that the peptide was highly specific and immunogenic for the production of the relevant antibodies.

The peptide was commercially synthesized and purified. For the generation of the polyclonal antibody, three rabbits were immunized with the peptide for 128 days according to the standard protocol (Pineda Antikörper Service, Berlin, Germany). Before the immunization, pre-immune sera were collected and tested, in order to choose rabbits which had the lowest background immunoreactivity on brain sections. After immunization, the blood was collected, and the antiserum was purified by affinity chromatography. The monoclonal antibodies were generated using standard procedures in the monoclonal antibody facilities of the Department of Biology of the LMU Munich.

Primary antibodies

Table 1. Primary antibodies

Antibody	Host Species	Source	Dilution
Agrin	Rabbit	Markus Ruegg	WB 1:2000 IHC 1:500 ICC 1:1000
TM-agrin (specific against intracellular-domain)	Rabbit	In house-made, #173	IHC 1:500 ICC 1:1000
TM-agrin (specific against intracellular-domain)	Mouse	In house-made	IHC 1:500 ICC 1:1000
α1-subunit $GABA_AR$	Rabbit	Merck:06-868	ICC 1:1000
α5-subunit $GABA_AR$	Rabbit	Synaptic Systems:224503	ICC 1:1000 IHC 1:1000
Amyloid precursor protein	Rabbit	Abcam:ab32136	ICC 1:1000 IHC 1:1000
Bassoon	Mouse	Thermo Scientific:MA1-20689	ICC 1:1000 IHC 1:1000
Collybistin	Rabbit	Synaptic systems:261003	ICC 1:1000 IHC 1:2000
GABA	Rabbit	Sigma:A2052	ICC 1:1000
Gephyrin	Rabbit	Synaptic Systems:147002	ICC 1:1000
GFP	Chicken	Abcam:ab13970	ICC 1:2000
HA affinity-purified	Rat	Roche:11867423001	ICC 1:1000
Neuroligin-1	Rabbit	Synaptic Systems:129013	ICC 1:1000
Neuroligin-2	Rabbit	Synaptic Systems:129203	ICC 1:1000
Neuronal nuclei (NeuN)	Mouse	Merck:mab377	ICC 1:500
PSD-95	Mouse	Merck:Mab68	ICC 1:1000
PSD-95	Rabbit	Abcam:ab18258	IHC 1:1000
RFP	Rabbit	Abcam: ab62341	ICC 1:2500
Tau	Rabbit	Sigma:	WB 1:1000
Tau	Mouse	Merck-Millipore:Mab3420	WB 1:1000
Tbr1	Mouse	Santa Cruz: sc-376258	ICC 1:1000
Tbr1	Rabbit	Abcam: ab31940	ICC 1:1000
Tbr1	Guinea Pig	Synaptic system:328005	ICC 1:1000
vGAT	Guinea Pig	Synaptic systems:131005	ICC 1:1000 IHC 1:1000
vGlut1	Guinea Pig	Synaptic systems: 135304	ICC 1:5000 IHC 1:5000

Secondary antibodies

Table 2. Secondary antibodies

Antibody	Flourescence tag	Source	Dilution
Goat anti-mouse IgG (H+L), highly cross-adsorbed	Alexa Fluor® 594	Thermo Fisher Scientific:A11032	ICC 1:1000 IHC 1:1000
Goat anti-mouse IgG (H+L), highly cross-adsorbed	Alexa Fluor® 647	Thermo Fisher Scientific:A21236	ICC 1:1000 IHC 1:1000
Goat anti-rabbit IgG (H+L), highly cross-adsorbed	Alexa Fluor® 594	Thermo Fisher Scientific:A11037	ICC 1:1000 IHC 1:1000
Goat anti-rabbit IgG (H+L), highly cross-adsorbed	Alexa Fluor® 647	Thermo Fisher Scientific:A21245	ICC 1:1000 IHC 1:1000
Donkey anti-rat IgG (H+L), highly cross-adsorbed	Alexa Fluor® 488	Thermo Fisher Scientific:A21208	ICC 1:1000 IHC 1:1000
Donkey anti-chicken IgY (H+L)	Alexa Fluor® 488	Thermo Fisher Scientific:A11039	ICC 1:1000 IHC 1:1000
Donkey anti-guinea pig	DyLight 649	Millipore: AP193SD	IHC 1:1000
Goat anti-mouse IgG (H+L)	IRDye 800CW	Li-Cor:925-32210	WB 1:20000
Goat anti-rabbit IgG (H+L)	IRDye 680LT	Li-Cor:925-68021	WB 1:20000

Buffers and solutions

Table 3. Buffers and solutions

Buffer/Solution	Components	Preparation / Final concentration	Manufacturer
Ampicillin stock, 100 mg/ml	1 g ampicillin, autoclaved ddH_2O	Ampicillin powder is dissolved in 10 ml ddH_2O	
4',6'-diamidino-2-phenylindole (DAPI) stock 2 mg/ml	2 mg DAPI 1 mL 1X PBS	DAPI powder is dissolved in the 1 ml PBS 1 X	
Kanamycin stock, 100 mg/ml	1 g kanamycin Autoclaved ddH_2O	Kanamycin powder is dissolved in 10 ml autoclaved ddH_2O	
Gel loading dye, purple (6 X)	-	-	New England BioLabs
Aqua-Poly/Mount	-	-	Polysciences, Inc
Paraformaldehyde 16% (PFA 16%)	-	-	Electron Microscopy Science
Paraformaldehyde 4% (PFA 4%)	1 volume PFA 16% 3 volume PBS 1 X	-	-
PBS 10 X			
PBS 1 X	1 Volume PBS 10 X 9 Volume ddH_2O		

Poly-D-Lysine (PDL) stock solution, 1 mg/ml	5 mg PDL ddH_2O	5 mg PDL powder is dissolved in 5 ml ddH_2O, then it is sterilized by filtering	
Poly-D-Lysine (PDL) working solution, 0.01 mg/ml	500 ul PDL stock solution 50 ml sterile PBS 1 X	500 ul of PDL stock solution is mixed with 50 ml sterile PBS 1 X	
RIPA buffer			
Electrophoresis running buffer 10 X , pH 8.5(Elo buffer 10 X)	30.2 g of Tris-BASE (MW = 121.14 g/mol), 144 g of Glycine (MW = 75.07 g/mol), 10 g of SDS (MW = 288.38 g/mol), ddH_2O	Tris-BASE, glycine and SDS are diluted in 900 ml ddH_2O. The pH is adjusted to 8.5, and then the ddH_2O is added up to 1 L.	
Elo buffer 1 X, working buffer	Elo buffer 10 X ddH_2O	100 ml of Elo buffer 10 X is diluted with 900 ml ddH_2O	
Transfer buffer 10 X	30.2 g of Tris-BASE (MW = 121.14 g/mol), 144 g of Glycine (MW = 75.07 g/mol), ddH_2O	Tris-BASe and glycine are dissolved in ddH_2O with the end volume 1 L.	
Transfer buffer 1 X, working buffer	Transfer buffer 10 X Ethanol 100 %	100 ml of transfer buffer 1 X, 200 ml of ethanol 100 % and 700 ml ddH_2O	
SDS 20%	20 g of SDS (MW = 288.38 g/mol) ddH_2O	20 g of SDS is dissolved in 80 ml ddH_2O at 65°C, and then the volume is added up to 100 ml.	
Tris HCl 1 M pH 8.5	TrisBASE powder (MW = 121.1 g/mol) HCl 6 N ddH_2O	60.5 g TrisBASE is dissolved in 450 ml ddH_2O. The pH is adjusted to 8.5 with HCl 6 N up to 500 ml volume.	
EDTA 0.5 M, pH 8.0	EDTA powder (MW = 372.24 g/mol) NaOH 32% ddH_2O	18.61 g of EDTA is dissolved in 80 ml ddH_2O. The pH is adjusted with NaOH 32%. The volume is adjusted up to 100 ml.	
NaCl 1 M	NaCl powder (MW = 58.44 g/mol) ddH_2O	22.22 g of NaCl is dissolved in 500 ml ddH_2O.	
Tris-Acetate-EDTA (TAE) buffer, 1 X	1 volume of TEA buffer 50 X ddH_2O		

LB broth			
LB Agar			
SDS-PAGE protein sample buffer 4 X	Tris-HCl 1 M pH 8.5, SDS 20 %, 100 % glycerol, □-mercaptoethanol 100 %, bromophenol blue, ddH_2O	5 mM of Tris-HCl pH 8.5, SDS 0.25 % (v/v), glycerol 25 % (v/v), □-mercaptoethanol 8 %, bromophenol blue 0.25 %	
APS 10 %	Ammonium persulfate (MW = 228.2 g/mol)	APS 20 % (w/v)	
Differentiation/maintenance medium	Neurobasal medium Penicillin-Streptomycin 1 X GlutaMAX™ 1 X B27 Supplement (Gibco®) 1 X		
Dissecting buffer	HBSS 50 mL 1 M HEPES 500 ul	1 M HEPES was added into cold HBSS, with the end concentration 100 uM	
Tissue lysis buffer	Tris-HCl pH 7.5 EDTA PMSF cOmplete™ Protease inhibitor cocktail (Co-Ro Roche)	Tris-HCl 10 mM pH 7.5 EDTA 10 mM PMSF 0.5 mM 1 tablet of protease inhibitor cocktail per 50 mL	
SDS sample buffer 4 X for S2 (supernatant-2) fraction	1 M Tris-HCl pH 8.5 Sodium dodecyl sulfate (SDS) Glycerol 2-mercaptoethanol Bromophenol blue	Tris-HCl 5 mM pH 8.5, SDS 1 %, glycerol 25 %, 2-mercaptoethanol 8 %, bromophenol blue 0.25 %	
SDS sample buffer 4 X for M (crude membrane) fraction	1 M Tris-HCl pH 8.5 Sodium dodecyl sulfate (SDS) Glycerol 2-mercaptoethanol Bromophenol blue Urea	Tris-HCl 5 mM pH 8.5, SDS 1 %, glycerol 25 %, 2-mercaptoethanol 8 %, bromophenol blue 0.25 %, Urea 8 M	
Proteinase K, stock 10 mg/ml	1 g of proteinase K powder ddH_2O	1 g of proteinase K powder is dissolved in 100 ml ddH_2O. The storage is -20 °C	Carl Roth, catalogue number 7528
Odyssey® blocking buffer (TBS)			Li-Cor
TBS 10 X, pH 8.0	Tris-BASE (MW = 121.14 g/mol), NaCl, ddH_2O	Tris-BASE 100 mM and NaCl 1.5 M are mixed in 900 ml ddH_2O. The pH is	

		adjusted to 8.0, then the volume is added up to 1 L.	
TBST 1 X	TBS 10 X, pH 8.0 Tween® 20, ddH_2O	TBS 1 X, Tween® 20 0.1 % (v/v), ddH_2O is added up to 1 L.	
WB staining solution	TBST 1 X, horse serum	horse serum 5 % (v/v) is added to 10 ml of TBST 1 X	
ICC blocking solution	Bovine serum albumin (BSA), triton X-100, PBS 1 X	BSA 2 % (m/v) is dissolved in PBS 1 X, triton X-100 0.2 % (v/v) in PBS 1 X.	
Sodium citrate buffer	Trisodium citrate (dihydrate), ddH_2O	Trisodium citrate 10 mM, pH 8	
IHC blocking solution	Normal Goat Serum (NGS), Triton X-100, PBS 1X	NGS 5 % (v/v), Triton X-100 0.3 % (v/v), PBS 1 X	
IHC staining solution	Bovine serum albumin (BSA), triton X-100, PBS 1 X	NGS 2.5 % (v/v), Triton X-100 0.1 % (v/v), PBS 1 X	
Tamoxifen powder	-	-	Sigma-Aldrich, Cat. No. T5648
Corn oil	-	-	Sigma-Aldrich, Cat. No. C8267
Tamoxifen for intraperitoneal injection	Tamoxifen powder, corn oil	Tamoxifen powder is dissolved in corn oil (2 mg/ml)	
Ketamine/xylazine mixture for perfusion	Ketamine hydrochloride 10 %, xylazine hydrochloride 2 %, NaCl 0.9 %		
Lipofectamine® 2000	-	-	Thermo Fisher Scientific
SV Total RNA Isolation System	-	-	Promega
Reverse-transcription			
Denaturing agarose gel	Formamide, Formaldehyde 37 %, Ethidium bromide		
MOPS buffer	MOPS, Na-acetate, EDTA	MOPS free acid 20 mM, Na-acetate 5 mM, EDTA 1mM	
Anesthesia solution	Ketamine hydrochloride 10 %, Xylazine hydrochloride 100 mg/ml, sterile physiological saline	1 mL ketamine hydrochloride, 0.25 mL xylazine hydrochloride, 2.5 sterile physiological saline solution	

Zyppy™ plasmid midiprep kit	-	-	Zymo Research
Plasmid Midi kit	-	-	Qiagen

Media and supplements

Table 4. Media and supplements

Medium	Manufacturer
HBSS, no calcium, no magnesium (Gibco™)	Thermo Fisher Scientific
HEPES 1M (Gibco™)	Thermo Fisher Scientific
Neurobasal, serum free medium	Thermo Fisher Scientific
B-27 supplement	Thermo Fisher Scientific
GlutaMAX™ supplement	Thermo Fisher Scientific

Cell lines

Table 5. Cell lines

Bacterial Strains	Manufacturer/Source
Top10 Chemically-competent E. coli TOP10	Invitrogen/Thermofisher
HEK 293T cells	Kind gift of Dr. Alex Lepier

Oligonucleotides

Table 6. Oligonucleotides

Sequence name	Application	Gene to be annealed	Sequence
prAS15	Genotyping	TM-agrin knock-in allele forward	TACTCCTCTACAATGGGCAG
prAS104	Genotyping	TM-agrin knock-in allele reverse	GCCACAACTCCTCATAAAGA
prAS116	Genotyping	CamKIIa-Cre$_{ERT2}$ transgene forward	GGTTCTCCGTTTGCACTCAGGA
prAS118	Genotyping	CamKIIa-Cre$_{ERT2}$ transgene reverse	GCTTGCAGGTACAGGAGGTAGT
oIMR1084	Genotyping	CamKIIa-Cre transgene forward	GCG GTC TGG CAG TAA AAA CTA TC
oIMR1085	Genotyping	CamKIIa-Cre	GTG AAA CAG CAT TGC TGT CAC TT

		transgene reverse	
oiMR9020	Genotyping	Rosa26 WT locus forward	AAGGGAGCTGCAGTGGAGTA
oiMR9021	Genotyping	Rosa26 WT locus reverse	CCGAAAATCTGTGGGAAGTC
L4Hpmf	Genotyping	Lrp4-WT	GGTGAGGAGAACAGCAATGT
43Br_FP	Genotyping	Lrp4-KO	TCCCAGGGTCAGTGTAACGATG
NsK-1	Genotyping	MuSK WT	ATGCCGCCCGAGTCTATCTTCTAC
NsK-2	Genotyping	MuSK WT-KO	TTCTCCTGGCAAACAATCAACTGG
Neo3	Genotyping	MuSK KO	CATAGCCTGAAGAACGAGATCAGCAGC
Bassoon left	qRT-PCR	Bsn	TTTAACCCAACACCGCATCT
Bassoon right	qRT-PCR	Bsn	GCCGCTTAGTTTGGCAGTT
GluR1-subunit of AMPAR left	qRT-PCR	Gria1	AGGGATCGACATCCAGAGAG
GluR1-subunit of AMPAR right	qRT-PCR	Gria1	TGCACATTTCCTGTCAAACC
NR1-subunit of NMDAR left	qRT-PCR	Grin1	AGGGATCGACATCCAGAGAG
NR1-subunit of NMDAR right	qRT-PCR	Grin1	AGCAGAGCCGTCACATTCTT
Synaptophysin left	qRT-PCR	Syp	CAAGGCTACGGCCAACAG
Synaptophysin right	qRT-PCR	Syp	TCGTGGGCTTCACTGACC
α1-subunit of $GABA_AR$ left	qRT-PCR	Gabra1	GCCCACTAAAATTCGGAAGC
α1-subunit of $GABA_AR$ right	qRT-PCR	Gabra1	CTTCTGCTACAACCACTGAACG
Gephyrin left	qRT-PCR	Gphn	TGGTCTCATCAGTTATTCCCATC
Gephyrin right	qRT-PCR	Gphn	CGAGAAATGATGGAGTCTGGA
Munc13-1 left	qRT-PCR	Unc13a	CAATGCCTTGGCAGATGATA
Munc13-1 right	qRT-PCR	Unc13a	GGGTCTTCAAAGGAACACTGG
Munc13-2 left	qRT-PCR	Unc13b	TGCCTTGGCAGATGATAATG
Munc13-2 right	qRT-PCR	Unc13b	AGCCCAAATAGGTCCAGTGA
HPRT left	qRT-PCR	Hprt	TCCTCCTCAGACCGCTTTT
HPRT right	qRT-PCR	Hprt	CCTGGTTCATCATCGCTAATC
Munc13-3 left	qRT-PCR	Unc13c	TCTGACACCAAGACAATGTGC
Munc13-3 right	qRT-PCR	Unc13c	CCTCCTGCATGAAAATATTGCT
PSD-95 left	qRT-PCR	Dlg4	ACTCCTGCTCCAGCTTCGT
PSD-95 right	qRT-PCR	Dlg4	GCTCCCTGGAGAATGTGCTA
Dystroglycan left	qRT-PCR	Dag1	CCAGGCAGTGTTGAAAACCT
Dystroglycan right	qRT-PCR	Dag1	CCAGGCAGTGTTGAAAACCT
Synaptotagmin-1 left	qRT-PCR	Syt1	ACCTTACTCAACTGGCATTTGTT
Synaptotagmin-1 right	qRT-PCR	Syt1	AGACTGCGGATGTTGGTTGT
Neuroligin-1 left	qRT-PCR	Nlgn1	CTATCGGCTTGGGGTACTTG

Neuroligin-1 right	qRT-PCR	Nlgn1	CAAGGAGCCCGTAGTTTCCT
Neuroligin-2 left	qRT-PCR	Nlgn2	CCTACGTGCAGAACCAGAGC
Neuroligin-2 right	qRT-PCR	Nlgn2	TCGCCTCGTCACGTTTTT

Plasmids

The full-length mouse TM-agrin-y4z0 cDNA was inserted into the multiple cloning sites (MCS) of a pMES-yeast-cassette vector (Schick, 2018). The pMES vector was chosen because it contains IRES-GFP, which enables visually the identification of transfected cells. All the constructs (Fig. 2, Table 7) used in this study were routinely sequenced (GATC Biotech, Konstanz, Germany) and were subjected to diagnostic restriction digest to exclude mutations.

Table 7. Plasmids

Plasmid Name	Vector backbone	Reporter/Tag Proteins	Source
Mouse TM-Agrin-y4z0 (pAS12)	pMES	IRES-GFP, HA-tag, myc-tag	Dr. Schick
pMES	-	IRES-GFP	Dr. Schick
Mouse TM-Agrin-y4z8	pAS12	IRES-GFP, HA-tag, myc-tag	Self-made/Genscript Biotech Corporation
Mouse TM-agrin-y0z0	pAS12	IRES-GFP, HA-tag, myc-tag	Restriction enzymes and ligation
miRNA Lrp4	pCAG-RFP	RFP	Karakatsani, 2017
miRNA control	pCAG-RFP	RFP	Karakatsani, 2017
Ch TM-agrin-y4z8 (chTM-agrin)	pGFPN-1	Fused-GFP	Porten, 2007
TMFD8	chTM-agrin	Fused-GFP	Porten, 2007
TMFD6	chTM-agrin	Fused-GFP	Porten, 2007
ΔEC-FL-Agrin	chTM-agrin	Fused-GFP	Porten, 2007
pGFPN-1		GFP	Clontech
S17A TM-agrin-y4z0	pAS12	IRES-GFP, HA-tag, myc-tag	Genscript Biotech Corporation
S17D TM-agrin-y4z0	pAS12	IRES-GFP, HA-tag, myc-tag	Genscript Biotech Corporation

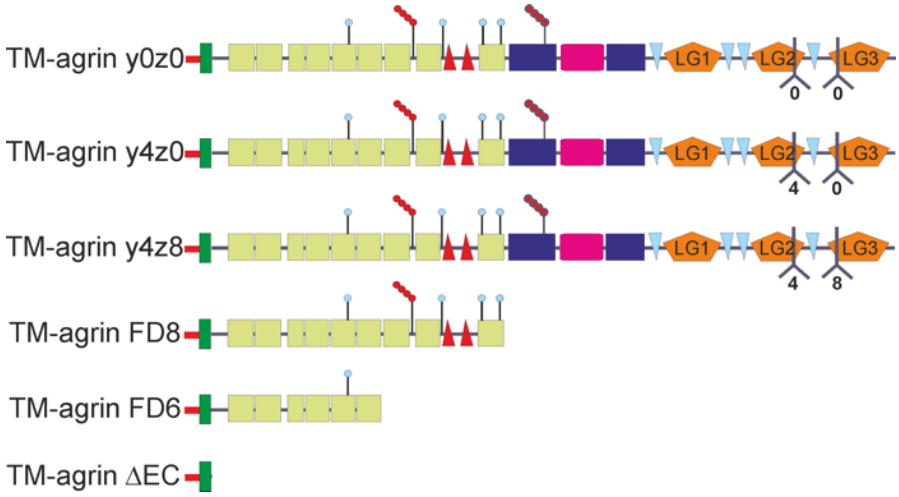

Figure 2. **Different constructs of TM-agrin used in this study.** TM-agrin-y4z8 is expressed mainly by the motoneurons. TM-agrin-y4z0 is the main isoform that is expressed by neurons in the CNS. TM-agrin-y0z0 is expressed by non-neuronal cells including glial cells. The FD8 construct lacks the C-terminal half of agrin, the FD6 construct lacks the C-terminus upstream of the 7th-follistatin-like domain and the ΔEC construct lacks the entire extracellular domain (adapted from Handara and Kröger (2019), submitted).

Methods

Breeding strategy

To investigate the effect of TM-agrin overexpression during the period of synaptic-plasticity, the TM-agrin knock-in line was cross-bred with CamKIIa-CreERT2 line. For breeding and maintenance of the colony, male CamKIIa-CreERT2 (homozygous)/TM-agrin KI (heterozygous) was bred with female CamKIIa-CreERT2 (WT)/TM-agrin KI (WT) mice.

DNA isolation from tails and genotyping

Adult mice were tailed 3 weeks after birth, whereas tails from embryos were dissected right before the cortical neuron preparation. The tails were lysed with the tail lysis buffer and Proteinase K in a shaker at 55oC overnight. After lysis, the DNA was purified using isopropanol. The purified DNA was genotyped by following the protocols (Table. 8). The CamKIIa-CreERT2 allele was analyzed with primer prAS116 and prAS118, whereas the TM-agrin knock-in allele was analyzed using primer prAS15 and prAS104. The WT allele for Rosa26 was analyzed using primer oiMR9020 and oiMR9021.

Table 8. Protocols for genotyping

Allele	Primers	Denaturation	Annealing	Elongation	Cycles	Note
TM-agrin knock-in	prAS15 prAS104	95$_o$C, 30s	55.1$_o$C, 60s	72$_o$C, 90s	40 cycles	DMSO; product size 1376 bp
CamKIIa-CreER$_{T2}$	prAS1162 prAS118	95$_o$C, 15s	62$_o$C, 45s	72$_o$C, 45s	35 cycles	Product size 375 bp
WT Rosa26 locus	oIMR9020 oIMR9021	1. 94$_o$C, 20s 2. 94$_o$C, 15s	1. 65$_o$C, 15s 2. 60$_o$C, 15s	1. 68$_o$C, 10s 2. 72$_o$C, 10s	1. 10 cycles (-0.5$_o$C / cycle) 2. 28 cycles	2 steps PCR, product size 297 bp
Lrp4$_{mitt}$	L4Hpfmf 43Br_FP	94$_o$C, 15 s	58$_o$C, 15 s	72$_o$C, 20 s	40 cycles	HpyCH4V digestion 37$_o$C overnight, mutant product 227bp, WT product 132bp + 69bp
MuSK-KO	Nsk1 Nsk2 Neo3	94$_o$C, 30 s	66$_o$C, 40 s	72$_o$C, 60 s	40 cycles	WT product 446bp, mutant product 300bp

Anesthesia and transcardial perfusion fixation

Mice were anesthetized by intraperitoneal injection of anesthesia solution, containing ketamine/xylazine cocktail (final concentration of ketamine is 10 mg/ml and of xylazine is 0.2 mg/ml in sterile normal saline). The injected volume was 0.1 ml per 10 g bodyweight. The withdrawal reflex was assessed by pinching the toe. The absence of the reflex indicates that the mice were well anesthetized and were eligible for the whole-body perfusion fixation procedure. To this end, the chest and abdominal cavities were opened to expose the heart and the liver. The needle was connected to a peristaltic pump and inserted into the left ventricle through the apical tip of the heart. The right atrium was then cut to let the blood flow out. Before the perfusion with the fixative, the blood in the vascular system was drained out and washed with cold 0.9% NaCl for 5 min or until the there was no blood coming out from the right atrium and the liver turned pale. After this washing step, the mice were perfused with cold 4% PFA for 10 min until the whole bodies appeared stiff. The indication of a successful perfusion was twitching of the tail and the heart appeared blanched. The brains were dissected and post-fixed by immersion in 4% PFA overnight at 4$_o$C. After post-fixation, the brains were washed with 1X PBS and then embedded in 4% agar dissolved in 1X PBS. The brain in agar was cut coronally freely floating with the thickness 40 μm using a vibratome (Leica, Wetzlar, Germany). The sections were stored in cryo-protectant solution (30 % glycerol, 30 % ethylene

glycol, in 0.05 M Na-Phosphate buffer, pH 7.4) at -20°C until processed for immunohistochemistry.

RNA extraction and quantitative reverse-transcription PCR

The RNA from the cortices was extracted two weeks after the induction of TM-agrin overexpression by tamoxifen administration. The mice were sacrificed by cervical dislocation. The brains were immediately extracted, and the cortices were dissected in cold PBS using the stereo binocular microscopy (Leica MZ6 with KL1500 LCD lamp. Schott AG, Mitterteich, Germany) and snap-frozen in liquid nitrogen.

Thirty mg of cortical tissue were ground with microtube-fitting pestles (Eppendorf micropestles, Sigma-Aldrich, Germany) on ice and the RNA was extracted using the SV Total RNA Isolation System kit (Promega, Mannheim, Germany) according to the protocol provided by the manufacturer. The RNA integrity was analyzed by denatured agarose gel electrophoresis using the intensity of the rRNA bands (28s rRNA band is twice as strong as the 18s rRNA band). The concentration and purity were assessed using a Nanodrop spectrophotometer (Thermo Fisher, Germany). The RNA was then reverse transcribed into cDNA using the Quantitect Reverse Transcription kit (Qiagen, Hilden, Germany).

Analysis of synapse-associated gene expression levels was performed using the cDNA. The oligonucleotides for this analysis were designed using the online Universal Probelibrary Assay Design Center (Table 6, Roche & Diagnostics). As the internal control (housekeeping gene), the Hypoxanthine-guanine-phosphoribosyltransferase (*HPRT)* gene was used.

Twenty microliters of reaction mixtures were added into each well of a 96-well plate and analyzed in a Light Cycler 480 (Roche Diagnostic, Unterhaching, Germany), using the Sybr green dye (SensiMix SYBR No-ROX Mastermix, Bioline, Luckenwalde, Germany). All genes were tested in technical triplicates. The specificity and efficiency of the reactions were analyzed with the melting curves assay. The specificity was indicated by a single peak in the melting curve and by a single band in the agarose gel analysis. The qPCR results were analyzed by double delta Ct (ΔΔCt-value) analysis.

Subcloning of mouse TM-agrin

The plasmid, pAS12, encoding full-length mouse TM-agrin-y4z0 was a kind gift from Dr. Anna Schick (LMU Munich). The full-length mouse NtA-agrin-y0z0 was a kind gift from Prof. Dr. Markus Ruegg (Biocenter, Basel, Switzerland). For generating the TM-agrin-y0z0, the plasmids were digested with SfiI and MfeI for 1 hour at 37°C, and the products were run in

1% agarose gel. The expected products were two bands, with the size of 12kb and 1kb. The smaller size bands were then swapped and mixed with the bigger size bands, and then ligated with the Quick Ligation™ kit (New England Biolabs, Frankfurt am Main, Germany). The ligation product was then used for bacterial transformation (Top10 Chemically Competent E. coli, Thermofisher Scientific). The transformed bacteria were inoculated into LB medium containing ampicillin and cultured overnight at 37^{o}C in the shaker at 150 rpm. After overnight incubation, a mini-prep was performed, and the plasmid was sequenced using the corresponding primers (Table 6).

The mouse TM-agrin-y4z8 isoform, serine-to-alanine TM-agrin-y4z0 and serine-to-aspartic acid TM-agrin-y4z0 were obtained by site-directed mutagenesis, outsourced to Genscript (New Jersey, USA). All final products of the cloning procedures were sequenced (GATC Biotech, Konstanz, Germany) to verify the sequence and to detect the mutations.

Brain tissue lysis and quantitative western blot analysis

For the preparation of adult mouse brain lysate, mice were sacrificed by cervical dislocation and the cortices were immediately dissected in cold 1X PBS and then snap-frozen in liquid nitrogen under a stereo microscope (Leica MZ6 with KL1500 LCD lamp, Schott). The tissue was gently homogenized in 10 w/v lysis buffer on ice using a glass pestle tissue grinder. After homogenization, lysates were centrifuged at 2500 x g for 30 min at 4^{o}C. The supernatant (S1-fraction) was collected and centrifuged at 34.000 x g for 30 min at 4^{o}C. The supernatant from the previous centrifugation was termed the S2-fraction. The S2-fraction was then denatured by adding 4X SDS sample buffer and heated at 95^{o}C for 3 min. The pellet of the second centrifugation (crude membrane fraction/M-fraction) was denatured by adding 4X SDS sample buffer with 8 M urea, and then heated at 37^{o}C for 10 min.

The proteins from the M-fractions were separated on 10% polyacrylamide gels by electrophoresis. The protein samples and a protein ladder (PageRuler prestained protein ladder, Thermo Scientific) were separated in running buffer at constant 80V and were transferred to nitrocellulose membranes (Protran, Schleicher & Schuell, Germany) at constant 140mA for 2h. The membranes were then incubated in blocking buffer (TBS Odyssey blocking buffer, Li-Cor, Germany) for 1h at RT. After blocking, the membranes were incubated with primary antibodies in 5% horse serum TBS-T for 3h at RT. The membranes were then washed three times 10min each in TBS-T and incubated with the secondary antibodies for 1h. After the last incubation, the membranes were washed three times for 10min. Tau protein was used as loading control.

Images from the WB membrane were obtained using the near-infrared fluorescent Odyssey Imaging system (Li-Cor, Bad Homburg, Germany), with the Image Studio Lite software (version 4.0). The analysis of the western blots was carried out by quantifying the pixel density of each bands using the Fiji Software (Schindelin et al., 2012). The pixel density of the protein of interests was subject to background subtraction and was normalized to the pixel density of tau protein as the loading control.

Coverslips preparation and coating

Round glass coverslips of 18 mm diameter were treated with solution containing 4 pellets of NaOH in 10 ml Milli-Q water and 35 ml of ethanol 70 % overnight on a shaker. The coverslips were then extensively washed with Milli-Q water and incubated with a solution containing 1 M HCl overnight on a shaker. The next day, the coverslips were washed with water and stored in absolute ethanol at $4^{o}C$ or processed for the dry heat sterilization ($160^{o}C$ for 2 hours) in the oven. One day before the cell culture preparation, the coverslips were coated with poly-D-lysine (PDL) working solution overnight, then washed with sterile water and dried under the laminar flow hood.

Transfection of monolayer cultures

Primary neuronal culture of E15 cortices from wildtype, Lrp4-KO and MuSK-KO were prepared by trypsinization and trituration with fire-polished Pasteur pipettes in dissecting medium under sterile condition (Handara et al., 2019; Karakatsani et al., 2017). The density of the dissociated cells was determined with trypan blue using a Neubauer chamber. The cells were seeded at a density of 100.000 cells per well (12-well plate, growth area 3.8 cm^2/well) in 1.5 mL maintenance medium and maintained for 14 days *in vitro*. The maintenance medium was changed on DIV 7 by replacing half of the old with fresh maintenance medium.

Cells were transfected on DIV 12 with Lipofectamine 2000 (Invitrogen, Karlsruhe, Germany) and incubated for two additional days before the fixation. For each well, two solutions for the transfection were prepared. The first solution contained 500 ng of plasmid DNA in 50 µl of neurobasal medium and the second solution contained 0.5 µl Lipofectamine in 50 µl of neurobasal medium. Both solutions were incubated for 5 min after mixing and then added to the well.

Immunocytochemistry

For routine staining, coverslips were washed once with warm PBS and then fixed with 4 % PFA in PBS for 10 min at RT. For the analysis of the NR1-subunit of the NMDA receptor, the coverslips were fixed with -20 ^{o}C methanol for 10 min. Fixation was blocked with ICC blocking solution for 60 min at RT. The coverslips were incubated with the primary antibodies in blocking solution at 4^{o}C overnight. On the next day, they were washed three times with 1X PBS and then incubated at 4^{o}C with the secondary antibodies in the blocking solution for 2 hours. The coverslips were counter-stained with 0.1 µg/ml DAPI in 1X PBS for 10 min at RT. The coverslips were then mounted onto glass slides using Aqua-Poly/Mount (Polysciences, Hirschberg, Germany). All incubation steps were performed on a rotating shaker.

Immunohistochemistry of freely floating fixed tissue sections

For the immunohistochemistry (IHC) of synaptic proteins, fixed freely floating brain sections were washed with 1X PBS. To unmask the antigens due to the methylene bridge generated by the PFA fixation, the antigenic epitopes were retrieved by heating the tissue at 85^{o}C with 10 mM sodium citrate buffer for 15 min. The sections were blocked with IHC blocking solution for 1 hour at RT and then incubated with primary antibodies in IHC staining solution for 48 hours at 4^{o}C. Thereafter, the sections were incubated with the secondary antibodies in the IHC staining solution for 1 hour at RT. Finally, they were mounted on glass slide in Fluoroshield™ mounting medium containing DAPI (Sigma-Aldrich, Taufkirchen. Germany).

Image acquisition

Images of monolayer cultures were obtained with an Axio ImagerM2 epiflourescence microscope (Carl Zeiss, Oberkochen, Germany). The images were acquired using the 40x water immersion objective. Images of fixed tissue sections were acquired using a Leica SP8X WLL upright confocal microscope (Leica, Wetzlar, Germany). Single confocal images from brain sections were obtained from cortical layer 2/3 in the region of the S1/S2 cortex. The images were acquired using an objective with the following specification HC PL APO 40x/1.30 oil CS2, working distance 0.24 mm. Images obtained with this objective lens were acquired with the digital zoom factor 3 x and a size of 1024 x 1024 pixel.

Quantitative analysis

The dendritic length of cortical neurons in μm was determined using the Fiji Simple Neurite Tracer plugin (Longair *et al.*, 2011). The number of primary dendrites emerging from the soma as well as the dendritic branch tip numbers were counted manually. Axons were excluded from the analysis. For analyses of the dendritic branching pattern, images were converted into 8-bit format and subjected to the thresholding for creating binary images. Sholl analysis was performed using the Sholl analysis plugin of the Fiji imaging program (Ferreira *et al.*, 2014).

Binary images were also analyzed for the synaptic puncta quantification. The synaptic puncta density was counted using the Analyze Particle toolbox of the Fiji software. The number of puncta labeled by antibodies against excitatory synapse-associated proteins per 20 μm was determined on dendrites outside a radius of 50 μm distance from the soma. In contrast, punctate immunoreactivity labeled by antibodies against inhibitory synapses-associated proteins per 20 μm was determined on dendrites within a radius of 50 μm from the soma (Klenowski et al., 2015).

Statistical analysis

Results are presented as mean +/- SEM. Unless stated otherwise, n represents the number of neurons or the number of brain sections analyzed and N represents the number of independent experiments, corresponding to the number of embryos/mice. With the assumption of normal distribution and homoscedasticity, significance was calculated with GraphPad Prism vs.8 (GraphPad Software, San Diego, California) using the unpaired t-test or the one-way ANOVA test with the Tukey's multiple comparison test. Data were evaluated for normal distribution using d'Agostino Pearson omnibus normality test and for homoscedasticity using Browne-Forsythe's test. Data that did not fulfil the assumption were investigated using the equivalent non-parametric tests, such as the Mann-Whitney rank sum test or the Kruskal-Wallis-test with Dunn's correction for multiple comparisons test. Outliers were analyzed by iterated Grubbs' test and were excluded. The results from qRT-PCR and WB were analyzed by the non-parametric test Mann-Whitney rank sum test. The type 1 statistical error was set to 5%, meaning that a p-value of < 0.05 was set as the level of statistical significance. 'n.s' was determined as $p > 0.05$, '*' as $p < 0.05$, '**' as $p < 0.01$ and '***' as $p < 0.001$.

Results

Generation and validation of the antiserum against TM-agrin

To investigate the selectivity and the specificity of the newly generated antiserum against the intracellular sequence of TM-agrin, I transiently transfected full-length mouse TM-agrin cDNA cloned into pMES vector under the cytomegalovirus (CMV) promoter into HEK293-T cells. The pMES vector contains an internal ribosome entry site (IRES) and the sequence coding for GFP to visualize the transfected cells. As a control, I used the empty pMES vector (control vector) encoding only the IRES-driven GFP. Two days after transfection, I confirmed the expression of TM-agrin using the antiserum in transfected cells. Only GFP-positive cells were stained with this antiserum, supporting the specificity of the antiserum for full-length mouse TM-agrin (Fig. 3A,B). Cells transfected with control vector were not stained, confirming the specificity of the antiserum for intracellular region of mouse TM-agrin. The antiserum was also tested in primary cortical neuron cultures, after transfection with plasmid containing full-length TM-agrin. I observed that the antiserum was specific against mouse TM-agrin, by reporting a strong signal in TM-agrin transfected neurons (Fig. 3C,D)

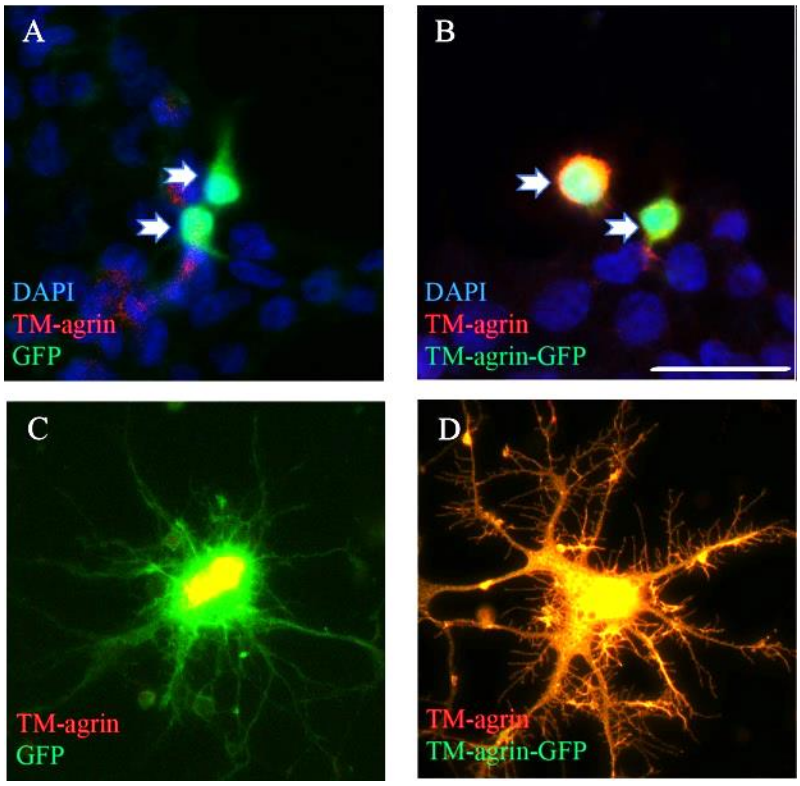

Figure 3. **Validation of the antiserum against TM-agrin**. HEK293 cells (A, B) or cortical neurons (C, D) were transfected with control (A, C) or full-length mouse TM-agrin (B, D). Arrows in A and B indicate transfected cells (GFP-positive cells, green). Only cells transfected with TM-agrin cDNA were stained by the antiserum against intracellular region of TM-agrin (red). Untransfected cells can be seen by the blue DAPI staining in A and B; scale bar 50 μm.

TM-agrin overexpression in cortical neurons increases the density of dendritic protrusions, but not the dendritic arborization

In primary cortical neuron culture, we recently reported an increase in the density of dendritic protrusions and complexity of dendritic arborization following overexpression of Lrp4 (Karakatsani et al., 2017). In order to investigate whether TM-agrin similarly affects the density of dendritic protrusions and of the dendritic arborization pattern, I transfected full-length TM-agrin-y4z8 into cultured cortical neurons and determined the number of primary dendrites (Fig. 4D) and the total dendritic branch tip number (TDBTN, Fig. 4E). I did not observe any differences in the number of primary dendrites and of the TDBTN between neurons transfected with the TM-agrin compared to neurons transfected with the control vector. However, TM-agrin overexpression increased the density of filopodia-like dendritic protrusions (Fig. 4F) similar to what has been previously reported (Annies et al., 2006; Porten et al., 2010). In addition, I observed a reduction in primary dendrite length in neurons transfected with TM-agrin compared to neurons transfected with the control vector (dashed line in Fig. 4B',C'; quantification in Fig. 4G). These results suggest a functional interaction between TM-agrin and Lrp4 during dendrite formation or maturation in embryonic cortical neurons *in vitro*. Moreover, my results are in line with the previously reported increase of dendritic complexity after Lrp4 overexpression (Karakatsani et al., 2017).

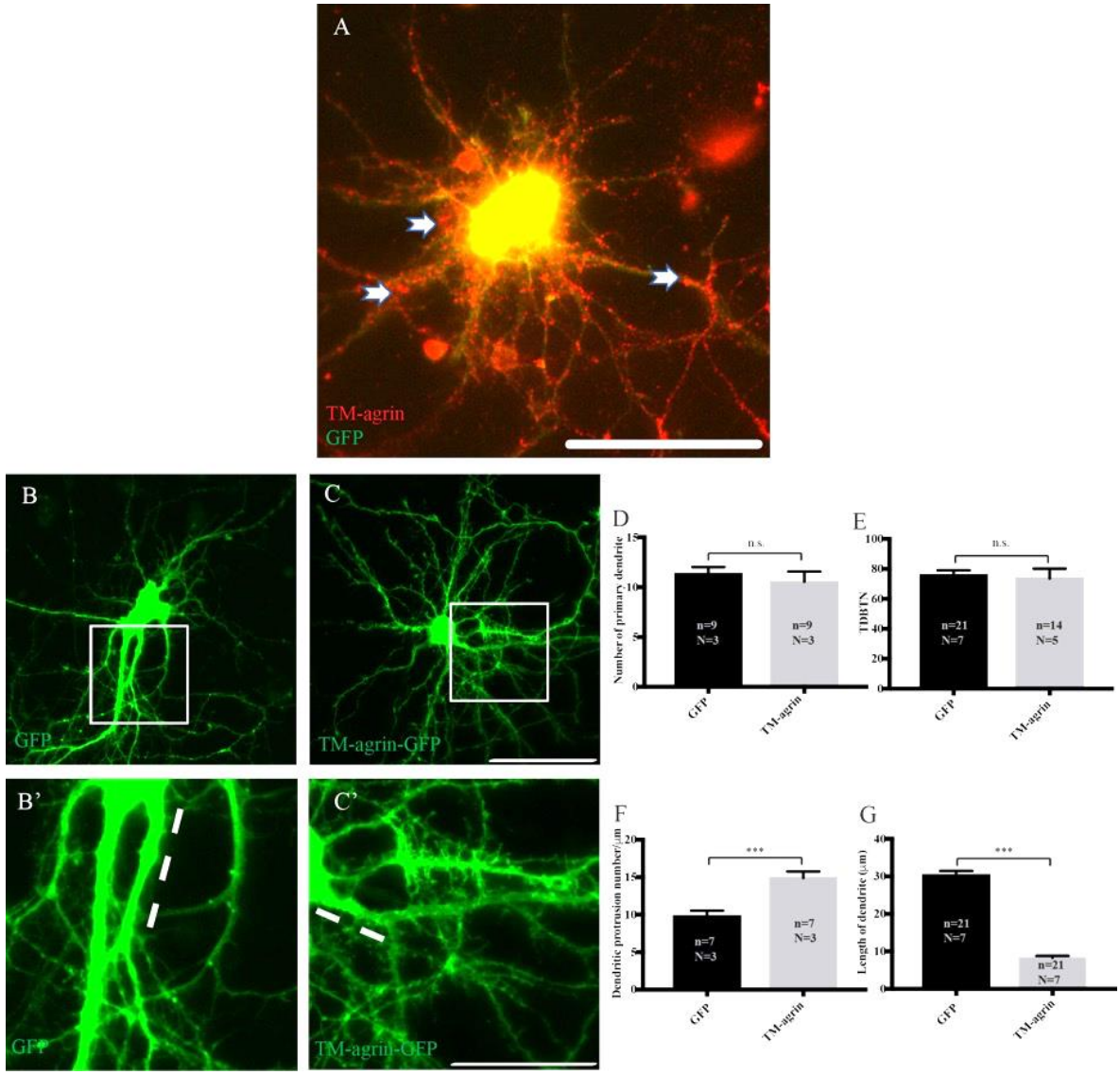

Figure 4. **TM-agrin overexpression in cortical neurons increases density of dendritic protrusions, but not dendritic arborization**. TM-agrin punctate staining (A) is widely distributed in the neuronal cell body and in neurites of transfected cortical neuron (white arrows). TM-agrin-y4z8 overexpression did not alter dendritic arborization complexity (B, C), number of primary dendrite (D) and TDBTN (E) but increased the density of dendritic protrusions (F) and shortened primary dendrites (dashed line in B', C' and in G for quantification). B' and C' are magnifications from selected region of interest in B and C; statistical analysis: unpaired t-test (D, E), Mann-Whitney test (C, D); scale bar 50 µm (A-C); scale bar 25 µm (B', C'). Note that the neuron in panel A is identical with the neuron in Fig. 3D.

Lrp4 is required for normal dendritic morphology

Neurons with a reduced level of Lrp4 upon miRNA transfection have a less complex dendritic arborization, reduced density of dendritic protrusions and longer primary dendrites (Karakatsani et al., 2017). To investigate if these changes were a microRNA-related artefact or directly caused by the reduced level of Lrp4 expression, I analyzed the dendritic morphology of cultured cortical neurons from Lrp4-KO embryos. No differences in neuronal density and neuronal composition in cultures from Lrp4-heterozygous embryos compared to cultures from Lrp4-KO embryos (Fig. 5A-E) were observed. However, Lrp4-KO neurons displayed a less

complex dendritic arborization compared to Lrp4-heterozygous neurons (Fig. 5F,G), including a significant reduction in the number of primary dendrites (Fig. 5J), TDBTN (Fig. 5K), dendritic protrusions density (Fig. 5L) and an increased length of the primary dendrite (Fig. 5M). These results show that knockdown of Lrp4 using miRNA and genetic ablation of Lrp4 expression have the same phenotype, demonstrating that the altered dendritic complexity is not a miRNA-related artefact.

In order to investigate the functional interaction between Lrp4 and TM-agrin during dendritic arborization, I transfected Lrp4-KO neurons with a full-length TM-agrin-y4z8. TM-agrin overexpression in Lrp4-KO neurons rescued all parameters considered in the analysis of dendritic complexity (Fig. 5J-M). Moreover, Sholl analysis (Fig. 5N), Schoenen ramification index (Fig. 5O) and maximal number of branching (Fig. 5P) confirmed the lower dendritic arborization complexity of Lrp4-KO neurons and the rescue by overexpressing TM-agrin. Congruently, TM-agrin overexpression restored dendritic arborization to a level comparable to that reported in Lrp4-heterozygous neurons (Fig. 5N–P). In summary, these results demonstrate that TM-agrin expression level controls normal dendritic arborization complexity and that this activity requires the expression of Lrp4.

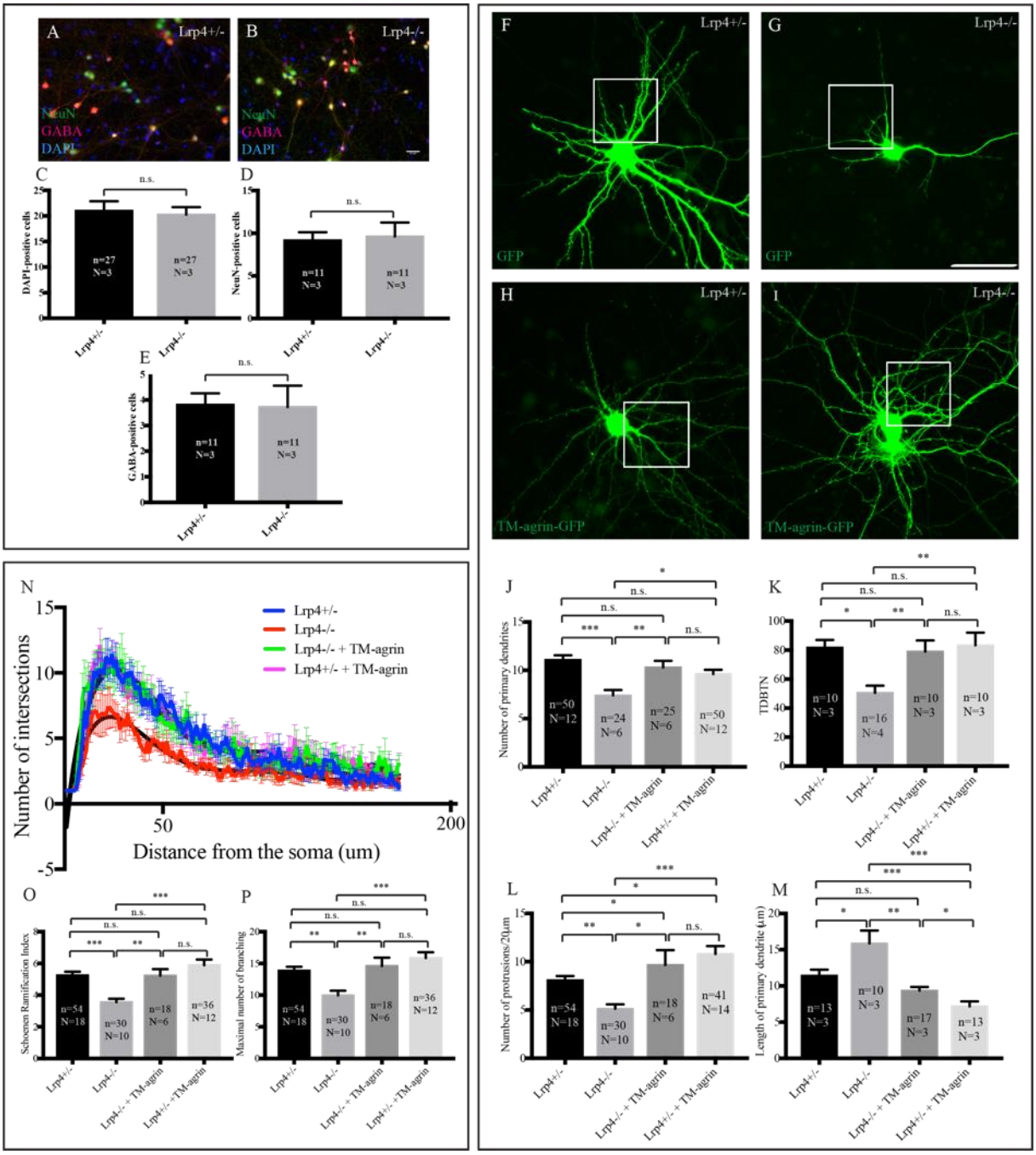

Figure 5. **Lrp4 is required for normal dendritic morphology**. (A-E) Cellular density, neuronal density and neuronal composition are comparable in Lrp4-heterozygous and in Lrp4-KO neuronal cultures. Viable cells density (DAPI-positive, blue, C), neuronal density (NeuN-positive, green, D) and neuronal composition (GABA-positive, red, E); statistical analysis: unpaired t-test; scale bar 25 µm (B). (F-M) Lrp4-KO neurons and TM-agrin overexpression in Lrp4-KO neurons affect the morphology of cortical neurons, which were indicated by number of primary dendrites (J), TDBTN (K), density of dendritic protrusions (L) and length of primary dendrite (M); statistical analysis: one-way ANOVA with Tukey's multiple comparison test (J, L); Kruskal-Wallis with Dunn's multiple comparisons test (K, M); scale bar 50 µm (G). (N-P) Less complex dendritic arborization in Lrp4-KO neurons is shown in Sholl plot (N), Schoenen Ramification Index (O) and maximal number of branching (P); statistical analysis: Kruskal-Wallis test with Dunn's multiple comparison test.

The C-terminal domain of TM-agrin is sufficient to rescue the complexity of dendritic arborization in Lrp4-KO neurons

Agrin is a large molecule and consists of several domains which could potentially interact with other proteins (Fig. 1). In order to determine which domain of agrin is required for the rescuing the dendritic arborization pattern in Lrp4-KO neurons, I transfected Lrp4-KO cortical neurons with different constructs of TM-agrin, including different full-length splice variants (TM-agrin-y4z0 and -y0z0) and a construct that lacks half of the C-terminal domain and is fused with GFP (FD8; Fig. 2 for details of the deletion constructs). Dendritic arborization in Lrp4-KO neurons was restored after transfection with full-length TM-agrin-y4z8 (Fig. 6A), TM-agrin-y4z0 (Fig. 6B) and TM-agrin-y0z0 (Fig. 6C), demonstrating that these splice variants contain the region necessary to restore dendritic arborization. In contrast, transfection with the FD8 construct lacking the C-terminal half of TM-agrin did not affect the dendritic arborization complexity of Lrp4-KO neurons (Fig. 6D). These observations were confirmed by quantification of the number of primary dendrites (Fig. 6E) and TDBTN (Fig. 6F) for each condition. In summary, the C-terminal half of TM-agrin was required for the establishment of the normal dendritic arborization pattern in Lrp4-KO neurons. However, a direct interaction between Lrp4 and TM-agrin was apparently not required, since isoforms which do not directly bind to Lrp4 (TM-agrin-y4z0, TM-agrin-y0z0) were as efficient as those, which directly interact with Lrp4 (TM-agrin-y4z8).

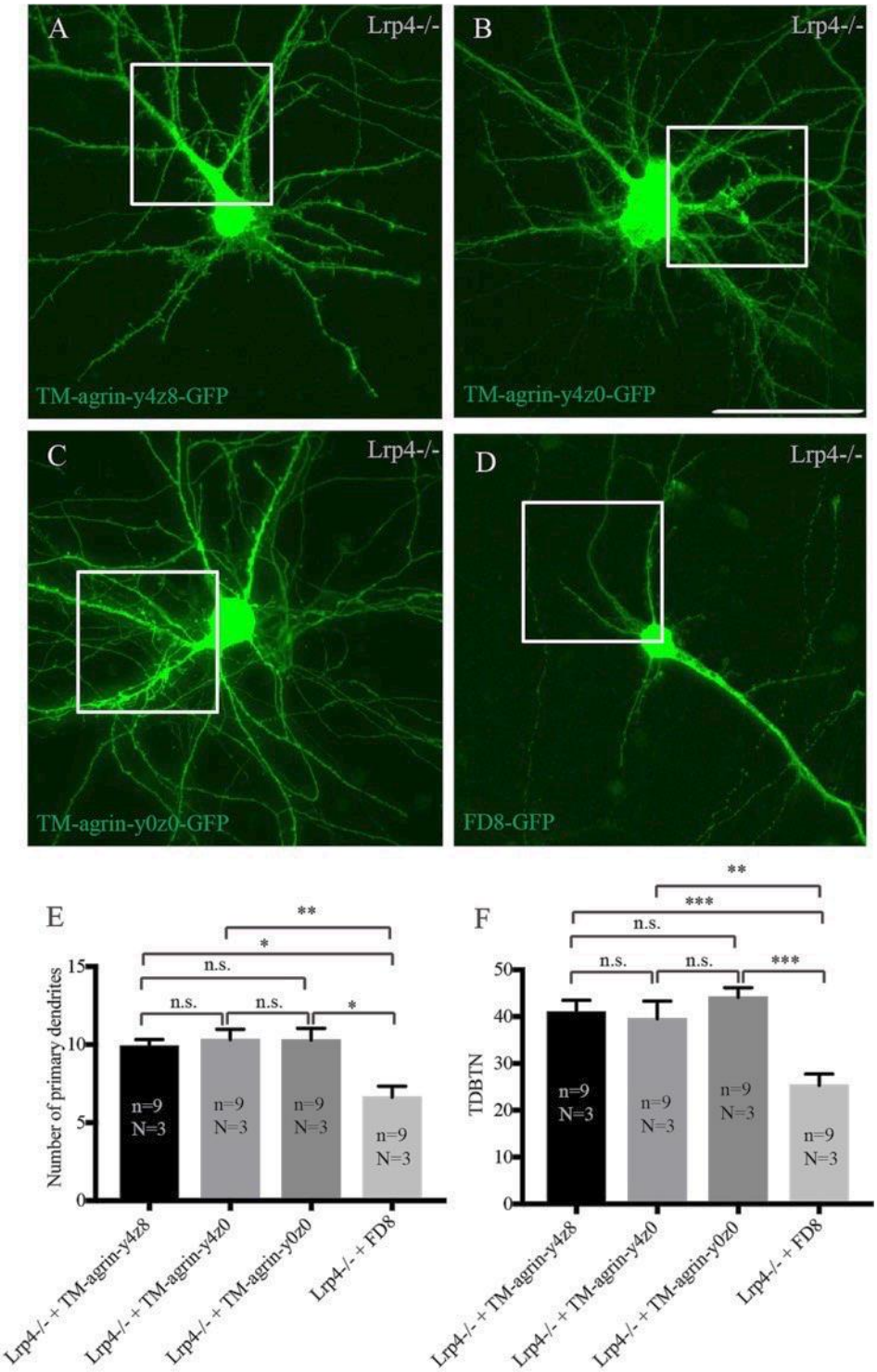

Figure 6. **The C-terminal half of TM-agrin is sufficient to rescue the complexity of dendritic arborization in Lrp4-KO cortical neurons**. (A-D) Transfection of Lrp4-KO neurons with TM-agrin-y4z8 (A), TM-agrin-y4z0 (B), TM-agrin-y0z0 (C), but not FD8 (D), restored dendritic arborization. Transfection of TM-agrin lacking half C-terminal could not restore number of primary dendrites (E) and TDBTN (F) in Lrp4-KO neurons; statistical analysis: Kruskal-Wallis with Dunn's multiple comparison test; scale bar 50 μm (B).

MuSK is required for normal dendritic morphology

At the developing NMJ, agrin requires MuSK for inducing the formation of synaptic specializations. Since MuSK is expressed in the CNS (Garcia-Osta et al., 2006), I investigated whether MuSK is required for normal dendritic arborization. To this end, I analyzed cultures of cortical neurons from MuSK-KO embryos and compared to the cultures from MuSK-heterozygous neurons. I observed no significant differences in cellular density, neuronal density and neuronal composition between MuSK-heterozygous and MuSK-KO cortical neuron cultures (Fig. 7A–E). Similar to Lrp4-KO neurons, MuSK-KO neurons displayed a less complex dendritic arborization pattern (Fig. 7G) compared to MuSK-heterozygous neurons (Fig. 7F). MuSK-KO neurons had fewer primary dendrites (Fig. 7J), a lower TDBTN value (Fig. 7K), a lower density of dendritic protrusions (Fig. 7L) and longer primary dendrites (Fig. 7M). The reduced dendritic arborization complexity in MuSK-KO neurons is reflected in the Sholl plot (Fig. 7N). Collectively my results suggest that, in addition to Lrp4 and TM-agrin, MuSK is also required for the establishment of the normal dendritic arborization, normal density of dendritic branches and normal length of primary dendrites.

Interestingly, TM-agrin overexpression in MuSK-heterozygous neurons and in MuSK-KO neurons (Fig. 7H,I) did not alter the dendritic morphology. However, TM-agrin overexpression increased the density of dendritic protrusions in neurons from both conditions. This demonstrates that the TM-agrin-mediated effect on dendritic protrusion density was not dependent on MuSK expression (Fig. 7L). In conclusion, TM-agrin overexpression in MuSK-KO neurons had no effect on dendritic arborization and on dendritic length, but it rescued the decreased dendritic protrusion density of neurons from MuSK-deficient neurons. This result stands in favor of an agrin-MuSK interaction-independent mechanism in controlling dendritic protrusion density.

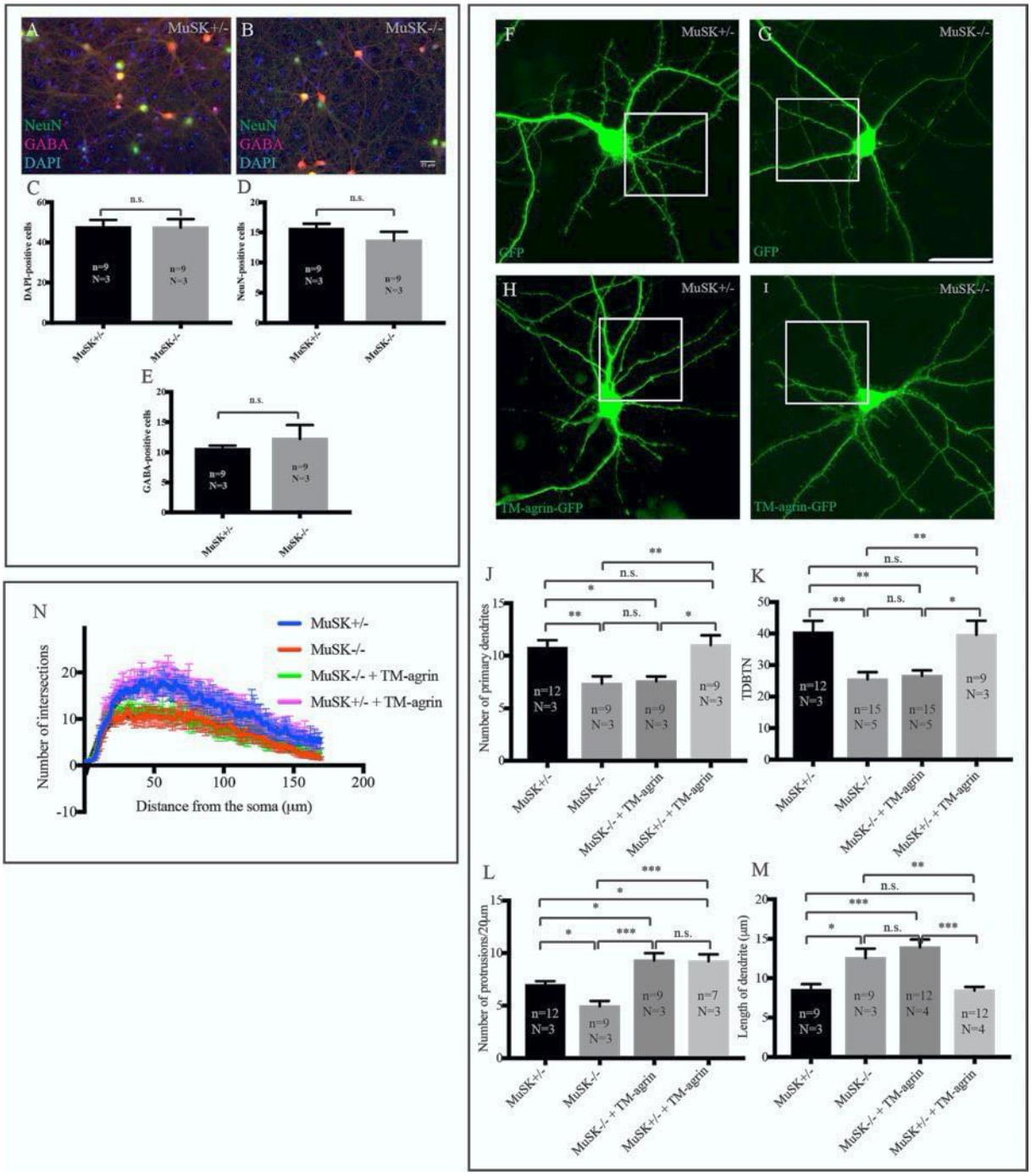

Figure 7. **MuSK is required for normal dendritic morphology**. (A-E) Cellular density, neuronal density and neuronal composition are comparable in MuSK-heterozygous (A) and MuSK-KO (B) cortical neuronal culture. Viable cells (DAPI-positive cells, blue, C), neuronal density (NeuN-positive cells, green, D) and neuronal composition (GABA-positive cells, red, E); statistical analysis: unpaired t-test; scale bar 25 µm (B). (F-N) The absence of MuSK in neurons affects the complexity of dendritic arborization and TM-agrin overexpression did not affect dendritic arborization in MuSK-heterozygous and MuSK-KO neurons, as had been indicated by number of primary dendrites (J), TDBTN (K) and length of primary dendrite (M). TM-agrin overexpression increased the density of dendritic filopodia in MuSK-heterozygous and MuSK-KO neurons. Sholl plot (N) showed the less complex dendritic arborization in MuSK-KO neurons; statistical analysis: Kruskal-Wallis test; scale bar 50 µm (G).

Overexpression of TM-agrin in cortical neurons increases excitatory synapses

The colocalization of TM-agrin with the post-synaptic density protein PSD-95 *in vitro* (McCroskery et al., 2009) and *in vivo* (Ksiazek et al., 2007) suggested the possibility that TM-agrin might be required to aggregate excitatory synapse-associated proteins. To address this question, I overexpressed TM-agrin-y4z8 in cortical neurons and analyzed the density of puncta containing the presynaptic vesicular glutamate transporter-1 (vGlut1) and of several postsynaptic proteins, including PSD-95 and the NR1-subunit of the NMDA receptor (NR1). I observed an increased density of vGlut1 (Fig. 8B,C), PSD-95 (Fig. 8E,F) and NR1 puncta (data not shown) on the dendritic segments at least 50 μm away from the cell bodies in TM-agrin-overexpressing neurons, compared to neurons transfected with the control vector (Fig. 8A,D). These results show that TM-agrin overexpression has the complementary effect to agrin deficiency: the former increased the density of excitatory synapses whereas the latter decreased it.

To investigate if agrin influences the formation of functional synapse, electrophysiological experiments were performed together with our collaborators, Dr. Hetsch and Prof. Rathjen from the MDC Berlin. Whole cell voltage clamp recordings were obtained from cortical neurons in a microisland culture system in the presence or absence of soluble agrin-y4z8. This microisland culture system is useful to investigate the basic mechanism of synaptic transmission and at the same time avoids neuronal network activity. Furthermore, the incubation of neurons with the soluble agrin-y4z8 isoform is a feasible approach since it is difficult to transfect a single neuron in a microisland culture system. Analysis of the spike traces (Fig. 8G) showed an increase in the frequency (Fig. 8H) and the amplitude (Fig. 8I) of miniature excitatory postsynaptic currents (mEPSCs). The increase in the number of dendritic pre- and postsynaptic specializations together with the electrophysiological data strongly suggest a role for TM-agrin in the formation and/or maintenance of pre- and postsynaptic specializations of excitatory synapses. It also suggests that the puncta observed on dendrites of cortical neurons after staining with antibodies against excitatory synapse-associated proteins, represent functional synapses.

To investigate if TM-agrin splice variants differ in their ability to increase the density of dendritic excitatory synapses, I transfected cortical neurons with cDNA constructs coding for different TM-agrin splice variants and analyzed the dendritic PSD-95 puncta density. As detailed above, transfection with TM-agrin-y4z0 cDNA significantly increased the density of PSD-95 puncta (Fig. 8N). In contrast, transfection of neurons with TM-agrin-y0z0 did not affect the density of PSD-95 compared to the neurons transfected with the empty vector. Thus, the

presence of the four amino acids at the y-splice site (y4) appeared to be critical for the increase puncta density of PSD-95 (Fig. 8N) and NR1 (Fig. 8O). Interestingly, the presence of eight amino acids at the z-splice site was not required for this increase (Fig. 8M-O). This supports the hypothesis that TM-agrin splice variant y4 controls excitatory synapses density, independent of the z splice variant and, therefore, independent of a direct binding to Lrp4.

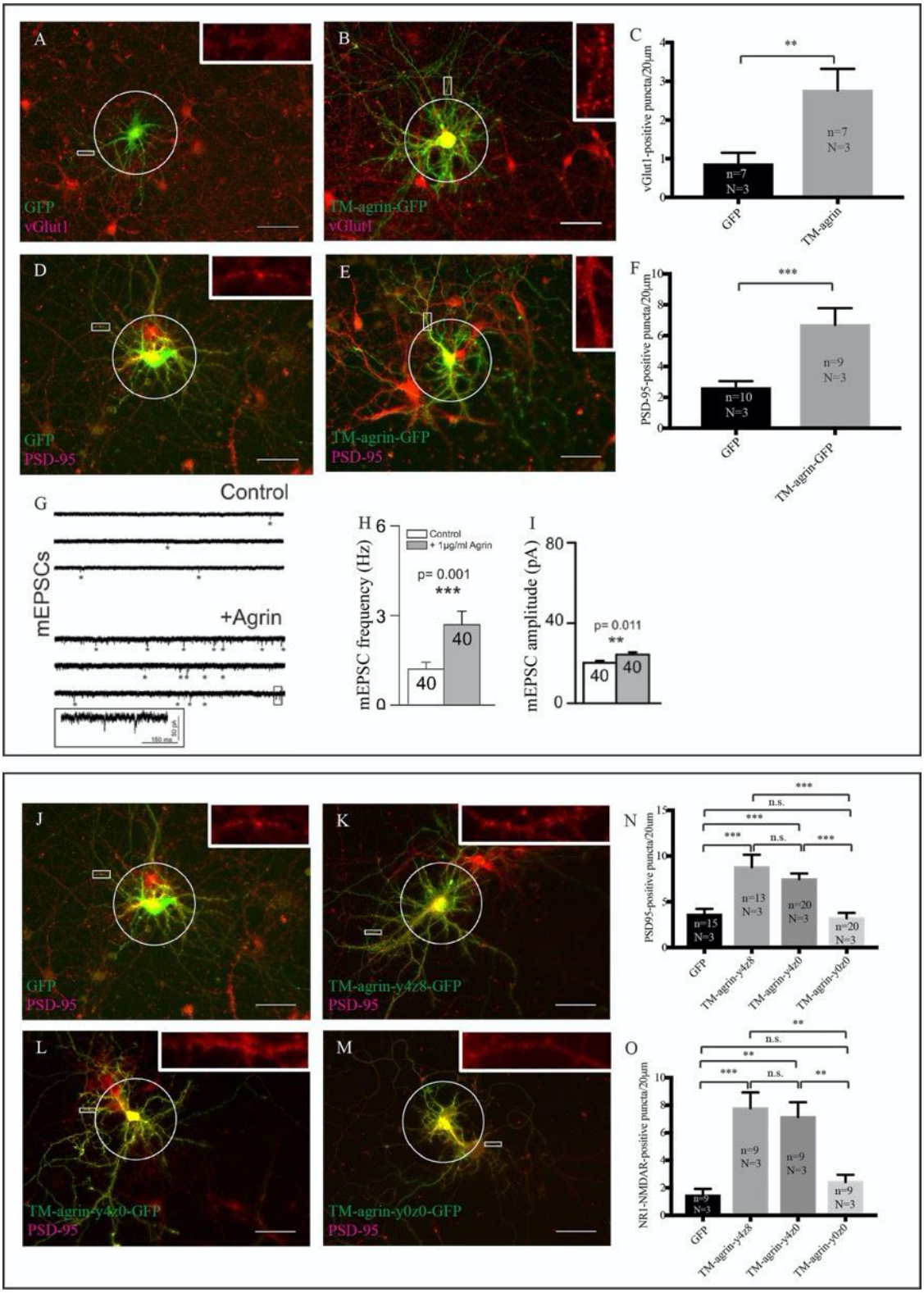

Figure 8. **TM-agrin overexpression affects the number of excitatory synapses and mEPSCs.** (A-F) TM-agrin overexpression increases the density of vGlut1 (A-C) and PSD-95 (D-F)); statistical analysis: Mann-Whitney test (C, F, H, I); scale bar 50 μm. (G-I) Soluble agrin incubation on cortical neurons in a microisland culture system increases the frequency (H) and amplitude (I) of miniature excitatory postsynaptic currents (mEPSCs), the mEPSCs were recorded at a holding potential -70 mV in the presence of tetrodotoxin (TTX). The number in the bars in (H) indicates the number of analyzed neurons. (J-O) Transfection of TM-agrin-y4z8 (K) and TM-agrin-y4z0 (L), but not of TM-agrin-y0z0 (M) increased PSD-95 (N) and NR1 (O) puncta density; statistical analysis: Kruskal-Wallis test with Dunn's multiple comparison test (N, O); scale bar 50 μm.

Lrp4, not MuSK, controls excitatory synapses density without direct but *in cis* interaction with TM-agrin

Since transfection of TM-agrin isoforms that did not directly interact with Lrp4 increased the density of dendritic excitatory synapses, I wanted to investigate whether Lrp4 expression was required for the formation of excitatory synapses. To this end, I analyzed PSD-95 puncta density in neurons from Lrp4-KO and Lrp4-heterozygous embryos. Interestingly, Lrp4-KO neurons had a lower PSD-95 puncta density compared to Lrp4-heterozygous neurons (Fig. 9A–E), suggesting that Lrp4 expression is required for the establishment of the normal excitatory synapse density. Moreover, TM-agrin overexpression in Lrp4-KO neurons failed to increase the density of PSD-95 puncta (Fig. 9D,E), on the other hand, it increased the PSD-95 puncta density in Lrp4-heterozygous neurons. This demonstrates that the expression of Lrp4 is required for the TM-agrin overexpression-mediated increase of the puncta density containing PSD-95.

Analysis of voltage clamp experiments (in collaboration with Dr. Hetsch and Prof. Rathjen) showed that incubation of Lrp4-KO neurons with the soluble agrin-y4z8 did not exert any effect on the mEPSCs frequency (Fig. 9G) and amplitude (Fig. 9H). In contrast, addition of soluble purified agrin-y4z8 to the WT neurons increased the mEPSCs frequency and amplitude (Fig. 8G–I). These results demonstrate that Lrp4 expression is necessary for the development/maintenance of the normal density and function of excitatory synapses. Since the increase of the number of excitatory synapses after transfection of TM-agrin was achievable with the isoform that did not directly interact with Lrp4, it must be considered that TM-agrin might need to interact indirectly via an additional binding partner with Lrp4 in order to exert its effect on excitatory synapses density.

In order to understand if this effect of TM-agrin was occurring in *cis* (i.e. in the same cell) or in *trans* (i.e. by an interaction between two cells), I overexpressed TM-agrin and at the same time knockdown Lrp4 (Lrp4-KD) by microRNA (miRNA-Lrp4) in the same WT cortical neuron (Fig. 9I–K). Lrp4-knockdown alone significantly reduced PSD-95 puncta density (Fig. 9K) similarly to the level observed in Lrp4-KO neurons (Fig. 9E; see also Karakatsani et al.,

2017). Co-transfection of TM-agrin and miRNA-Lrp4 could not increase the PSD-95 puncta density compared to neurons transfected with TM-agrin and miRNA-scrambled, suggesting that Lrp4 expression in the same neuron was essential for the TM-agrin-mediated effect on the increased density of excitatory synapses. Therefore, a *cis*-interaction between TM-agrin and Lrp4 is likely to be necessary for the increase of excitatory synapses after TM-agrin overexpression.

To investigate if MuSK is required for the formation of excitatory synapse-associated specializations, I analyzed the density of puncta containing PSD-95 in MuSK-KO neurons. MuSK-KO neurons displayed no significant changes in the density of PSD-95 puncta compared to MuSK-heterozygous neurons (Fig. 9L–P). Consistently, the overexpression of TM-agrin in MuSK-heterozygous (Fig. 9N) and MuSK-KO neurons (Fig. 9O) increased the density of PSD-95 puncta (Fig. 9P), similarly to the effect of TM-agrin overexpression in WT neurons. This demonstrates that MuSK expression is apparently not required for the formation or maintenance of excitatory synapses or for the TM-agrin-mediated increase in the excitatory synapse density.

In conclusion, while MuSK expression does not seem to be required for TM-agrin-mediated formation/maintenance of excitatory synapses, Lrp4, on the other hand, is required and might indirectly interact with TM-agrin to regulate the density of dendritic excitatory synapses.

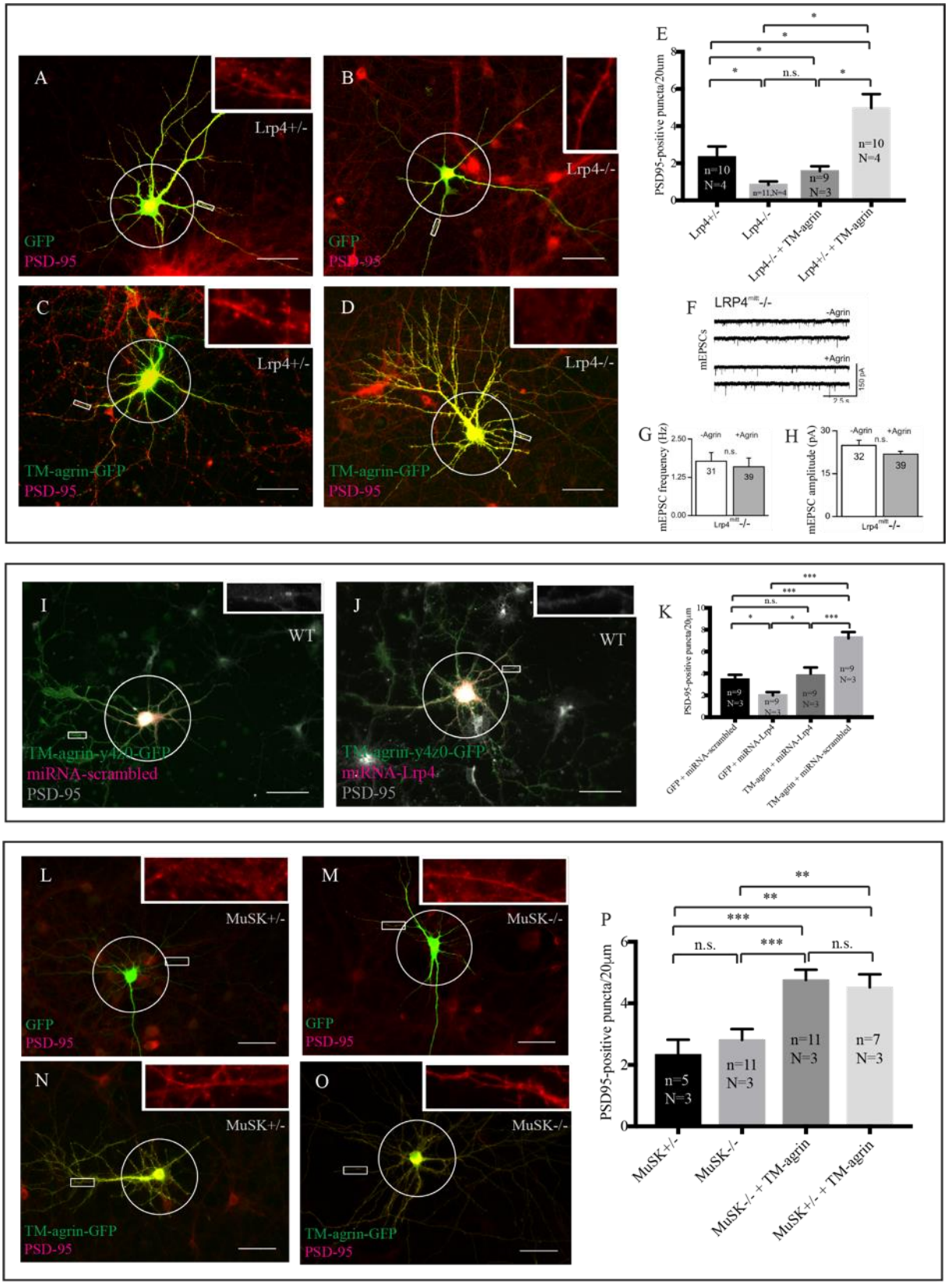

Figure 9. **Lrp4, not MuSK, controls excitatory synapses density with a non-direct *cis*-interaction with TM-agrin.** (A-H) Lrp4-KO neurons (B) showed a reduced PSD-95 puncta density compared to Lrp4-heterozygous neurons (A). TM-agrin overexpression increased PSD-95 puncta density only in Lrp4-heterozygous neurons (C), but not Lrp4-KO neurons (D). Agrin incubation on Lrp4-KO neurons did not change the trace of mEPSCs (F) as analyzed in mEPSCs frequency (G) and amplitude (H, during recording, the voltage was holded at -70 mV, number in the bar indicates number of analyzed neurons, collaboration with Dr. Hetsch and Prof. Rathjen); statistical analysis for E: Kruskal-Wallis test with Dunn's test for multiple comparison (omnibus test), Lrp4-heterozygous

vs Lrp4-KO was tested with unpaired t-test. (I-K) WT neurons with miRNA-Lrp4 knockdown showed reduced PSD-95 puncta density. TM-agrin overexpression increased the PSD-95 puncta density when co-transfected with miRNA-scrambled (I) but not when co-transfected with miRNA-Lrp4 (J, K); statistical analysis: Kruskal-Wallis test with Dunn's test for multiple comparison. (L-P) No difference in the density of PSD-95 puncta density between MuSK-heterozygous neurons (L) compared to MuSK-KO neurons (M). TM-agrin overexpression in MuSK-heterozygous (N) and in MuSK-KO neurons (O) increased PSD-95 puncta density; statistical analysis: Kruskal-Wallis test with Dunn's test for multiple comparison; scale bar 50 μm.

APP is a candidate for the agrin/Lrp4-dependent effect on excitatory synapses

The results reported above led to the conclusion that Lrp4 expression is necessary for the formation of a normal density of excitatory synapse-like specializations and required for the TM-agrin-mediated effect on excitatory synapses. Since agrin splice variants that do not bind to Lrp4, i.e. without an eight, eleven or nineteen amino acid insert at the z-site, increased the density of excitatory synapses, I hypothesized that an indirect interaction between both proteins via a third protein might be required for the Lrp4-dependent TM-agrin-mediated effect. A well-characterized partner of both Lrp4 and agrin at the NMJ is the amyloid precursor protein (APP; Choi et al., 2013). To investigate whether APP is affected by TM-agrin overexpression in cortical neurons, I analyzed APP puncta density in WT neurons following TM-agrin overexpression. Interestingly, TM-agrin overexpression significantly increased APP puncta density (Fig. 10E), but only when a cDNA coding for TM-agrin-y4 was transfected (Fig. 10B,C). This result is very preliminary, but it supports a potential interplay of APP in the agrin/Lrp4-dependent effect on excitatory synapses formation or maintenance. Clearly, more refined experiments are required to substantiate this hypothesis.

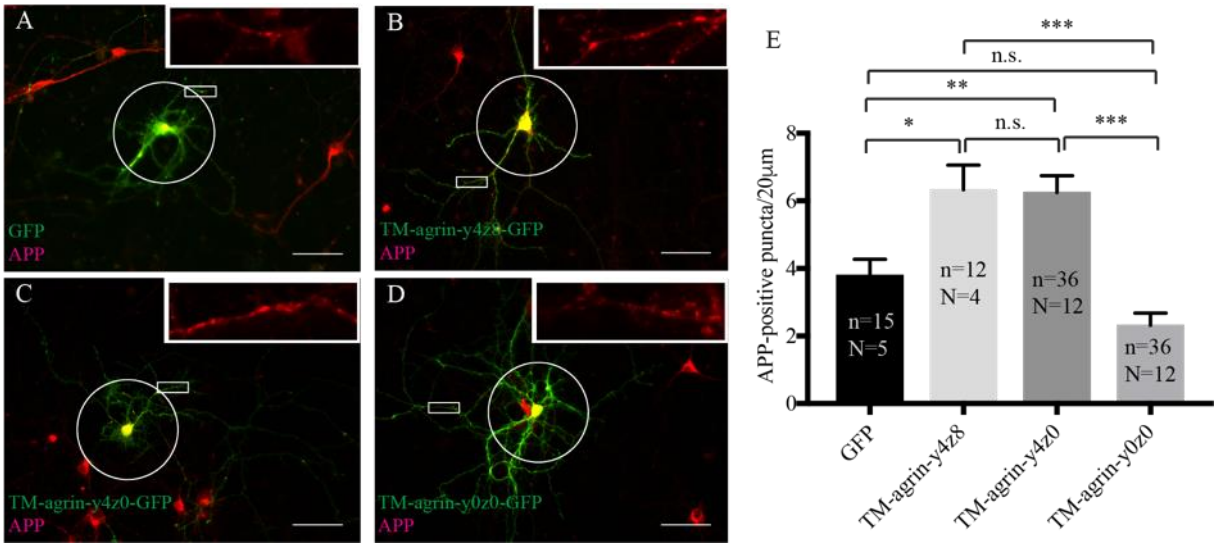

Figure 10. **APP is a candidate-binding partner of agrin and Lrp4 in controlling excitatory synapses**. APP puncta density was increased after TM-agrin-y4z8 (B) and TM-agrin-y4z0 overexpression. TM-agrin-y0z0 overexpression had no effect on the APP puncta density (D, E); statistical analysis: one-way ANOVA with Dunn's multiple comparison test; scale bar 50 μm.

TM-agrin controls the density of inhibitory synapses

In order to assess whether TM-agrin overexpression also affects the density of inhibitory synapses, I analyzed the effect of TM-agrin overexpression on the distribution of several inhibitory synapse-associated proteins. Transfection of WT neurons with the full-length TM-agrin-y4z8 cDNA decreased the density of puncta containing the presynaptic vesicular GABA transporter (vGAT; Fig. 11A–C), as well as of the postsynaptic protein collybistin (Fig. 11D,E), the α1-subunit of the $GABA_A$ receptor (Fig. 11G-I), gephyrin (Fig. 11M) and neuroligin-2 (Fig. 11N). Interestingly, no difference was observed in the density of puncta containing the non-synaptic α5-subunit of the $GABA_A$ receptor (Fig. 11J–L), demonstrating that the effect of TM-agrin was specific to the synaptic GABAergic receptors and its associated scaffolding proteins. These results stand in favor of TM-agrin being able to control inhibitory synapse density. Moreover, TM-agrin appears to affect excitatory and inhibitory synapses in opposite ways, i.e. TM-agrin overexpression increased the density of excitatory synapses and decreased the density of inhibitory synapses.

To investigate if TM-agrin overexpression affects the density of a synaptic marker that is located in both types of synapses (excitatory and inhibitory synapses), I analyzed the effect of TM-agrin overexpression on the density of immunoreactive puncta containing the pan-synaptic marker bassoon. I observed that TM-agrin overexpression did not alter the density of bassoon puncta (Fig. 11O-Q). This result congruently supports my previous observations that the TM-agrin overexpression regulated the density of excitatory and inhibitory synapses in the opposite directions.

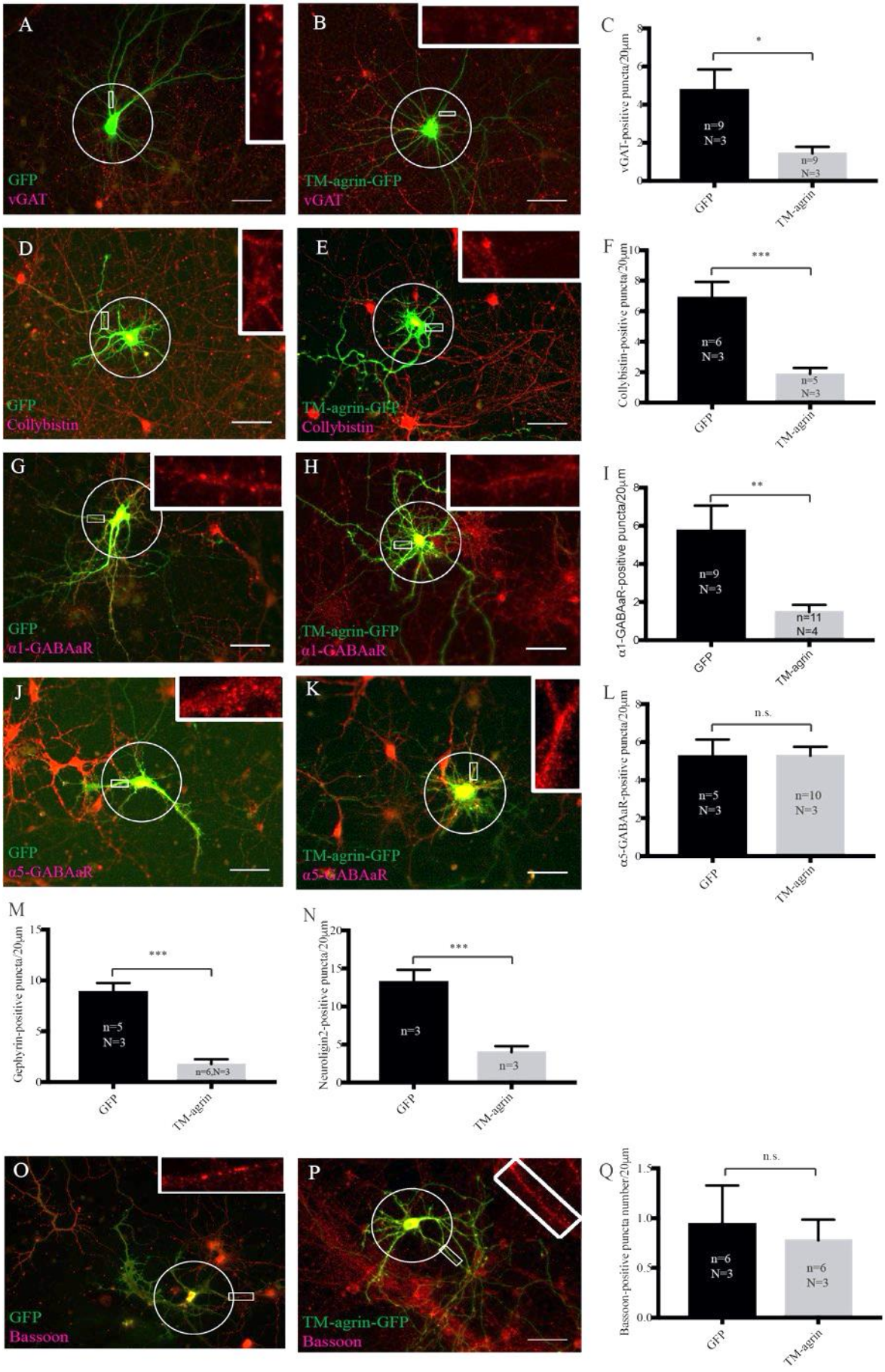
A
GFP
vGAT
B
TM-agrin-GFP
vGAT
C
vGAT-positive puncta/20μm
*
n=9
N=3
n=9
N=3
GFP
TM-agrin
D
GFP
Collybistin
E
TM-agrin-GFP
Collybistin
F
Collybistin-positive puncta/20μm
***
n=6
N=3
n=5
N=3
GFP
TM-agrin
G
GFP
α1-GABAaR
H
TM-agrin-GFP
α1-GABAaR
I
α1-GABAaR-positive puncta/20μm
**
n=9
N=3
n=11
N=4
GFP
TM-agrin
J
GFP
α5-GABAaR
K
TM-agrin-GFP
α5-GABAaR
L
α5-GABAaR-positive puncta/20μm
n.s.
n=5
N=3
n=10
N=3
GFP
TM-agrin
M
Gephyrin-positive puncta/20μm
***
n=5
N=3
n=6,N=3
GFP
TM-agrin
N
Neuroligin2-positive puncta/20μm
***
n=3
n=3
GFP
TM-agrin
O
GFP
Bassoon
P
TM-agrin-GFP
Bassoon
Q
Bassoon-positive puncta number/20μm
n.s.
n=6
N=3
n=6
N=3
GFP
TM-agrin

Figure 11. **TM-agrin controls the density of inhibitory synapses.** TM-agrin overexpression decreased presynaptic inhibitory protein vGAT (A, B, C), postsynaptic inhibitory proteins, collybistin (D, E, F), the α1-subunit of the $GABA_AR$ (G, H, I), but not the α5-subunit of the $GABA_AR$ (J, K, L). Gephyrin (M) and neuroligin-2 (N) puncta densities were also reduced after TM-agrin overexpression; statistical analysis: Mann-Whitney test (F, I), unpaired t-test (C, L, M, N); scale bar 50 μm. (O-Q) TM-agrin overexpression did not change the density of pan-synaptic marker bassoon; statistical analysis: Mann-Whitney test (Q); scale bar 50 μm.

The extracellular region of TM-agrin is not required for the TM-agrin overexpression-mediated decrease in inhibitory synapses

The increase of excitatory synapses after TM-agrin overexpression is regulated by the extracellular region of TM-agrin, specifically by the presence of four amino acids at the y-splice site, whereas the presence of eight amino acids at the z-splice site does not appear to be essential. To investigate if the different splice variants of TM-agrin differentially affect inhibitory synapses, I analyzed the effect of several splice variants of TM-agrin on gephyrin puncta density. Following overexpression of TM-agrin-y4z8 (Fig. 12B), TM-agrin-y4z0 (Fig. 12C) and TM-agrin-y0z0 (Fig. 12D) in WT cortical neurons, gephyrin puncta density was reduced compared to neurons transfected with the control vector (Fig. 12A). Thus, the TM-agrin-mediated reduction of inhibitory synapses does not depend on C-terminal splicing of TM-agrin.

Transfection of neurons with truncated constructs, i.e. the deletion of the C-terminal half of TM-agrin (FD8, Fig. 12E), the 7_{th}-follistatin-like domain (FD6) or the entire extracellular domain of TM-agrin (ΔEC-TM-agrin, Fig. 12F) decreased gephyrin puncta density similar to the level after transfection with full-length TM-agrin cDNA. Therefore, TM-agrin overexpression reduced gephyrin puncta density independently of the entire extracellular region of TM-agrin. This suggests that this effect depends on TM-agrin's intracellular and/or the transmembrane region.

To investigate if the presence of the extracellular region of agrin affects the function of inhibitory synapse, the frequency and amplitude of miniature inhibitory postsynaptic currents (mIPSCs) were investigated in the presence and absence of soluble agrin (with collaboration with Dr. Hetsch and Prof. Rathjen, MDC Berlin). Voltage clamp experiments, in which the cortical neurons were incubated with purified soluble agrin-y4z8, showed no changes in the frequency (Fig. 12I) and the amplitude (Fig. 12J) of the mIPSCs. Consistent with the transfection results, the effect of TM-agrin overexpression on the density and function of the inhibitory synapses appears to be dependent on the presence of either the intracellular and/or the transmembrane region of the TM-agrin.

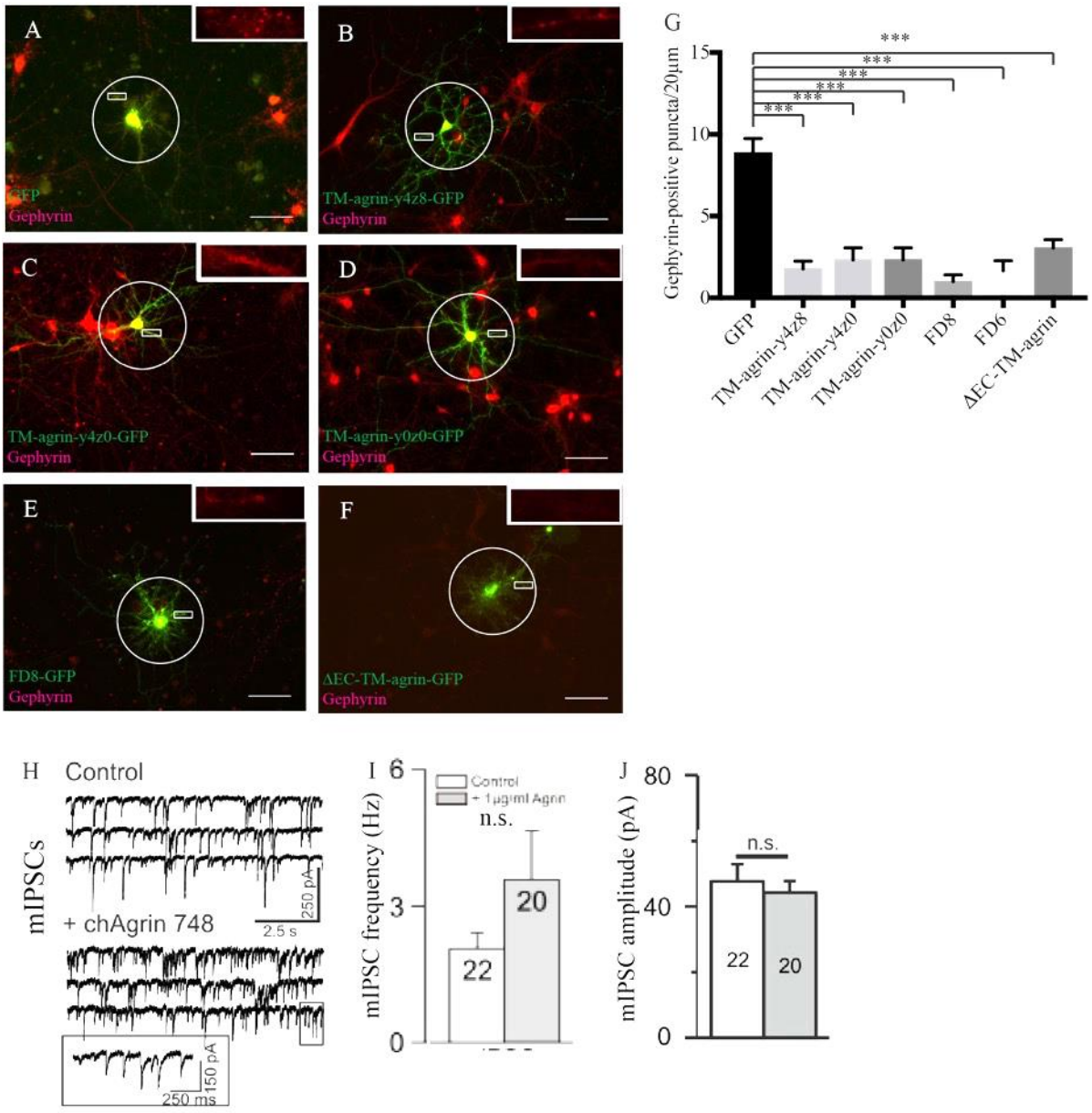

Figure 12. **The extracellular region of TM-agrin was not required for the TM-agrin overexpression-mediated decrease in inhibitory synapses**. (A-G) Gephyrin puncta reduction after TM-agrin overexpression was not dependent on TM-agrin splice variants -y4z8 (B), -y4z0 (C), -y0z0 (D), half C-terminal of TM-agrin (E), 7th follistatin-like domain (FLD) and the whole extracellular region (F, ΔEC-TM-agrin; in panel G, number of independent experiments for each group is 3). (H-J) Incubation of cortical neurons with full-length purified soluble agrin-y4z8, which lacking of intracellular and transmembrane region of TM-agrin, showed no difference on the mIPSCs traces (H) compared to the control, as indicated in the analysis of the frequency (I) and amplitude (J) of miniature inhibitory postsynaptic currents (mIPSCs, number in the bar represents number of analyzed neurons, under collaboration with Dr. Hetsch and Prof. Rathjen); statistical analysis: ordinary one-way ANOVA with Dunn's multiple comparison test (G), Mann-Whitney test (I, J); scale bar 50 μm.

Phosphorylation of a conserved serine-residue in agrin intracellular domain is required for TM-agrin-mediated reduction of inhibitory synapses

To investigate which part of TM-agrin is required for the decrease of inhibitory synapses after TM-agrin overexpression, I analyzed the amino acid sequence of the intracellular region of TM-agrin and compared it among several vertebrate species using a multiple sequence alignment program (Clustal Omega, https://www.ebi.ac.uk/Tools/msa/clustalo/). This analysis revealed a conserved motif in the TM-agrin intracellular domain containing a serine residue at position 17 (S17) in human and mouse.

In order to predict whether the S17 residue was phosphorylated, based on the amino acid sequence and the predicted secondary structure of TM-agrin (Blom et al., 1999; Blom et al., 2004), I performed *in silico* analysis of the intracellular amino acid sequence using the online open-access platform Netphos3.1 (http://www.cbs.dtu.dk/services/NetPhos). This analysis confidently confirmed that serine 17 is a potential phosphorylation site within TM-agrin's intracellular region (Fig. 13) and predicts TM-agrin as a substrate for cyclin-dependent kinase 1 (CDK1; encoded by the *cdc2* gene).

Given these results, I hypothesized that this serine residue might act as phosphorylation site of TM-agrin and that this phosphorylation is functionally important for the reduction of inhibitory synapse puncta density after TM-agrin overexpression. To test this hypothesis, I transfected cortical neurons with TM-agrin cDNA constructs containing point mutations in the TM-agrin cDNA. These mutations were generated by substituting serine with the non-phosphorylatable alanine residue (S17A, Fig. 13) or with the phosphomimetic aspartic acid residue (S17D, Fig. 13). Overexpression of S17A-TM-agrin did not reduce the density of puncta of the inhibitory synapse-associated proteins gephyrin (Fig. 13C-G), the α1-subunit of the $GABA_AR$ (Fig. 13H), collybistin (Fig. 13I) and neuroligin-2 (Fig. 13J). In contrast, transfection of the S17D-TM-agrin cDNA significantly reduced the puncta density of all inhibitory synapse-associated proteins. These results demonstrate that the presence of S17 in the intracellular part of TM-agrin is required for the formation or maintenance of inhibitory synapses.

Together these data suggest that the reduction of inhibitory puncta density indeed requires the presence and the phosphorylation of S17 in TM-agrin. However, further experiments are needed to formally validate the phosphorylation of TM-agrin and its effect on inhibitory synapses.

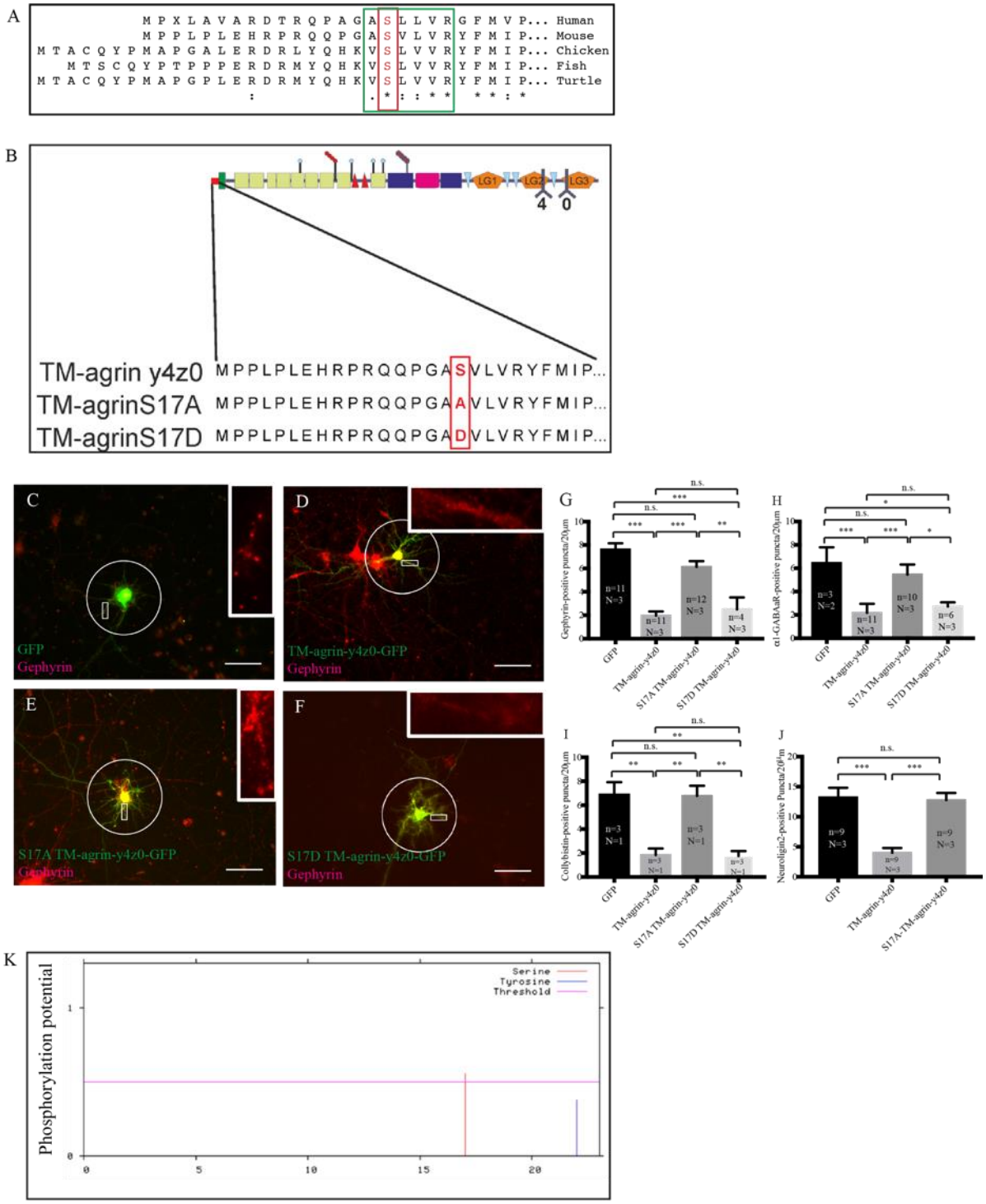

Figure 13**. Phosphorylation of a conserved serine-residue in agrin intracellular domain is required for TM-agrin-mediated reduction of inhibitory synapses.** (A) Multiple sequence alignment analysis of intracellular region of TM-agrin revealed an unknown conserved amino acid motif (green box) and a conserved intracellular serine-residue at position 17 (S17, red box, in human and mouse) among species in vertebrate. ('*' conserved site; ':' conservative replacement; '.' semi-conservative replacement; ' ' non-conservative replacement). (B) Different constructs containing point-mutation of serine-to-alanine (S17A, non-phosphorylated mutant) and of serine-to-aspartic-acid (S17D, phosphomimetic-mutant) were generated for further analysis. (C-J) The presence and the phosphorylation of S17 in TM-agrin cDNA is required for TM-agrin overexpression-mediated decrease of gephyrin, the α1-subunit of the $GABA_AR$, collybistin and neuroligin-2 puncta density; statistical analysis: Kruskal-Wallis test with Dunn's multiple comparison test (G-I); scale bar 50 µm. (K) Serine residue at the position-17 is predicted to be a potential phosphorylation site (above the threshold line, pink-colored line) according to the *in silico* analysis of amino acid sequence (Netphos3.1).

Lrp4 and TM-agrin, but not MuSK, differentially control inhibitory synapses

Previously, I showed that Lrp4 is necessary to control excitatory synapse density (Fig. 9). To investigate if Lrp4 is also necessary for inhibitory synapse formation or maintenance, I analyzed the puncta density of inhibitory synapses in Lrp4-KO neurons. The density of gephyrin (Fig. 14B,E) and of the α1-subunit of the $GABA_AR$ (Fig. 14 G,J) in Lrp4-KO neurons were significantly reduced compared to Lrp4-heterozygous neurons (Fig. 14A,F), supporting a role of Lrp4 in inhibitory synapses formation and/or maintenance. TM-agrin overexpression in Lrp4-heterozygous neurons consistently reduced gephyrin (Fig. 14C,E) and the α1-subunit of the $GABA_AR$ (Fig. 14C,E) puncta density, similarly to the effect in WT neurons (Fig. 11). Moreover, no additional reduction of gephyrin (Fig. 14D) and of the α1-subunit of the $GABA_AR$ puncta density (Fig. 14I) were observed following TM-agrin overexpression in Lrp4-KO neurons. These results suggest that in contrast to the formation of excitatory synapses where the expression of Lrp4 is required, Lrp4 seems not to be required for the TM-agrin-mediated reduction of inhibitory synapses. Thus, in the case of inhibitory synapses, Lrp4 and TM-agrin act independently of each other.

Previously, I showed that MuSK is not required for the formation of excitatory synapses (Fig. 9). To investigate if MuSK affects the formation of inhibitory synapses, I investigated the density of puncta containing inhibitory synapses markers in MuSK-KO neurons and compared their density to the density of puncta on dendrites from MuSK-heterozygous neurons. MuSK-heterozygous neurons showed a comparable puncta density containing gephyrin (Fig. 14K) or the α1-subunit of the $GABA_AR$ (Fig. 14P) compared to MuSK-KO neurons (Fig. 14L). These results suggest that MuSK expression is not required for the formation of inhibitory synapses. Moreover, TM-agrin overexpression similarly decreased gephyrin puncta density in MuSK-heterozygous (Fig. 14M,P) and MuSK-KO neurons (Fig. 14N,P), demonstrating that TM-agrin does not need MuSK expression to reduce the density of inhibitory synapses. These results stand in favor of MuSK not being required for controlling inhibitory synaptic density, similar to the observations regarding the TM-agrin-overexpression-mediated effect on excitatory synapses.

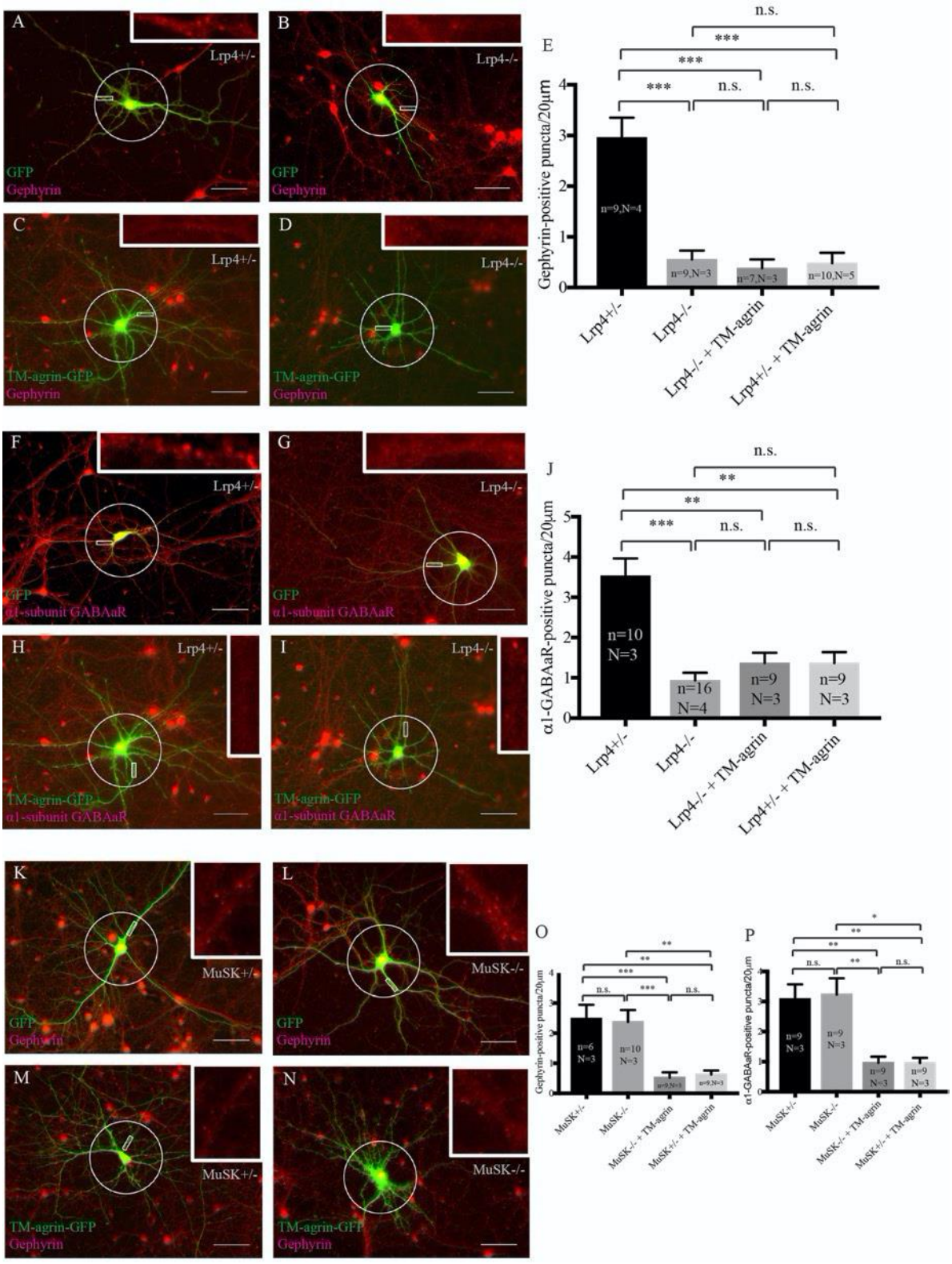

Figure 14. **Lrp4 and TM-agrin, but not MuSK, control inhibitory synapses.** (A-J) Lrp4-KO neurons showed lower density of gephyrin (E) and the α1-subunit of the GABAAR (J) compared to Lrp4-heterozygous neurons. TM-agrin overexpression decreased gephyrin (D) and the α1-subunit of the GABAAR (I) puncta density in Lrp4-heterozygous neurons which did not decrease further in Lrp4-KO neurons. (K-P) MuSK-heterozygous neurons (K) showed comparable gephyrin (O) and the α1-subunit of the GABAAR (P) puncta density compared to MuSK-KO neurons (L). TM-agrin overexpression reduced gephyrin and the α1-subunit of the GABAAR puncta density in MuSK-heterozygous (M) and MuSK-KO neurons (N); statistical analysis: Kruskal-Wallis test with Dunn's multiple comparison test (E, J), one-way ANOVA with Dunn's multiple comparison test (O, P); scale bar 50 µm.

Conditional TM-agrin overexpression in adult murine cortex

In order to investigate whether TM-agrin expression levels affect the formation/maintenance of synapses *in vivo*, I took advantage of a conditional TM-agrin knock-in (KI) mouse model. In this mouse line, the overexpression of TM-agrin is regulated in a time- and space-specific manner, by exploiting the loxP/cre-ERT2 inducible system (Erdmann et al., 2007; Metzger et al., 1995; Schwenk et al., 1998). A knock-in mouse line with a floxed stop cassette upstream of the TM-agrin cDNA was crossed with a mouse line expressing cre-ERT2 under the CamKIIa promoter. This results in the overexpression of TM-agrin upon tamoxifen application. The CamKIIa promoter of the Cre recombinase provides spatial specificity to the Cre expression, i.e. in glutamatergic neurons of the neocortex and hippocampus (Fig. 15).

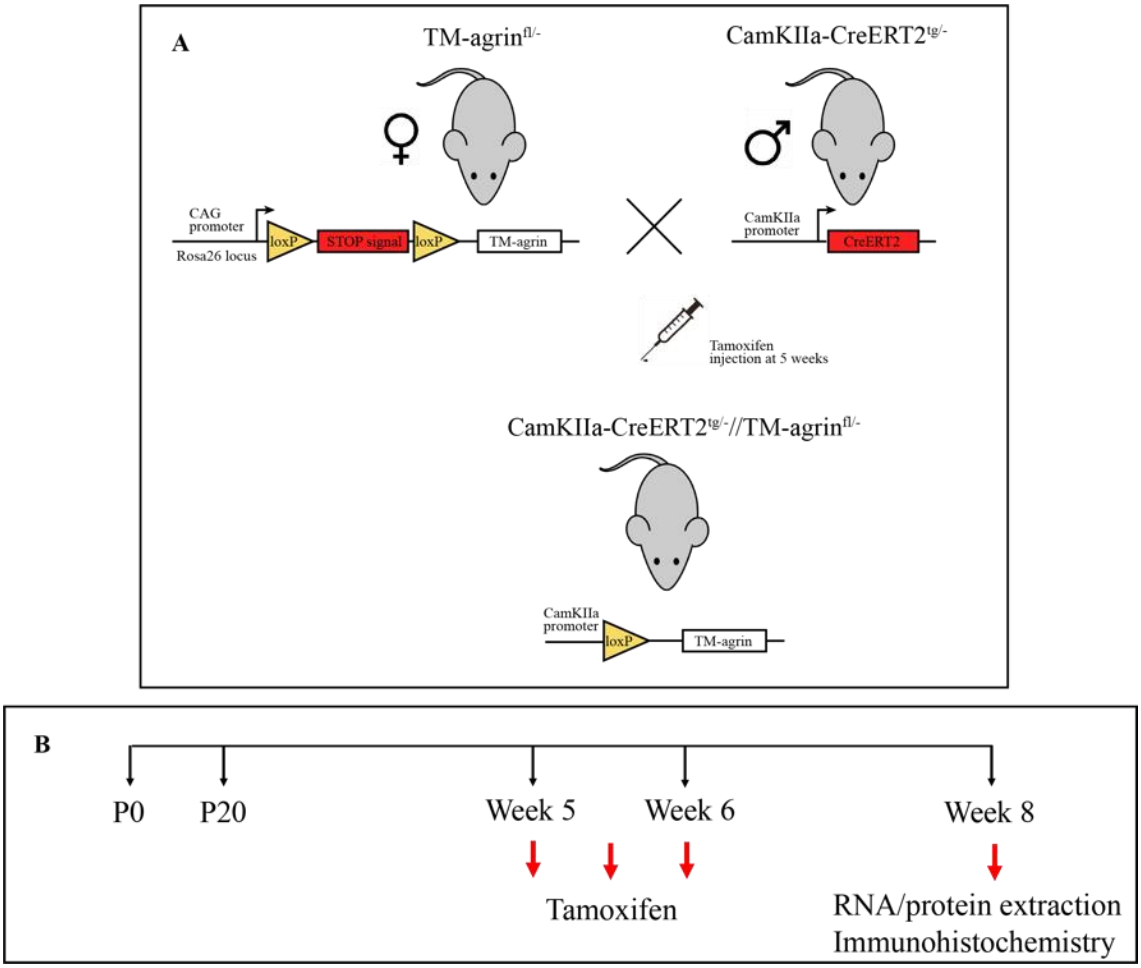

Figure 15. **Breeding and induction scheme of TM-agrin overexpressing mice**. A. Breeding strategy of generating the CamKIIa-Cre$^{+/-}$//TM-agrin$^{fl/-}$ (Cre+/TM-agrin KI). B. Induction scheme of TM-agrin overexpression under tamoxifen administration. Tamoxifen in corn oil was injected intraperitoneally three times into 5-week-old mice. Two weeks after the last tamoxifen administration, the mice were sacrificed for further analyses.

To validate the system of the inducible TM-agrin overexpression, I injected tamoxifen intraperitoneally three times in Cre$^{+/-}$/TM-agrin$^{fl/-}$ (Cre+/TM-agrin KI) and Cre$^{+/-}$/TM-agrin$^{-/-}$ (Cre+/TM-agrin WT) mice at the age of 5-weeks. Two weeks after the last injection, I observed

a significant increase in agrin puncta density (Fig. 16C) and puncta size (Fig. 16D), protein level (Fig. 16E,F) and transcript level (Fig. 16G). On the protein level, TM-agrin was approximately 8-fold overexpressed. This set of data confirms that in the conditional TM-agrin overexpressing mice, injection of tamoxifen induces a significant increase of TM-agrin mRNA and protein.

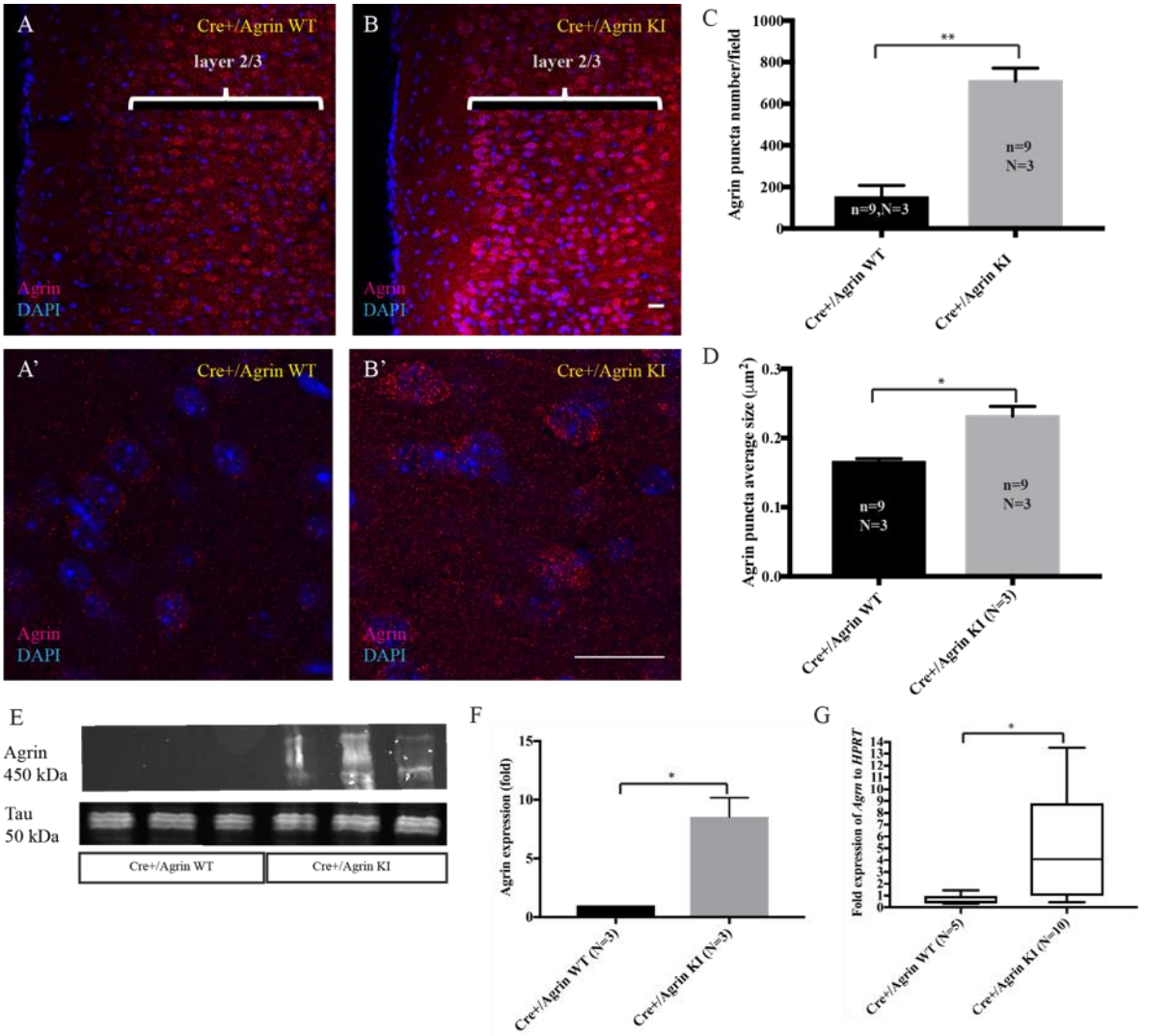

Figure 16. **Tamoxifen-induced overexpression of TM-agrin *in vivo***. Tamoxifen administration in Cre+/TM-agrin KI increased the TM-agrin puncta density (C), size (D). In WB analyses, the ratio of the pixel densities between mutant and control were normalized to the expression level of the tau protein (E, F). The ratio of *agrn* transcript level in mutant and in control mice was normalized to the transcript level of *hprt* (G). Panel A' and B' represent higher magnifications of the areas indicated in panel A and B, respectively; N indicates number of mice; statistical analysis: unpaired t-test (C, D, F), Mann-Whitney test (G); scale bar 50 μm (B, B').

TM-agrin overexpression affects transcript levels of several synapse-associated proteins

In order to understand whether TM-agrin overexpression affects synapse-associated proteins *in vivo*, I performed qRT-PCR analyses of several synaptic protein transcripts. Transcript levels of several pan-synaptic proteins, *bsn* (bassoon), *syp* (synaptophysin) and

vamp2 (synaptobrevin), were not altered after TM-agrin overexpression *in vivo* (Table. 9). Interestingly, transcript levels of excitatory synapse-associated proteins, such as *dlg4* (PSD-95) and *grin1* (the NR1-subunit of the NMDAR), were significantly increased (Table. 9, green). On the other hand, the transcript levels of the inhibitory synapse-associated proteins, including *gphn* (gephyrin) and *gabra1* (the α1-subunit of the GABAAR), were significantly decreased (Table. 9, red). These results are in line with the changes observed in cultures of embryonic cortical neurons *in vitro* and suggest that the TM-agrin overexpression affects these proteins on the transcript level.

Table 9. **Transcript levels of several synapse-associated proteins after tamoxifen administration in adult Cre+/TM-agrin KI and Cre+/TM-agrin WT**.
TM-agrin overexpression did not change pan-synaptic markers transcript levels (*bsn, syp and vamp2)*, increased transcript levels of *dlg4* and *grin1* (green-colored) and reduced transcript levels of *gphn* and *gabra1* (red-colored); statistical analysis: Mann-Whitney-Test.

Gene Protein	8-week-old mice Mean ± Standard error of the mean (SEM) Cre+/Agrin WT (N)	Cre+/Agrin KI (N)	Fold difference	*p-value*
Presynaptic Proteins				
Bsn Bassoon	11,90 ± 3,7 (N=3)	10,08 ± 7,38 (N=4)	0,23	0,4
Syp Synaptophysin	27,22 ± 6,41 (N=3)	24,41 ± 23,63 (N=3)	0,9	0,7
Vamp2 Synaptobrevin	7,11 ± 0,80 (N=3)	6,012 ± 2,96 (N=4)	0,85	0,63
Postsynaptic and Scaffolding Proteins				
Dlg4 PSD-95	72,97 ± 31,11 (N=5)	165,6 ± 61,16 (N=8)	2,27	0,04
Gphn Gephyrin	0,07 ± 0,002 (N=5)	0,002 ± 0,0003 (N=5)	0,04	0,03
Ionotrophic Receptors				
Grin1 NR1-NMDAR	25,65 ± 5,56 (N=6)	69,64 ± 5,57 (N=3)	2,71	0,02
Gabra1 α1-GABAAR	35,81 ± 3,02 (N=3)	5,67 ± 3,10 (N=5)	0,24	0,04

*The qRT-PCR was carried out under a supervision by Dr. Schick.

TM-agrin does not colocalize with gephyrin but colocalizes with PSD-95 *in vivo*

Several changes reported in the qRT-PCR analysis (table 9) suggested that TM-agrin might differentially regulate the expression level of excitatory and inhibitory synapse-associated proteins *in vivo*. To investigate the spatial distribution of TM-agrin in relation to excitatory and inhibitory synapses in sections of cortices from wildtype adult mice, I analyzed the distribution of TM-agrin with respect to the distribution of gephyrin or of PSD-95. I observed that TM-agrin did not colocalize with gephyrin (Fig. 17A,A'). On the other hand, TM-agrin puncta partially colocalized with PSD-95 puncta (Fig. 17B,B'). These results demonstrate that TM-agrin is concentrated at least at a subset of excitatory synapses, but not at inhibitory synapses.

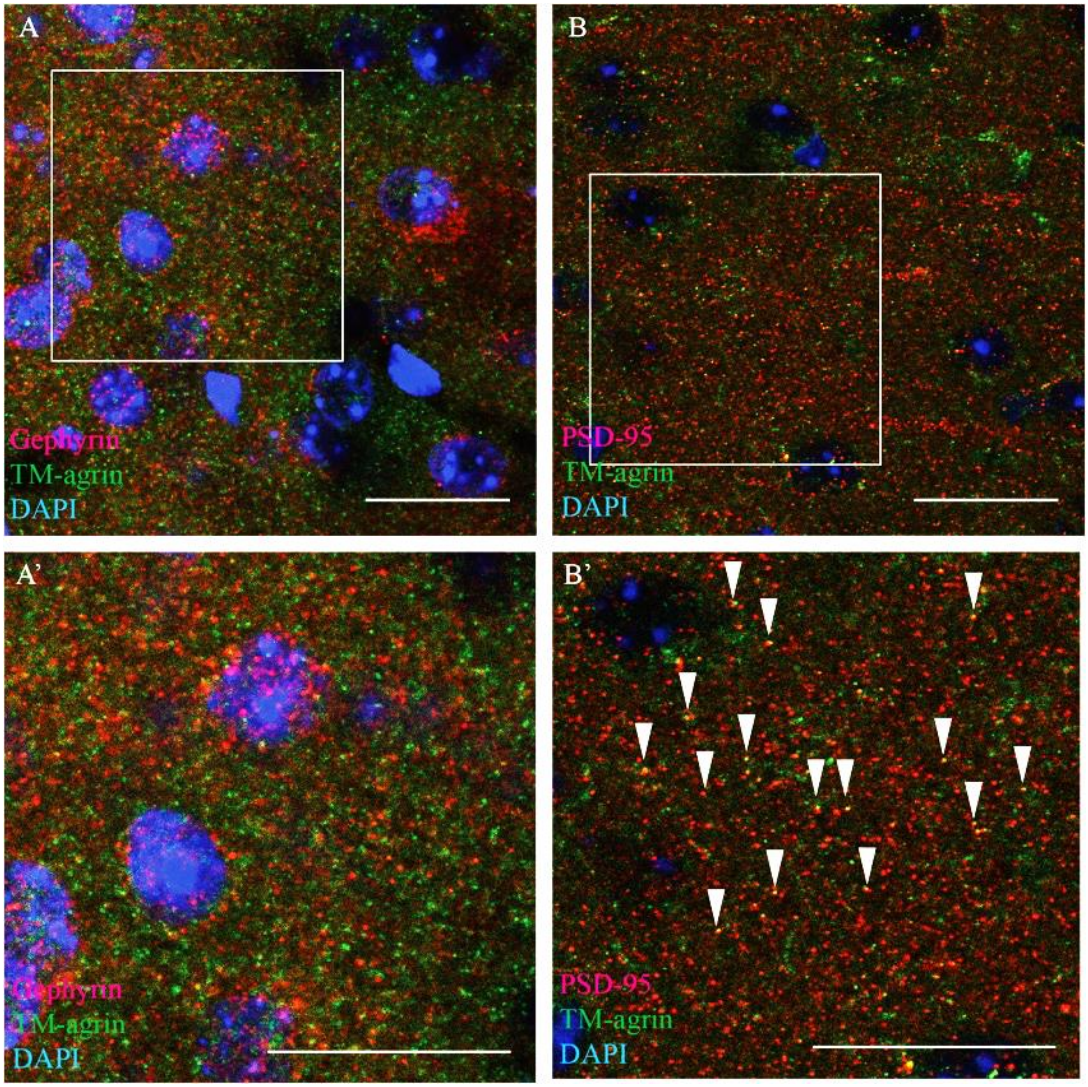

Figure 17. **A non-colocalization of TM-agrin with gephyrin and a colocalization of TM-agrin with PSD-95 in WT cortical sections.** (A, A') TM-agrin puncta distribution (green) does not colocalize with gephyrin puncta (red). (B, B') TM-agrin puncta (green) colocalizes with PSD-95 puncta (red, white head arrow), A' and B' panels are the magnifications of the corresponding panel A and B; scale bar 25 μm. The images were taken as a single focal plane.

TM-agrin controls excitatory and inhibitory synapses *in vivo*

In order to confirm the changes observed in the transcript levels, I analyzed the distribution of the corresponding proteins by performing immunohistochemical analyses in TM-agrin KI mice. In agreement with the lack of changes on the transcript level (Table. 9) and in agreement with the *in vitro* data (Fig. 11O–Q), the pan-synaptic protein marker, bassoon, was not affected in terms of puncta density or puncta size in TM-agrin overexpressing brains (Fig. 18A–D).

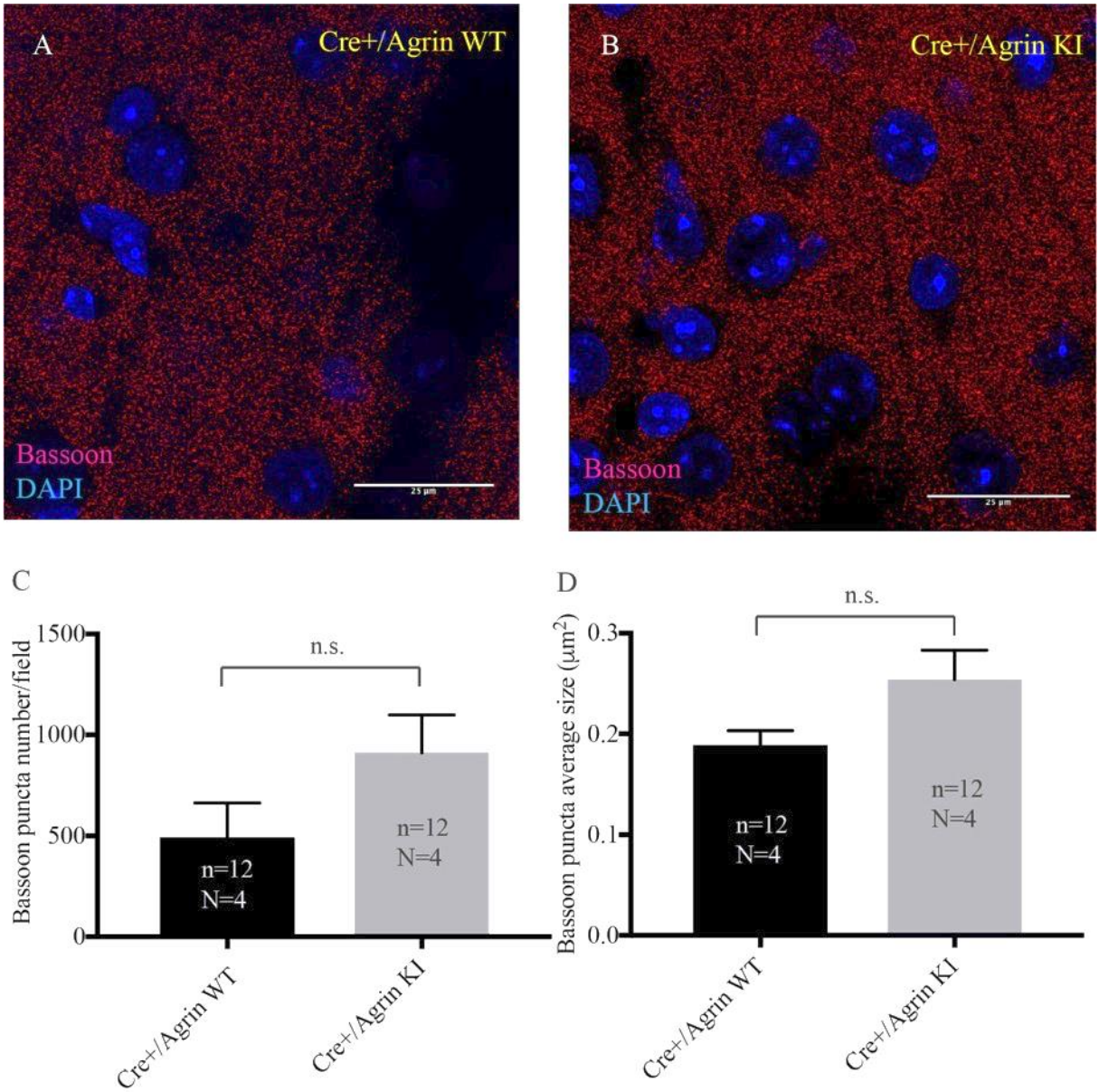

Figure 18. **TM-agrin overexpression did not alter bassoon puncta density and size**, statistical analysis: unpaired t-test (C, D); scale bar 25 µm.

In contrast, a significant increase of presynaptic excitatory vGlut1 puncta density was observed in Cre+/TM-agrin KI neocortical sections compared to the control Cre+/TM-agrin

WT (Fig. 19A-D). Similarly, excitatory postsynaptic PSD-95, the NR1- and the NR2B-subunit of the NMDAR puncta density were also significantly increased (Fig. 19E-P). Together, these data suggest that TM-agrin overexpression in adulthood *in vivo* increases the density of excitatory pre- and postsynaptic synapses in a similar way as it does in cultures of cortical neurons.

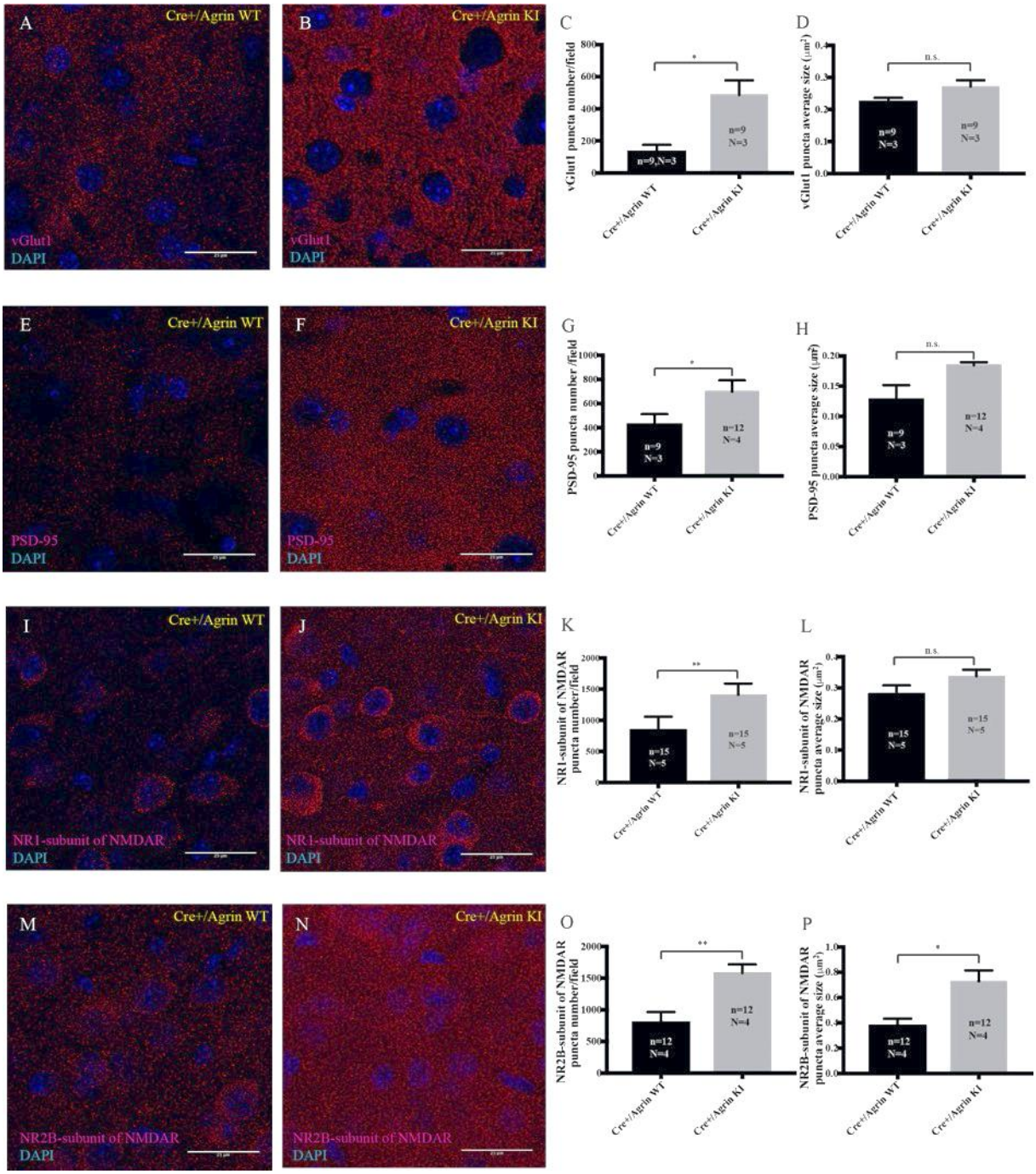

Figure 19. **TM-agrin controls excitatory synapses density *in vivo*.** TM-agrin overexpression in adulthood increased the puncta density of vesicular glutamate transporter-1 (A-C), PSD-95 (E-G), the NR1-subunit of the NMDAR (I-K) and the NR2B-subunit of the NMDAR (M-O); statistical analysis: Mann-Whitney test (C, G, H, K, O, P), unpaired t-test (D, L); scale bar 25 μm.

In order to confirm the changes at the transcript levels of inhibitory synapse-associated proteins, the distribution of the corresponding proteins in Cre+/TM-agrin KI neocortices was analyzed. I observed a significant reduction in the density of puncta containing presynaptic protein vGAT (Fig. 20A–D) as well as postsynaptic gephyrin (Fig. 20E–H), collybistin (Fig. 20I–L) and the α5-subunit of the $GABA_AR$ (Fig. 20M-O), demonstrating a reduction in transcript and protein levels of the inhibitory synapses after TM-agrin overexpression in adulthood *in vivo*.

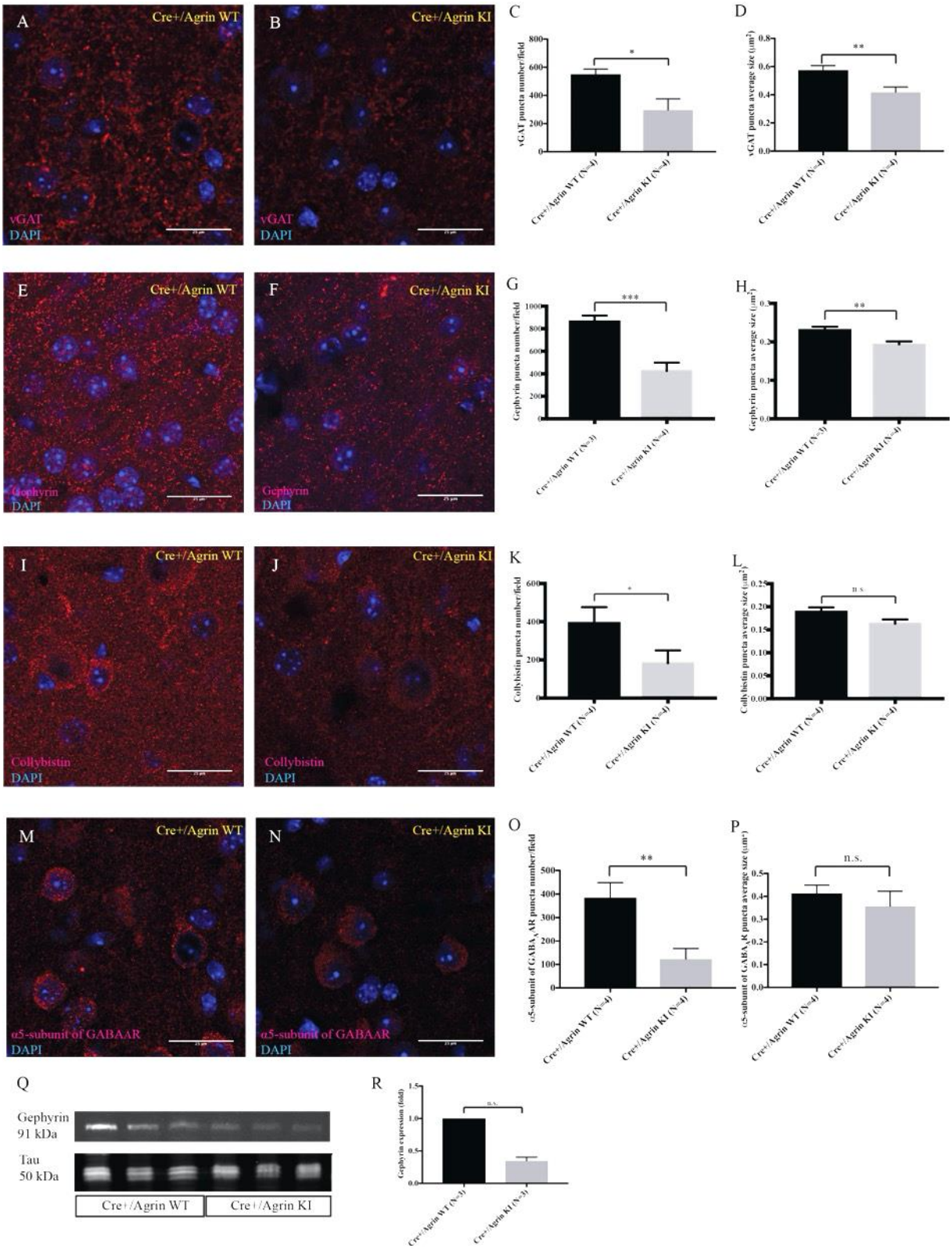

Figure 20. **TM-agrin controls inhibitory synapses density *in vivo*.** TM-agrin overexpression in adulthood *in vivo* reduced the puncta density containing vesicular GABA transporter (A-C), gephyrin (E-G), collybistin (I-K) and the α5-subunit of the GABAAR (M-O). WB analysis on the membrane fraction did not show significant reduction on the gephyrin protein level (Q, R); statistical analysis: unpaired t-test (C, G, O, P), Mann-Whitney test (D, H, K, L, R); scale bar 25 μm.

Collectively, these data confirm that the overexpression of TM-agrin in neurons *in vitro* and *in vivo* differentially regulates the formation/maintenance of synapses. On one side, the overexpression of TM-agrin increases the transcript and protein levels of excitatory synapse-associated proteins. On the other side, TM-agrin's overexpression reduces the transcript and protein levels of inhibitory synapse-associated proteins.

Discussion

Several lines of evidence have demonstrated the essential role of agrin, MuSK and Lrp4 during formation, maintenance and regeneration of the NMJ (Tintignac et al., 2015). However, the role of these organizers in the CNS is poorly understood even though they are present in the CNS and concentrated at synapses (Kröger and Pfister, 2009). The widespread expression of these molecules, the diversity of their isoforms and the developmental regulation of their expression in neuronal and non-neuronal cells complicate the analysis of their functions and interactions. In my thesis, I carried out gain- and loss-of-function experiments, in order to better understand the role of agrin and its receptor complex during dendritic development and synaptogenesis in neocortical neurons *in vitro* and *in vivo*. My results are summarized in Table 10. Since the complete knockout of either agrin, Lrp4 or MuSK is lethal, their specific function in the CNS remains largely to be unveiled. Although knockout or overexpressing these proteins is a non-physiologically situation, these approaches in general are considerably useful to investigate the interplay of agrin and its partners and their possible roles in developmental processes and in adulthood.

Table 10. Summary: the effect of TM-agrin, Lrp4 and MuSK in dendritic arborization and synaptogenesis

1. Differences of Lrp4-KO and MuSK-KO neurons compared to Lrp4-heterozygous or MuSK-heterozygous neurons

Phenotype	Lrp4-KO	MuSK-KO
Dendritic arbor complexity	Reduced complexity compared to Lrp4-heterozygous	Reduced complexity compared to MuSK-heterozygous
Excitatory synapses	Reduced excitatory synapses compared to Lrp4-heterozygous	Unaffected compared to MuSK-heterozygous
Inhibitory synapses	Reduced inhibitory synapses compared to Lrp4-heterozygous	Unaffected compared to MuSK-heterozygous

2. The effect of TM-agrin overexpression on Lrp4-heterozygous and MuSK-heterozygous compared to heterozygous neurons transfected with GFP only

Phenotype	Lrp4-heterozygous plus TM-agrin	MuSK-heterozygous plus TM-agrin
Dendritic arborization complexity	Unaffected	Unaffected

Excitatory synapses	Increased excitatory synapses	Increased excitatory synapses
Inhibitory synapses	Reduced inhibitory synapses	Reduced inhibitory synapses

3. The effect of TM-agrin overexpression on wildtype neurons

Phenotype	Wildtype neurons + TM-agrin
Dendritic arborization complexity	Unaffected
Pan-synaptic marker	Unaffected
Excitatory synapses	Increased excitatory synapses which depends on the y4, not the z8.
Inhibitory synapses	Reduced inhibitory synapses which depends on the presence and the phosphorylation of S17 residue.

4. The effect of TM-agrin overexpression on Lrp4-KO and MuSK-KO neurons

Phenotype	Lrp4-KO + TM-agrin	MuSK-KO + TM-agrin
Dendritic arborization complexity	Restored complexity similar to Lrp4-heterozygous	No effect; the complexity remained less complex similar to MuSK-KO
Excitatory synapses	No increased of excitatory synapses; density similar to transfected Lrp4-KO neurons, lower compared to Lrp4-heterozygous	n.a.
Inhibitory synapses	No further reduction of inhibitory synapses; density similar to transfected Lrp4-KO	n.a.

5. The effect of soluble agrin incubation in neurons microisland culture compared to non-treated neurons

Phenotype	Wildtype neurons plus soluble agrin 748	Lrp4-KO neurons plus soluble agrin 748
mEPSCs frequency and amplitude	Increased compared to neurons without agrin treatment	Unchanged compared to neurons without agrin treatment
Number/area of VGluT1+2/AMPAR or VGluT1+2/PSD95 puncta	Increased compared to neurons without agrin treatment	n.d.

mIPSCs frequency and amplitude	Unchanged compared to neurons without agrin treatment	Unchanged compared to neurons without agrin treatment

6. The effect of TM-agrin-y4z0 overexpression in brains from adult mice *in vivo*

Phenotype	TM-agrin overexpressing adult brains
Pan-synaptic marker	Unaffected
Excitatory synapses	Increased transcript and protein levels of excitatory synapse-associated proteins.
Inhibitory synapses	Reduced transcript and protein levels of inhibitory synapse-associated proteins.

n.d.: not determined; n.a.: not applicable

TM-agrin, Lrp4 and MuSK affect dendritic arbor complexity

I investigate the role of TM-agrin, Lrp4 and MuSK on dendritic arborization in cortical neurons *in vitro*. To this end, I compared the effect of an overexpression of the neuronal TM-agrin in WT neurons, in Lrp4-KO neurons and in MuSK-KO neurons with the effect of an overexpression in neurons from the corresponding heterozygous embryos. After transfection with TM-agrin, neurons from WT embryos showed no differences in dendritic arborization (number of primary dendrites extending from the cell body and total dendritic branch tip number) compared to neurons transfected with control vector encoding GFP. However, neurons transfected with TM-agrin have significantly shorter primary dendrites. My results are compatible to previous studies where agrin knockdown by shRNA in hippocampal neurons led to an increase in dendritic length (McCroskery et al., 2006). In contrast, incubation of hippocampal neurons with recombinant agrin increased dendritic branching and dendritic elongation, whereas inhibiting agrin's translation by antisense oligonucleotides showed the opposite effect (Ferreira, 1999; Mantych and Ferreira, 2001). Potential explanations why I did not observe any change in the dendritic branching pattern after TM-agrin overexpression could be due to differences in the type of the neurons analyzed (cortical vs hippocampal neurons) or due to the isoforms of agrin used to transfect the neurons. In my experiments, I prepared primary cultures of embryonic neocortical neurons, whereas in the previous studies the analyses were mostly carried out in cultures of hippocampal neurons. Furthermore, I transfected the transmembrane-form of agrin whereas the other studies incubated with recombinant soluble agrin. In any case, my results show that TM-agrin controls dendritic length in cultures from cortical neurons. The exact mechanism of how TM-agrin influences the length of dendrites remains to be determined.

Interestingly, the reduction of Lrp4 expression via miRNA lead to a similar phenotype in cortical neurons (Karakatsani et al., 2017) as the genetic deletion of Lrp4 expression. In both cases, the neurons have a lower density of dendritic spines and a lower number but longer primary dendrites (Karakatsani et al., 2017). Since the miRNA technique has several disadvantages, such as off-target effects (Singh et al., 2011), the possibility remained that the effect of Lrp4 knockdown was due to non-physiological side effects. However, genetic deletion of Lrp4 gene affected dendritic arborization in neocortical neurons in the same way as neuron-specific knockdown of Lrp4 by miRNA *in vitro* and *in vivo* (Karakatsani et al., 2017). This clearly demonstrates that the miRNA effect was specific and suggests that the altered dendritic arborization pattern was not due to off target effects of the miRNA. On the other hand, mice lacking Lrp4 in the adult CNS showed no gross anatomical changes in adult neocortex, hippocampus and cerebellum (Gomez et al., 2014; Pohlkamp et al., 2015). It should be noted, however, that the effect of Lrp4 knockdown and overexpression in cortical neurons *in vitro* on the number of primary dendrites disappeared overtime as the neurons matured, suggesting the activation of compensatory or redundant mechanisms *in vivo* which maintained the dendritic tree structure (Karakatsani et al., 2017). Indeed, compensatory mechanisms for Lrp4 have been previously described during skeletal muscle development, such as functional compensation via Lrp1, which shares a high degree of homology with Lrp4 (Lane-Donovan et al., 2014; Li et al., 2010). Similar to Lrp1, Lrp4 is concentrated in the PSD fraction similar to Lrp4. Moreover, due to their homologous structure, another LDLR family member, Lrp10, might similarly compensate the effect that was observed after Lrp4 manipulation *in vivo* (Brodeur et al., 2012; Lane-Donovan et al., 2014). In summary, Lrp4 is required for the normal dendritic arborization in the developing neurons, but its function *in vivo* in mature neurons might be compensated by functionally redundant proteins.

While Lrp4 is involved in regulating the dendritic arborization pattern, the question remains open whether MuSK is also involved. I showed that the absence of MuSK in cortical neurons led to a reduction of the number of primary dendrites and of the total dendritic branch tip number. This is the first evidence demonstrating a critical function of MuSK in regulating dendritic tree complexity and opens the questions of how MuSK regulates the dendritic morphology. One possible explanation is the interaction of MuSK with Wnt morphogens via its Frizzled-like/cysteine-rich domain. It was previously shown that the Frizzled-like domain in MuSK interacts with Wnt morphogens to maintain NMJ structural integrity (Messeant et al., 2015). Moreover, pharmacological Wnt inhibition led to a reduction of the dendritic arborization in cultured cortical neurons (Hiester et al., 2013; Remedio et al., 2016). Thus,

MuSK could affect the formation of the normal dendritic arborization pattern by being a receptor for Wnt proteins during CNS development.

Interestingly, while TM-agrin overexpression could restore the dendritic arborization deficit in Lrp4-KO neurons, it had no such effect in MuSK-KO neurons. This suggests that MuSK, but not Lrp4, is required for the TM-agrin-induced changes in dendritic arborization. Of note, agrin is not able to directly bind to MuSK (Glass et al., 1996a). This suggests that in the developing CNS, TM-agrin might require additional proteins mediating the TM-agrin – MuSK interaction in order to regulate dendritic arborization. These proteins remain to be identified.

The C-terminal half of TM-agrin was essential for rescuing the loss of the dendritic arborization complexity in Lrp4-KO neurons. This effect was independent of the C-terminal splicing isoforms and thus independent of a direct agrin-Lrp4 interaction. In fact, all of the splice variants of TM-agrin restored dendritic arborization complexity observed in Lrp4-deficient neurons. Several molecules of the agrin signaling cascade have been shown to affect dendritic arborization. For example, agrin could regulate dendritic arborization via its interaction with dystroglycan (Bijata et al., 2015). Supporting this hypothesis, the C-terminal half of agrin, the binding domain between agrin and dystroglycan, was required for the TM-agrin-mediated effect on dendritic arborization restoration in Lrp4-KO neurons. Alternatively, agrin's effect could also be mediated by several other molecules, possibly interacting with agrin's glycosaminoglycan side chains. For example, a previous report has shown a neuroprotective effect of the GAG-side chains, promoting dendritic arborization (Dudas et al., 2008). In addition, the effect of agrin on dendritic arborization could be mediated by the activation of the mitogen-activated protein kinase (MAPK) pathway, which has been reported to be important for regulating dendritic tree complexity (Jan and Jan, 2010) and which has been shown to be reduced in agrin-deficient brains (Ksiazek et al., 2007). Thus, agrin regulates dendritic arborization under certain conditions and this function requires its half C-terminus and potentially an interaction with other molecules.

Interestingly, neurons from Lrp4-KO and MuSK-KO mice displayed longer primary dendrites compared to control neurons suggesting a negative correlation between dendritic arborization complexity and length of primary dendrites, *i.e.* the more complex the dendritic arborization, the shorter the dendritic length. A similar observation has been reported in Lrp4-miRNA-treated neurons (Karakatsani et al., 2017). This suggests that both parameters, the dendritic arborization and the dendritic length, might depend on each other. However, further

investigations are clearly needed to assess whether these parameters are causally and functionally related.

Together these results stand in favor of multiple mechanisms through which TM-agrin might regulate dendritic complexity. Conclusions on how agrin controls dendritic tree morphology should be taken carefully, since TM-agrin overexpression in WT neurons did not cause any changes in dendritic arborization. Therefore, the effect of agrin on dendritic complexity might only take place selectively under specific conditions, such as when the conditions for dendritic arborization development is not optimal, as in the case in neurons which lack of Lrp4-expression.

The role of TM-agrin, Lrp4 and MuSK in excitatory synapse development and spine formation

To investigate the effect of neuronal agrin during the development of excitatory synapses, I quantified the density of excitatory pre- and postsynaptic-related proteins after TM-agrin overexpression in WT neocortical neuronal cultures. I observed a significant increase in the density of the excitatory presynaptic marker vGlut1, as well as of postsynaptic markers PSD-95 and the NR1-subunit of the NDMA receptor. This observation is in line with previous loss-of-function experiments where the agrin-deficiency in hippocampal cultures and in mice *in vivo* reduced the density of dendritic spines, PSD-95 puncta density and frequency and amplitude of mEPSCs (Ksiazek et al., 2007; McCroskery et al., 2009). However, only a 30% loss of synaptic density was observed in agrin-deficient brains, suggesting that compensatory mechanisms are activated to take over the function of agrin during synapse formation and/or maintenance (Ksiazek et al., 2007). Moreover, previous studies reported an impairment of excitatory synapse formation after blockade of agrin's translation with antisense oligonucleotide (Bose et al., 2000; Ferreira, 1999). In contrast, synaptic puncta analysis in cultures from agrin-deficient cortical and hippocampal neurons did not show any change in the number of synapses (Li et al., 1999; Serpinskaya et al., 1999). The reason for this discrepancy is unknown. However, since the effect of overexpression or of the knockdown was only quantitative in the range of 30 %, the possibility exists that this minimal effect escaped the analysis. In any case, the vast majority of evidence stands in favor of TM-agrin playing a role in the formation or maintenance of excitatory synapses.

Analysis of Lrp4-KO neurons showed that Lrp4 is required for spinogenesis and excitatory synapses formation. In Lrp4-KO neurons, the density of dendritic spines and of PSD-95 puncta were lower compared to wildtype neurons. Thus, Lrp4 expression is required for the

formation of excitatory synapses and dendritic spines. A function of Lrp4 in controlling the formation of dendritic spines and excitatory synapses has been previously suggested using a knockdown approach *in vitro* (Karakatsani et al., 2017) and *in vivo* (Gomez et al., 2014; Pohlkamp et al., 2015). *In vitro*, the reduction of Lrp4 level in hippocampal and cortical neurons led to a reduction of the spine density and of the puncta density containing PSD-95, whereas the overexpression displayed the opposite phenotypes (Karakatsani et al., 2017). In all cases, Lrp4 deficiency led to an approximately 50% reduction of mEPSCs frequency, impairment of the hippocampal LTP and of a longer latency of learning of the mutant mice to reach the platform in the Morris water maze test (Gomez et al., 2014). My results together with the previously published evidence confirm Lrp4 as a key player during spinogenesis, synaptogenesis and synaptic plasticity.

To investigate whether TM-agrin and Lrp4 cooperate in regulating spinogenesis and synaptogenesis, I overexpressed TM-agrin in Lrp4-KO neurons. The overexpression of TM-agrin under these conditions showed no increase in PSD-95 puncta density compared to TM-agrin overexpression in WT cortical neurons. Therefore, it can be concluded, that Lrp4 expression is necessary to control excitatory synapse density, and that TM-agrin might cooperate with Lrp4 to exert its effect on excitatory synapses.

Overexpression of TM-agrin together with Lrp4 miRNA in the same WT neuron showed that the knockdown of Lrp4 level abolished the TM-agrin-mediated increase of excitatory synapses. Based on the previous observation that agrin requires Lrp4 to exert its effect on excitatory synapses. I conclude that the presence of Lrp4 in the same neuron, which overexpresses TM-agrin, is required for controlling excitatory synapses. The increase of excitatory synapses that was exerted by TM-agrin overexpression in miRNA-Lrp4 treated cells and is therefore very likely due to a *trans* interaction between TM-agrin and synaptic or non-neuronal Lrp4 in non-transfected cells. Alternatively, the effect might be caused by the residual Lrp4, which is still expressed at a low-level in the knockdown experiments. Therefore, the presence of Lrp4 in the same cells appears to be required for the TM-agrin overexpression-mediated effect in regulating the excitatory synapses.

In the CNS, Lrp4 is expressed in neuronal and non-neuronal cells, such as glial cells (Lein et al., 2006; Sun et al., 2016; Tian et al., 2006). Neuronal and glial Lrp4 might have different functions during CNS development. Astroglial Lrp4 modulates synaptic transmission at glutamatergic synapses by acting as a glutamatergic transmission modulator via suppression of ATP/adenosine through adenosine A1 receptor on glutamatergic neurons (Sun et al., 2016). The genetic deletion of Lrp4 in astrocyte leads to an increase secretion of ATP which then

suppresses the glutamatergic transmission in the hippocampus (Sun et al., 2016). Interestingly, the absence of astroglial Lrp4 has no effect on the dendritic spine density in the hippocampus (Sun et al., 2016).

Several lines of evidences showed that neuronal Lrp4 affects synapses. Neuronal Lrp4 expression levels regulate the development of excitatory synapses (Karakatsani et al., 2017). Moreover, Lrp4 is concentrated in synaptosomal fractions and has been described to play a critical role in synaptogenesis and synaptic-related plasticity (Gomez et al., 2014; Karakatsani et al., 2017; Mosca et al., 2017; Pohlkamp et al., 2015). Interestingly, the absence of Lrp4 in the CNS does not disturb the overall anatomical organization of the brain (Gomez et al., 2014). Instead, neuronal Lrp4 might account for controlling synapse density, synaptic function as well as hippocampal LTP (Gomez et al., 2014; Pohlkamp et al., 2015). Further evidence strengthening the hypothesis of a role of neuronal Lrp4 in synapse formation and/or maintenance such as that the knockdown of Lrp4 in neurons resulted in lower dendritic spine density, fewer excitatory synapse-like specializations and fewer presynaptic cells labelled by trans-synaptic tracing with rabies virus (Karakatsani et al., 2017). Furthermore, mice without Lrp4 displayed impairment in cognitive tasks related to learning and memory (Gomez et al., 2014). Overall, these evidences suggest that neuronal Lrp4 is required for the formation or maintenance of the excitatory synapses, whereas the astroglial Lrp4 is important for modulating the glutamatergic synaptic transmission.

I did not observe a change in the development of excitatory synapses, i.e. PSD-95 puncta density, in MuSK-KO neurons. Thus, MuSK expression is apparently not required for the formation of the normal density of excitatory synapses. However, MuSK-KO neurons showed fewer dendritic spines compared to control neurons. These contradictory observations could be explained by the fact that MuSK might establish the structural anatomy of excitatory synapses but does not recruit PSD-95 into the newly formed spines. Previous evidence suggested that the presence of PSD-95 does not always correlate with the presence of dendritic spines, meaning that the spines without PSD-95 are subject to be modified, being retracted compared to those that contain PSD-95 (Cane et al., 2014). Furthermore, the downregulation of the PSD-95 expression level does not affect dendritic spines formation (Woods et al., 2011).

TM-agrin overexpression in MuSK-KO neurons increased the density of excitatory synapses compared to the corresponding control neurons. Therefore, in contrast to Lrp4, MuSK expression is apparently not required for the TM-agrin overexpression-mediated increase of excitatory synapses. TM-agrin was still able to exert its effect on excitatory synapses formation in the absence of MuSK. In conclusion, the mechanism of dendritic spine and excitatory

synapses formation in the CNS does not require MuSK suggesting a different molecular mechanism for TM-agrin activity during synaptogenesis in the CNS and at the NMJ.

Besides a less complex dendritic tree, Lrp4- and MuSK-KO neurons have lower densities of dendritic protrusions compared to control neurons. It has been hypothesized that immature dendritic filopodia-like protrusions evolve into dendritic mature mushroom-like protrusions, which eventually transform into contact sites between pre- and post-synaptic excitatory specializations (McCroskery et al., 2006; Miermans et al., 2017). Previous studies reported that TM-agrin overexpression in various cell types causes the formation of filopodia-like protrusions (Annies et al., 2006; McCroskery et al., 2006; Ramseger et al., 2009) and it was hypothesized that these protrusions might be precursors for dendritic spines. Thus, TM-agrin might enhance synapse formation by promoting these filopoda-like protrusions. In my experiments, the overexpression of TM-agrin increased the density of dendritic protrusions in neocortical neuronal culture, independently of the presence of Lrp4 and MuSK. This confirmed that TM-agrin is able to induce filopodia-like processes. Moreover, the induction of filopodia-like processes by TM-agrin depends on the formation of lipid rafts and requires the activation of MAPK and Fyn kinases (Ramseger et al., 2009). In addition, the filopodia formation induced after TM-agrin overexpression in SH-SY5Y neuronal cells requires Cdc42, the Rho family GTPase (McCroskery et al., 2006). The impetus of Cdc42 has been shown to be able to further activate MAP kinase pathway (Kang et al., 2008). The formation of the filopodia-like protrusions required the 7$_{th}$-follistatin-like domain (Porten et al., 2010), whereas the formation of excitatory synapses required a 4 amino acid insertion at splice site y. Thus, the formation of filopodia-like protrusions and the formation of excitatory synapses might be controlled by different domains within TM-agrin. This would suggest that the TM-agrin-mediated formation of the filopodia-like protrusions might not be related to the formation of excitatory synapses. Therefore, the physiological role of dendritic filopodia-like protrusions remains unclear and needs to be further investigated.

Domain of TM-agrin that regulates excitatory synapse development

Agrin is a large multidomain protein. However, little is known about the function of individual domains in the developing CNS. In my study, I showed that specific splice variants of TM-agrin regulate excitatory synapse development. The increase of excitatory synapses was observed after transfection of TM-agrin-y4z8 and TM-agrin-y4z0, but not of TM-agrin-y0z0. Therefore, the TM-agrin overexpression-mediated increase of excitatory synapses required the four amino acid insert at the y-splice site of the LG2 domain. The importance of the LG2

domain for TM-agrin's interaction with chick ciliary neurons has been shown previously (Burgess et al., 2002). Interestingly, the presence of eight amino acids at the z-site, which is essential for the effective binding between agrin and Lrp4, was not required for excitatory synapse formation. The current finding at the same time rejected also our hypothesis in which TM-agrin-mediated filopodia-like processes act as the precursors of excitatory synapses. These two events are induced by two different domains: the y-splice site for the excitatory synapse formation and the 7th-follistatin-like domain for the filopodia-induce activity. This finding is the first evidence for a role of the y-splice site of agrin and allows us to gain insights into new functions of agrin mRNA splicing in neocortical excitatory synapse development: while the formation of cholinergic specialization at the NMJ is regulated by agrin-y4z8, glutamatergic synapses in the CNS appear to be regulated by agrin-y4z0.

The TM-agrin-mediated-increase of excitatory synapses required the expression of Lrp4. However, it did not require direct binding of TM-agrin to Lrp4. Thus, the formation of the NMJ and of excitatory synapses in the CNS differ in their requirement of a direct interaction of Lrp4 and TM-agrin. I hypothesize that there might be an indirect interaction between both molecules. In principle, this could be mediated by several candidate molecules. One potential candidate is the amyloid precursor protein (APP). APP, Lrp4 and agrin have been shown to cooperate and bind to each other during synaptogenesis and maintenance of the NMJ (Choi et al., 2013; Cotman et al., 2000). APP and agrin share a heparin/heparan-sulfate binding domain: the E2 domain of APP is required for APP's binding to heparansulfate, whereas the presence of four amino acid insert at y-splice site of agrin increases the binding affinity of TM-agrin with heparansulfate (Gesemann et al., 1996). In addition, Lrp4 binds directly to APP via its extracellular domain (Pohlkamp et al., 2015). Therefore, it is possible that TM-agrin together with APP and Lrp4 form a complex which regulates the formation of excitatory synapses in the CNS, possibly via the intracellular domain containing PDZ-containing domain of Lrp4 (Tian et al., 2006).

To investigate the hypothesis of an agrin/APP interaction, I analyzed APP puncta density following overexpression of distinct TM-agrin splice variants. TM-agrin-y4z8 and TM-agrin-y4z0, but not TM-agrin-y0z0, increased the density of APP puncta on dendrites. This suggests that the presence of the four amino acid insert at the y-splice site, but not the Lrp4-binding domain itself, was required for the increase of APP puncta density after TM-agrin overexpression *in vitro.* A similar effect of TM-agrin overexpression was observed in the case of the excitatory synapse markers PSD-95 and NR1, further supporting the idea that APP

cooperates with TM-agrin and Lrp4 to increase the density of excitatory synapse-associated specializations.

The role of TM-agrin, Lrp4 and MuSK during inhibitory synapse development

Since the pan-synaptic marker bassoon did not display any change following TM-agrin overexpression *in vitro*, I hypothesized that the increase in excitatory synapse density might be accompanied by a similar decrease of inhibitory synapses. This would indicate that TM-agrin controls inhibitory synapse formation as well. In agreement with the hypothesis, I observed a reduction in the density of synaptic puncta containing inhibitory specializations, such as vGAT, gephyrin, collybistin and the α1-subunit of the $GABA_AR$, after TM-agrin overexpression *in vitro*. Moreover, overexpression of TM-agrin affected only synapse-associated proteins, but not extrasynaptic inhibitory-associated protein, such as the α5-subunit of the $GABA_AR$. These results demonstrate that TM-agrin overexpression specifically altered excitatory and inhibitory synapse density and that both type of synapses were affected in the opposite direction, i.e. an increase of excitatory- and a decrease of inhibitory synaptic specializations, without influencing the distribution of the inhibitory extrasynaptic neurotransmitter receptors. Since inhibitory neurotransmitter receptors exist in synaptic as well as in extrasynaptic pools, it remains to be determined, if agrin selectively affects either one of these pools or if it affects the relative distribution of proteins between both pools.

The effect of TM-agrin overexpression on inhibitory synapses was independent of the presence of MuSK. Thus, similar to the effect of TM-agrin overexpression on excitatory synapses, MuSK was not required for the TM-agrin-mediated effect to downregulate inhibitory synapses in neocortical cultures. Surprisingly, Lrp4 acted in an opposite manner compared to TM-agrin, i.e. TM-agrin-overexpression and Lrp4-deficiency reduced the density of inhibitory synapses. This would support the hypothesis that both molecules, Lrp4 and TM-agrin, control inhibitory synapse formation via independent mechanisms. Moreover, Lrp4-deficient brains *in vivo* were previously reported to have a significant reduction of the γ2-subunit of the $GABA_AR$ expression level in the hippocampus (Gomez et al., 2014), suggesting a crucial function of Lrp4 in regulating the formation and/or maintenance of inhibitory synapses, *in vitro* and *in vivo.*

Domain of TM-agrin that regulates inhibitory synapse development

In my thesis, I provide evidence that the presence of the conserved serine 17 was necessary for the TM-agrin-mediated effect on inhibitory synapses. Point mutation of serine to aspartic acid (phosphomimetic mutation) could reduce inhibitory synapse density, whereas the

point mutation of serine to alanine (an amino acid that cannot be phosphorylated) showed no reduction. This demonstrates the importance of serine 17 for inhibitory synapse formation and further suggests that the phosphorylation of serine 17 might regulate TM-agrin's effect on inhibitory synapses.

Phosphorylation is a common post-translational modification, which controls the function of many proteins. Gephyrin itself, for example, is subject to post-translational phosphorylation and this modification regulates the aggregation of gephyrin at synapses via putative extracellular signal regulated kinase 1/2 and glycogen synthase kinase 3β (Battaglia et al., 2018; Bausen et al., 2010; Kuhse et al., 2012; Tyagarajan et al., 2011). Mutating serine 17 to alanine or aspartic acid did not affect excitatory synapse density (data not shown), demonstrating that the serine-residue influenced specifically inhibitory synapses. This stands in favor of opposing effects of TM-agrin overexpression on glutamatergic and GABAergic synapses, with two different domains within TM-agrin being responsible for excitatory and inhibitory synapse formations.

The effect of TM-agrin overexpression in synapse-related plasticity in adult cortex

In wildtype mice, immunoreactivity with an antibody specific for TM-agrin in the cortices colocalized with a subset of excitatory synapses, but not with inhibitory synapses. This is consistent with previously published data (Ksiazek et al., 2007) which showed a colocalization of PSD-95 with a pan-specific anti-agrin antiserum and an absence of colocalization with the α2-subunit of the $GABA_AR$. The absence of a colocalization of TM-agrin and gephyrin suggests that the reduction of inhibitory synapses after TM-agrin's overexpression does not require the concentration of TM-agrin at inhibitory synapses. It seems likely, therefore, that the activation of an intracellular signaling cascade possibly via serine 17 phosphorylation is sufficient for the formation of the postsynaptic specialization of inhibitory synapses. In addition, I observed that not all of the PSD-95 puncta colocalized with TM-agrin, suggesting that only specific isoforms of TM-agrin are concentrated at excitatory synapses or that only a subset of excitatory synapses is immunopositive for TM-agrin. Further studies are clearly required to elucidate the molecular mechanisms and the intracellular signaling cascades activated by TM-agrin which regulate the density of excitatory and inhibitory synapses *in vivo.*

Agrin is not only essential during NMJ development, but also for stabilizing synaptic specializations at adult NMJ (Samuel et al., 2012). It has previously been shown also that agrin expression is upregulated following traumatic brain injury (Falo et al., 2008), suggesting a role of agrin also during periods of synaptic-plasticity in the adult brain. To learn if TM-agrin might

similarly be involved in synapse maintenance in the adult brain, I characterized mice that conditionally overexpressed TM-agrin-y4z0 after tamoxifen administration, under the control of the CamKIIa promoter, which is selectively expressed in glutamatergic neurons of the neocortex (Schick, 2018). Following validation of TM-agrin overexpression by analyzing TM-agrin transcript and protein levels, I investigated the expression of synapse-associated proteins. I observed a significant increase in vGlut1, PSD-95, the NR1-subunit of the NMDAR transcript levels. This increase in mRNA levels was accompanied by a concomitant increase in their dendritic puncta densities. Both changes occurred in adult mice 14 days after tamoxifen-induced TM-agrin overexpression. In addition, Anna Schick showed that spine head size and PSD-95 puncta intensity were specifically increased in the apical dendrite of pyramidal neurons of the neocortex and hippocampus of TM-agrin-overexpressing mice (Schick, 2018). These morphological changes at excitatory synapses were in agreement with a previous publication showing that agrin-deficient brain had fewer dendritic spines and a reduction of mEPSCs frequency, suggesting that these mice have fewer functional excitatory synapses (Ksiazek et al., 2007). Together these results support a critical role of TM-agrin not only during synaptogenesis in the developing brain, but also in the maintenance of synapses in the adult brain *in vivo*.

Analysis of the inhibitory synapse density has shown that TM-agrin overexpression led to a decrease of both pre- and postsynaptic inhibitory synaptic proteins, such as vGAT, gephyrin and collybistin. Although these results were in line with my *in vitro* evidence, they represent a discrepancy to the lack of changes at inhibitory synapses as well as in mIPSCs frequency and amplitude in agrin-deficient brains (Ksiazek et al., 2007). My identification of serine 17 as an essential part of TM-agrin required for the downregulation of inhibitory synapses might offer an explanation for this discrepancy. The mouse line with an agrin-deficient brain was generated by crossing agrin knockout mice with a mouse line in which NtA-agrin was expressed selectively in HB9-positive neurons, *i.e.* motoneurons (Ksiazek et al., 2007). This rescued the perinatal lethality of the mice and allowed the analysis of agrin-deficient brains. The agrin knockout mice were generated by inserting a neomycin cassette downstream of exon 5, leading to a deletion of exons 6-33. However, exon 1-5 might still be transcribed (Lin et al., 2001). Accordingly, these mice might still express a truncated TM-agrin protein containing the intracellular and the transmembrane domains of TM-agrin. Since this part of TM-agrin was sufficient for the downregulation of inhibitory synapses, the distribution and expression of inhibitory synapse-associated proteins might not be observed in this agrin-deficient brain. Along the same line: the identification of serine 17 as essential for TM-agrin's downregulation also explains, why the addition of soluble agrin, in which the intracellular domain is not present,

to cortical microisland cultures showed no effect on the frequency and the amplitude of mIPSCs (Handara et al., 2019).

Interestingly, unlike the unaffected extrasynaptic inhibitory component during synaptogenesis *in vitro*, TM-agrin overexpression *in vivo* affected all inhibitory synapse-associated proteins, including the extrasynaptic α5-subunit of the $GABA_AR$. One possible explanation why this subunit was affected *in vivo* but not *in vitro* could be that TM-agrin might exert different effects on GABAergic synapses depending on the developmental status (i.e. developing vs adult neurons) of the synapses. Moreover, it should be kept in mind that the exact role of the extrasynaptic α5-subunit of the $GABA_AR$ during synapse development and adulthood is not entirely clear (Brady and Jacob, 2015), which precludes a precise interpretation of how TM-agrin might differentially regulate synaptic and extrasynaptic inhibitory neurotransmitter receptors.

In agreement with the *in vitro* result, the density of puncta labeled by the pan-synaptic protein bassoon was also not altered *in vivo* following TM-agrin overexpression. Therefore, the opposing effects of TM-agrin overexpression on excitatory and inhibitory synapses might keep the total number of synapses at a relatively constant level, suggesting a possibly role of TM-agrin in the maintenance of an adequate excitatory/inhibitory balance.

Conclusion

In summary, both Lrp4 and MuSK are required for normal dendritic arborization and TM-agrin affects dendritic arborization by acting in concert with MuSK. TM-agrin's effect on excitatory synapses requires Lrp4, whereas the TM-agrin-mediated downregulation of inhibitory synapse does not require Lrp4. MuSK appears not to be involved at all in synapse development. Two different regions of TM-agrin affect the control of the two types of synapses: the presence of four amino acids at the y-splice site of TM-agrin is essential for excitatory synapse regulation, whereas the presence of the conserved intracellular serine residue 17 regulates the inhibitory synapses. Together these data unveil specific and selective roles for TM-agrin, Lrp4 and MuSK in dendritic arborization and synapse formation during development *in vitro* and in the adult CNS *in vivo*. Moreover, my results further support the hypothesis that the formation and maintenance of the neuromuscular junction and of synapses in the CNS share common molecular determinants.

Acknowledgments

I would like to thank my Ph.D. supervisor, **Prof. Stephan Kröger,** for the opportunity to conduct my research project in his lab. Thank you for all the supports and the exchange of ideas. Importantly, thank you for the patience to teach me how to give a scientific talk, write a thesis and create a scientific poster. Moreover, I am also grateful to have the freedom to explore and conduct my Ph.D. project.

Furthermore, I would like to thank **Prof. Magdalena Götz** and the Graduate School **HELENA** at the Helmholtz Center München for the funding during my Ph.D and also for supporting me to participate in several workshops, conferences and lab-exchanges.

Thank you **Prof. Fritz Rathjen** for the opportunity to do experiments at the MDC Berlin. Thank you for providing and organizing the breeding of the Lrp4-KO and the MuSK-KO mice.

I am so grateful to have a wonderful colleagues **Laura Gerwin**, **Anna Schick**, **Martina Bürkle, Ilaria Vitali** and **Johannes Geisinger**. Thank you so much for all the advises, cares and great time together. For Martina and Ilaria, thank you so much for your technical assistances! Martina, thank you for teaching me how to speak german. Ilaria, thank you for critically reading my whole thesis and also for providing the figure 15a.

Thank you **Ines Mühlhahn** for your help in the cloning lab. **Tatiana Simon-Ebert**, thank you for organizing the plug-check of the mice. Thank you Chu-Lan Lao, Sergio Gascon, Corinna Haupt, Elisa Murenu and Riccardo Bocchi, for the opinions and all the discussions.

Thank you **Sarah Rossmanith**, **Hedwig Barbey** and **Michel Knörr** for being presence in the lab and your inputs during the lab meetings.

I would like to thank **Elsa Melo**, **Lana Polero**, **Eva-Maria Bushart** and **Suada** for their administrative supports.

Also, I thank my fellow friends **Iris Marti** and **Marie-Claire Ung**. Thank you for your supports during my Ph.D. period.

Last but not least, thank you so much to my parent (papa **Budi,** mama **Regina,** tante **Linda**), sisters (**Monna, Maria, Xessyl, Novi**), brothers (**Ano and Cello**) and cousins (ci **Feni** and ci **Lia**). Thank you for always being there, although we're physically separated for almost 10.901 km away. I love you all!

Gerry

Bibliography

Alldred, M.J., Mulder-Rosi, J., Lingenfelter, S.E., Chen, G., Luscher, B., 2005. Distinct gamma2 subunit domains mediate clustering and synaptic function of postsynaptic GABAA receptors and gephyrin. *J Neurosci* 25, 594-603.

Annies, M., Bittcher, G., Ramseger, R., Loschinger, J., Woll, S., Porten, E., Abraham, C., Ruegg, M.A., Kröger, S., 2006. Clustering transmembrane-agrin induces filopodia-like processes on axons and dendrites. *Mol Cell Neurosci* 31, 515-524.

Barber, A.J., Lieth, E., 1997. Agrin accumulates in the brain microvascular basal lamina during development of the blood-brain barrier. *Dev Dyn* 208, 62-74.

Battaglia, S., Renner, M., Russeau, M., Come, E., Tyagarajan, S.K., Levi, S., 2018. Activity-Dependent Inhibitory Synapse Scaling Is Determined by Gephyrin Phosphorylation and Subsequent Regulation of GABAA Receptor Diffusion. *eNeuro* 5.

Bauerfeind, R., Huttner, W.B., 1993. Biogenesis of constitutive secretory vesicles, secretory granules and synaptic vesicles. *Curr Opin Cell Biol* 5, 628-635.

Bausen, M., Weltzien, F., Betz, H., O'Sullivan, G.A., 2010. Regulation of postsynaptic gephyrin cluster size by protein phosphatase 1. *Mol Cell Neurosci* 44, 201-209.

Bedet, C., Bruusgaard, J.C., Vergo, S., Groth-Pedersen, L., Eimer, S., Triller, A., Vannier, C., 2006. Regulation of gephyrin assembly and glycine receptor synaptic stability. *J Biol Chem* 281, 30046-30056.

Béïque, J.-C., Lin, D.-T., Kang, M.-G., Aizawa, H., Takamiya, K., Huganir, R.L., 2006. Synapse-specific regulation of AMPA receptor function by PSD-95. *Proc Natl Acad Sci USA* 103, 19535-19540.

Bezakova, G., Helm, J.P., Francolini, M., Lomo, T., 2001. Effects of purified recombinant neural and muscle agrin on skeletal muscle fibers in vivo. *J Cell Biol* 153, 1441-1452.

Biederer, T., Kaeser, P.S., Blanpied, T.A., 2017. Transcellular Nanoalignment of Synaptic Function. *Neuron* 96, 680-696.

Bijata, M., Wlodarczyk, J., Figiel, I., 2015. Dystroglycan controls dendritic morphogenesis of hippocampal neurons in vitro. *Front Cell Neurosci* 9, 199.

Blom, N., Gammeltoft, S., Brunak, S., 1999. Sequence and structure-based prediction of eukaryotic protein phosphorylation sites. *J Mol Biol* 294, 1351-1362.

Blom, N., Sicheritz-Ponten, T., Gupta, R., Gammeltoft, S., Brunak, S., 2004. Prediction of post-translational glycosylation and phosphorylation of proteins from the amino acid sequence. *Proteomics* 4, 1633-1649.

Bose, C.M., Qiu, D., Bergamaschi, A., Gravante, B., Bossi, M., Villa, A., Rupp, F., Malgaroli, A., 2000. Agrin controls synaptic differentiation in hippocampal neurons. *J Neurosci* 20, 9086-9095.

Brady, M.L., Jacob, T.C., 2015. Synaptic localization of alpha5 GABA (A) receptors via gephyrin interaction regulates dendritic outgrowth and spine maturation. *Dev Neurobiol* 75, 1241-1251.

Bresler, T., Shapira, M., Boeckers, T., Dresbach, T., Futter, M., Garner, C.C., Rosenblum, K., Gundelfinger, E.D., Ziv, N.E., 2004. Postsynaptic density assembly is fundamentally different from presynaptic active zone assembly. *J Neurosci* 24, 1507-1520.

Brodeur, J., Theriault, C., Lessard-Beaudoin, M., Marcil, A., Dahan, S., Lavoie, C., 2012. LDLR-related protein 10 (LRP10) regulates amyloid precursor protein (APP) trafficking and processing: evidence for a role in Alzheimer's disease. *Mol Neurodegener* 7, 31.

Burgess, R.W., Dickman, D.K., Nunez, L., Glass, D.J., Sanes, J.R., 2002. Mapping sites responsible for interactions of agrin with neurons. *J Neurochem* 83, 271-284.

Burgess, R.W., Nguyen, Q.T., Son, Y.J., Lichtman, J.W., Sanes, J.R., 1999. Alternatively spliced isoforms of nerve- and muscle-derived agrin: their roles at the neuromuscular junction. *Neuron* 23, 33-44.

Burgess, R.W., Skarnes, W.C., Sanes, J.R., 2000. Agrin isoforms with distinct amino termini: differential expression, localization, and function. *J Cell Biol* 151, 41-52.

Burk, K., Desoeuvre, A., Boutin, C., Smith, M.A., Kröger, S., Bosio, A., Tiveron, M.C., Cremer, H., 2012. Agrin-signaling is necessary for the integration of newly generated neurons in the adult olfactory bulb. *J Neurosci* 32, 3759-3764.

Cane, M., Maco, B., Knott, G., Holtmaat, A., 2014. The relationship between PSD-95 clustering and spine stability in vivo. *J Neurosci* 34, 2075-2086.

Carlin, R.K., Grab, D.J., Cohen, R.S., Siekevitz, P., 1980. Isolation and characterization of postsynaptic densities from various brain regions: enrichment of different types of postsynaptic densities. *J Cell Biol* 86, 831-845.

Cartaud, A., Stetzkowski-Marden, F., Maoui, A., Cartaud, J., 2011. Agrin triggers the clustering of raft-associated acetylcholine receptors through actin cytoskeleton reorganization. *Biology of the cell* 103, 287-301.

Chen, L., Chetkovich, D.M., Petralia, R.S., Sweeney, N.T., Kawasaki, Y., Wenthold, R.J., Bredt, D.S., Nicoll, R.A., 2000. Stargazin regulates synaptic targeting of AMPA receptors by two distinct mechanisms. *Nature* 408, 936-943.

Chen, W.J., Goldstein, J.L., Brown, M.S., 1990. NPXY, a sequence often found in cytoplasmic tails, is required for coated pit-mediated internalization of the low density lipoprotein receptor. *J Biol Chem* 265, 3116-3123.

Choi, H.Y., Liu, Y., Tennert, C., Sugiura, Y., Karakatsani, A., Kröger, S., Johnson, E.B., Hammer, R.E., Lin, W., Herz, J., 2013. APP interacts with LRP4 and agrin to coordinate the development of the neuromuscular junction in mice. *Elife* 2, e00220.

Coba, M.P., Pocklington, A.J., Collins, M.O., Kopanitsa, M.V., Uren, R.T., Swamy, S., Croning, M.D., Choudhary, J.S., Grant, S.G., 2009. Neurotransmitters drive combinatorial multistate postsynaptic density networks. *Sci Signal* 2(68):ra19

Colonnier, M., 1968. Synaptic patterns on different cell types in the different laminae of the cat visual cortex. An electron microscope study. *Brain Res* 9, 268-287.

Cotman, S.L., Halfter, W., Cole, G.J., 2000. Agrin binds to beta-amyloid (Abeta), accelerates abeta fibril formation, and is localized to Abeta deposits in Alzheimer's disease brain. *Mol Cell Neurosci* 15, 183-198.

Couteaux, R., Pecot-Dechavassine, M., 1970. [Synaptic vesicles and pouches at the level of "active zones" of the neuromuscular junction]. Comptes rendus hebdomadaires des seances de l'Academie des sciences. Serie D: Sciences naturelles 271, 2346-2349.

Craig, A.M., Graf, E.R., Linhoff, M.W., 2006. How to build a central synapse: clues from cell culture. *Trends Neurosci* 29, 8-20.

Daniels, M.P., 2012. The role of agrin in synaptic development, plasticity and signaling in the central nervous system. *Neurochem Int* 61, 848-853.

De Roo, M., Klauser, P., Garcia, P.M., Poglia, L., Muller, D., 2008a. Spine dynamics and synapse remodeling during LTP and memory processes. *Prog Brain Res* 169, 199-207.

De Roo, M., Klauser, P., Mendez, P., Poglia, L., Muller, D., 2008b. Activity-dependent PSD formation and stabilization of newly formed spines in hippocampal slice cultures. *Cerebral Cortex* (New York, N.Y. : 1991) 18, 151-161.

De Roo, M., Klauser, P., Muller, D., 2008c. LTP promotes a selective long-term stabilization and clustering of dendritic spines. *PLoS Biology* 6, e219.

DeChiara, T.M., Bowen, D.C., Valenzuela, D.M., Simmons, M.V., Poueymirou, W.T., Thomas, S., Kinetz, E., Compton, D.L., Rojas, E., Park, J.S., Smith, C., DiStefano, P.S., Glass, D.J., Burden, S.J., Yancopoulos, G.D., 1996. The receptor tyrosine kinase MuSK is required for neuromuscular junction formation in vivo. *Cell* 85, 501-512.

Dejanovic, B., Semtner, M., Ebert, S., Lamkemeyer, T., Neuser, F., Luscher, B., Meier, J.C., Schwarz, G., 2014. Palmitoylation of gephyrin controls receptor clustering and plasticity of GABAergic synapses. *PLoS biology* 12, e1001908.

Denzer, A.J., Hauser, D.M., Gesemann, M., Ruegg, M.A., 1997. Synaptic differentiation: the role of agrin in the formation and maintenance of the neuromuscular junction. *Cell Tissue Res* 290, 357-365.

Dong, Y.N., Waxman, E.A., Lynch, D.R., 2004. Interactions of Postsynaptic Density-95 and the NMDA Receptor 2 Subunit Control Calpain-Mediated Cleavage of the NMDA Receptor. *J Neurosci* 24, 11035-11045.

Dudas, B., Rose, M., Cornelli, U., Pavlovich, A., Hanin, I., 2008. Neuroprotective properties of glycosaminoglycans: potential treatment for neurodegenerative disorders. *Neuro-degenerative diseases* 5, 200-205.

Ehlers, M.D., 2003. Activity level controls postsynaptic composition and signaling via the ubiquitin-proteasome system. *Nat Neurosci* 6, 231-242.

Ehrlich, I., Klein, M., Rumpel, S., Malinow, R., 2007. PSD-95 is required for activity-driven synapse stabilization. *Proc Natl Acad Sci USA* 104, 4176-4181.

El-Husseini, A.E., Schnell, E., Chetkovich, D.M., Nicoll, R.A., Bredt, D.S., 2000. PSD-95 involvement in maturation of excitatory synapses. *Science* 290, 1364-1368.

Elias, G.M., Elias, L.A., Apostolides, P.F., Kriegstein, A.R., Nicoll, R.A., 2008. Differential trafficking of AMPA and NMDA receptors by SAP102 and PSD-95 underlies synapse development. *Proc Natl Acad Sci USA* 105, 20953-20958.

Erdmann, G., Schutz, G., Berger, S., 2007. Inducible gene inactivation in neurons of the adult mouse forebrain. *BMC Neurosci* 8, 63.

Ethell, I.M., Pasquale, E.B., 2005. Molecular mechanisms of dendritic spine development and remodeling. *Prog Neurobiol* 75, 161-205.

Falo, M.C., Reeves, T.M., Phillips, L.L., 2008. Agrin expression during synaptogenesis induced by traumatic brain injury. *J Neurotrauma* 25, 769-783.

Feng, G., Tintrup, H., Kirsch, J., Nichol, M.C., Kuhse, J., Betz, H., Sanes, J.R., 1998. Dual requirement for gephyrin in glycine receptor clustering and molybdoenzyme activity. *Science* 282, 1321-1324.

Ferns, M., Deiner, M., Hall, Z., 1996. Agrin-induced acetylcholine receptor clustering in mammalian muscle requires tyrosine phosphorylation. *J Cell Biol* 132, 937-944.

Ferreira, A., 1999. Abnormal synapse formation in agrin-depleted hippocampal neurons. *J Cell Sci* 112 (Pt 24), 4729-4738.

Fischer, F., Kneussel, M., Tintrup, H., Haverkamp, S., Rauen, T., Betz, H., Wassle, H., 2000. Reduced synaptic clustering of GABA and glycine receptors in the retina of the gephyrin null mutant mouse. *J Comp Neurol*427, 634-648.

Fuhrmann, J.C., Kins, S., Rostaing, P., El Far, O., Kirsch, J., Sheng, M., Triller, A., Betz, H., Kneussel, M., 2002. Gephyrin interacts with Dynein light chains 1 and 2, components of motor protein complexes. *J Neurosci* 22, 5393-5402.

Funke, L., Dakoji, S., Bredt, D.S., 2005. Membrane-associated guanylate kinases regulate adhesion and plasticity at cell junctions. *Annu Rev Biochem* 74, 219-245.

Furshpan, E.J., Potter, D.D., 1957. Mechanism of nerve-impulse transmission at a crayfish synapse. *Nature* 180, 342-343.

Garcia-Osta, A., Tsokas, P., Pollonini, G., Landau, E.M., Blitzer, R., Alberini, C.M., 2006. MuSK expressed in the brain mediates cholinergic responses, synaptic plasticity, and memory formation. *J Neurosci* 26, 7919-7932.

Gardiol, A., Racca, C., Triller, A., 1999. Dendritic and postsynaptic protein synthetic machinery. *J Neurosci* 19, 168-179.

Gautam, M., DeChiara, T.M., Glass, D.J., Yancopoulos, G.D., Sanes, J.R., 1999. Distinct phenotypes of mutant mice lacking agrin, MuSK, or rapsyn. Brain research. *Dev Brain Res* 114, 171-178.

Gautam, M., Noakes, P.G., Moscoso, L., Rupp, F., Scheller, R.H., Merlie, J.P., Sanes, J.R., 1996. Defective neuromuscular synaptogenesis in agrin-deficient mutant mice. *Cell* 85, 525-535.

Gerrow, K., El-Husseini, A., 2006. Cell adhesion molecules at the synapse. *Frontiers Bioscience* 11, 2400-2419.

Gerrow, K., Romorini, S., Nabi, S.M., Colicos, M.A., Sala, C., El-Husseini, A., 2006. A preformed complex of postsynaptic proteins is involved in excitatory synapse development. *Neuron* 49, 547-562.

Gesemann, M., Brancaccio, A., Schumacher, B., Ruegg, M.A., 1998. Agrin is a high-affinity binding protein of dystroglycan in non-muscle tissue. *J Biol Chem* 273, 600-605.

Gesemann, M., Cavalli, V., Denzer, A.J., Brancaccio, A., Schumacher, B., Ruegg, M.A., 1996. Alternative splicing of agrin alters its binding to heparin, dystroglycan, and the putative agrin receptor. *Neuron* 16, 755-767.

Gesemann, M., Denzer, A.J., Ruegg, M.A., 1995. Acetylcholine receptor-aggregating activity of agrin isoforms and mapping of the active site. *J Cell Biol* 128, 625-636.

Glass, D.J., Bowen, D.C., Stitt, T.N., Radziejewski, C., Bruno, J., Ryan, T.E., Gies, D.R., Shah, S., Mattsson, K., Burden, S.J., DiStefano, P.S., Valenzuela, D.M., DeChiara, T.M., Yancopoulos, G.D., 1996a. Agrin acts via a MuSK receptor complex. *Cell* 85, 513-523.

Glass, D.J., DeChiara, T.M., Stitt, T.N., DiStefano, P.S., Valenzuela, D.M., Yancopoulos, G.D., 1996b. The receptor tyrosine kinase MuSK is required for neuromuscular junction formation and is a functional receptor for agrin. *Cold Spring Harb Symp Quant Biol* 61, 435-444.

Gomez, A.M., Froemke, R.C., Burden, S.J., 2014. Synaptic plasticity and cognitive function are disrupted in the absence of Lrp4. *Elife* 3, e04287.

Gotthardt, M., Trommsdorff, M., Nevitt, M.F., Shelton, J., Richardson, J.A., Stockinger, W., Nimpf, J., Herz, J., 2000. Interactions of the low density lipoprotein receptor gene family with cytosolic adaptor and scaffold proteins suggest diverse biological functions in cellular communication and signal transduction. *J Biol Chem* 275, 25616-25624.

Grady, R.M., Zhou, H., Cunningham, J.M., Henry, M.D., Campbell, K.P., Sanes, J.R., 2000. Maturation and maintenance of the neuromuscular synapse: genetic evidence for roles of the dystrophin--glycoprotein complex. *Neuron* 25, 279-293.

Graf, E.R., Zhang, X., Jin, S.X., Linhoff, M.W., Craig, A.M., 2004. Neurexins induce differentiation of GABA and glutamate postsynaptic specializations via neuroligins. *Cell* 119, 1013-1026.

Gramolini, A.O., Burton, E.A., Tinsley, J.M., Ferns, M.J., Cartaud, A., Cartaud, J., Davies, K.E., Lunde, J.A., Jasmin, B.J., 1998. Muscle and neural isoforms of agrin increase utrophin expression in cultured myotubes via a transcriptional regulatory mechanism. *J Biol Chem* 273, 736-743.

Gray, E.G., 1959. Axo-somatic and axo-dendritic synapses of the cerebral cortex: an electron microscope study. *J Anat* 93, 420-433.

Grutzendler, J., Kasthuri, N., Gan, W.B., 2002. Long-term dendritic spine stability in the adult cortex. *Nature* 420, 812-816.

Handara, G., Hetsch, F.J.A., Juttner, R., Schick, A., Haupt, C., Rathjen, F.G., Kröger, S., 2019. The role of agrin, Lrp4 and MuSK during dendritic arborization and synaptogenesis in cultured embryonic CNS neurons. *Dev Biol*. 1;445(1):54-67.

Harris, K.M., Jensen, F.E., Tsao, B., 1992. Three-dimensional structure of dendritic spines and synapses in rat hippocampus (CA1) at postnatal day 15 and adult ages: implications for the maturation of synaptic physiology and long-term potentiation. *J Neurosci* 12, 2685-2705.

Herculano-Houzel, S., 2009. The human brain in numbers: a linearly scaled-up primate brain. *Front Hum Neurosci* 3, 31.

Hiester, B.G., Galati, D.F., Salinas, P.C., Jones, K.R., 2013. Neurotrophin and Wnt signaling cooperatively regulate dendritic spine formation. *Mol Cell Neurosci* 56, 115-127.

Holtmaat, A., De Paola, V., Wilbrecht, L., Knott, G.W., 2008. Imaging of experience-dependent structural plasticity in the mouse neocortex in vivo. *Behav Brain Res* 192, 20-25.

Holtmaat, A.J., Trachtenberg, J.T., Wilbrecht, L., Shepherd, G.M., Zhang, X., Knott, G.W., Svoboda, K., 2005. Transient and persistent dendritic spines in the neocortex in vivo. *Neuron* 45, 279-291.

Hopf, C., Hoch, W., 1996. Agrin binding to alpha-dystroglycan. Domains of agrin necessary to induce acetylcholine receptor clustering are overlapping but not identical to the alpha-dystroglycan-binding region. *J Biol Chem* 271, 5231-5236.

Hopf, C., Hoch, W., 1998. Tyrosine phosphorylation of the muscle-specific kinase is exclusively induced by acetylcholine receptor-aggregating agrin fragments. *Eur J Biochem* / FEBS 253, 382-389.

Hormuzdi, S.G., Filippov, M.A., Mitropoulou, G., Monyer, H., Bruzzone, R., 2004. Electrical synapses: a dynamic signaling system that shapes the activity of neuronal networks. *Biochimica Biophysica Acta* 1662, 113-137.

Huganir, R.L., Delcour, A.H., Greengard, P., Hess, G.P., 1986. Phosphorylation of the nicotinic acetylcholine receptor regulates its rate of desensitization. *Nature* 321, 774-776.

Huganir, R.L., Greengard, P., 1983. cAMP-dependent protein kinase phosphorylates the nicotinic acetylcholine receptor. *Proc Natl Acad Sci USA* 80, 1130-1134.

Huganir, R.L., Miles, K., 1989. Protein phosphorylation of nicotinic acetylcholine receptors. *Crit Rev Biochem Mol Biol* 24, 183-215.

Iki, J., Inoue, A., Bito, H., Okabe, S., 2005. Bi-directional regulation of postsynaptic cortactin distribution by BDNF and NMDA receptor activity. *Eur J Neurosci* 22, 2985-2994.

Inoue, A., Sanes, J.R., 1997. Lamina-specific connectivity in the brain: regulation by N-cadherin, neurotrophins, and glycoconjugates. *Science* 276, 1428-1431.

Irie, M., Hata, Y., Takeuchi, M., Ichtchenko, K., Toyoda, A., Hirao, K., Takai, Y., Rosahl, T.W., Sudhof, T.C., 1997. Binding of neuroligins to PSD-95. *Science* 277, 1511-1515.

Jan, Y.N., Jan, L.Y., 2010. Branching out: mechanisms of dendritic arborization. *Nat Rev Neurosci* 11, 316-328.

Janin, J., 1979. Surface and inside volumes in globular proteins. *Nature* 277, 491-492.

Jedlicka, P., Papadopoulos, T., Deller, T., Betz, H., Schwarzacher, S.W., 2009. Increased network excitability and impaired induction of long-term potentiation in the dentate gyrus of collybistin-deficient mice in vivo. *Mol Cell Neurosci* 41, 94-100.

Jennings, C.G., Dyer, S.M., Burden, S.J., 1993. Muscle-specific trk-related receptor with a kringle domain defines a distinct class of receptor tyrosine kinases. *Proc Natl Acad Sci USA* 90, 2895-2899.

Jing, L., Lefebvre, J.L., Gordon, L.R., Granato, M., 2009. Wnt signals organize synaptic prepattern and axon guidance through the zebrafish unplugged/MuSK receptor. *Neuron* 61, 721-733.

Ju, W., Morishita, W., Tsui, J., Gaietta, G., Deerinck, T.J., Adams, S.R., Garner, C.C., Tsien, R.Y., Ellisman, M.H., Malenka, R.C., 2004. Activity-dependent regulation of dendritic synthesis and trafficking of AMPA receptors. *Nat Neurosci* 7, 244-253.

Kang, J.S., Bae, G.U., Yi, M.J., Yang, Y.J., Oh, J.E., Takaesu, G., Zhou, Y.T., Low, B.C., Krauss, R.S., 2008. A Cdo-Bnip-2-Cdc42 signaling pathway regulates p38alpha/beta MAPK activity and myogenic differentiation. *J Cell Biol* 182, 497-507.

Karakatsani, A., Marichal, N., Urban, S., Kalamakis, G., Ghanem, A., Schick, A., Zhang, Y., Conzelmann, K.K., Ruegg, M.A., Berninger, B., de Almodovar, C.R., Gascon, S., Kröger, S., 2017. Neuronal LRP4 regulates synapse formation in the developing CNS. *Development*.

Kasai, H., Matsuzaki, M., Noguchi, J., Yasumatsu, N., Nakahara, H., 2003. Structure-stability-function relationships of dendritic spines. *Trends Neurosci* 26, 360-368.

Kennedy, M.B., 2000. Signal-processing machines at the postsynaptic density. *Science* 290, 750-754.

Kennedy, M.J., Ehlers, M.D., 2006. Organelles and trafficking machinery for postsynaptic plasticity. *Annu Rev Neurosci* 29, 325-362.

Khan, A.A., Bose, C., Yam, L.S., Soloski, M.J., Rupp, F., 2001. Physiological regulation of the immunological synapse by agrin. *Science* 292, 1681-1686.

Kim, E.Y., Schrader, N., Smolinsky, B., Bedet, C., Vannier, C., Schwarz, G., Schindelin, H., 2006. Deciphering the structural framework of glycine receptor anchoring by gephyrin. *EMBO* 25, 1385-1395.

Kim, N., Stiegler, A.L., Cameron, T.O., Hallock, P.T., Gomez, A.M., Huang, J.H., Hubbard, S.R., Dustin, M.L., Burden, S.J., 2008. Lrp4 is a receptor for Agrin and forms a complex with MuSK. *Cell* 135, 334-342.

Kins, S., Betz, H., Kirsch, J., 2000. Collybistin, a newly identified brain-specific GEF, induces submembrane clustering of gephyrin. *Nat Neurosci* 3, 22-29.

Kirsch, J., Wolters, I., Triller, A., Betz, H., 1993. Gephyrin antisense oligonucleotides prevent glycine receptor clustering in spinal neurons. *Nature* 366, 745-748.

Klenowski, P.M., Fogarty, M.J., Belmer, A., Noakes, P.G., Bellingham, M.C., Bartlett, S.E., 2015. Structural and functional characterization of dendritic arbors and GABAergic synaptic inputs on interneurons and principal cells in the rat basolateral amygdala. *J Neurophysiol* 114, 942-957.

Kneussel, M., Haverkamp, S., Fuhrmann, J.C., Wang, H., Wassle, H., Olsen, R.W., Betz, H., 2000. The gamma-aminobutyric acid type A receptor (GABAAR)-associated protein GABARAP interacts with gephyrin but is not involved in receptor anchoring at the synapse. *Proc Natl Acad Sci USA* 97, 8594-8599.

Kornau, H.C., Schenker, L.T., Kennedy, M.B., Seeburg, P.H., 1995. Domain interaction between NMDA receptor subunits and the postsynaptic density protein PSD-95. *Science* 269, 1737-1740.

Koulen, P., Honig, L.S., Fletcher, E.L., Kröger, S., 1999. Expression, distribution and ultrastructural localization of the synapse-organizing molecule agrin in the mature avian retina. *Eur J Neurosci* 11, 4188-4196.

Kröger, S., Pfister, H., 2009. Agrin in the nervous system: synaptogenesis and beyond. *Future Neurology* 4, 67-86.

Ksiazek, I., Burkhardt, C., Lin, S., Seddik, R., Maj, M., Bezakova, G., Jucker, M., Arber, S., Caroni, P., Sanes, J.R., Bettler, B., Ruegg, M.A., 2007. Synapse loss in cortex of agrin-deficient mice after genetic rescue of perinatal death. *J Neurosci* 27, 7183-7195.

Kuhse, J., Kalbouneh, H., Schlicksupp, A., Mukusch, S., Nawrotzki, R., Kirsch, J., 2012. Phosphorylation of gephyrin in hippocampal neurons by cyclin-dependent kinase CDK5 at Ser-270 is dependent on collybistin. *J Biol Chem* 287, 30952-30966.

Lane-Donovan, C., Philips, G.T., Herz, J., 2014. More than cholesterol transporters: lipoprotein receptors in CNS function and neurodegeneration. *Neuron* 83, 771-787.

Langosch, D., Hoch, W., Betz, H., 1992. The 93 kDa protein gephyrin and tubulin associated with the inhibitory glycine receptor are phosphorylated by an endogenous protein kinase. *FEBS Lett* 298, 113-117.

Lardi-Studler, B., Smolinsky, B., Petitjean, C.M., Koenig, F., Sidler, C., Meier, J.C., Fritschy, J.M., Schwarz, G., 2007. Vertebrate-specific sequences in the gephyrin E-domain regulate cytosolic aggregation and postsynaptic clustering. *J Cell Sci* 120, 1371-1382.

Lein, E.S., Hawrylycz, M.J., Ao, N., Ayres, M., Bensinger, A., Bernard, A., Boe, A.F., Boguski, M.S., Brockway, K.S., Byrnes, E.J., Chen, L., Chen, L., Chen, T.M., Chin, M.C., Chong, J., Crook, B.E., Czaplinska, A., Dang, C.N., Datta, S., Dee, N.R., Desaki, A.L., Desta, T.,

Diep, E., Dolbeare, T.A., Donelan, M.J., Dong, H.W., Dougherty, J.G., Duncan, B.J., Ebbert, A.J., Eichele, G., Estin, L.K., Faber, C., Facer, B.A., Fields, R., Fischer, S.R., Fliss, T.P., Frensley, C., Gates, S.N., Glattfelder, K.J., Halverson, K.R., Hart, M.R., Hohmann, J.G., Howell, M.P., Jeung, D.P., Johnson, R.A., Karr, P.T., Kawal, R., Kidney, J.M., Knapik, R.H., Kuan, C.L., Lake, J.H., Laramee, A.R., Larsen, K.D., Lau, C., Lemon, T.A., Liang, A.J., Liu, Y., Luong, L.T., Michaels, J., Morgan, J.J., Morgan, R.J., Mortrud, M.T., Mosqueda, N.F., Ng, L.L., Ng, R., Orta, G.J., Overly, C.C., Pak, T.H., Parry, S.E., Pathak, S.D., Pearson, O.C., Puchalski, R.B., Riley, Z.L., Rockett, H.R., Rowland, S.A., Royall, J.J., Ruiz, M.J., Sarno, N.R., Schaffnit, K., Shapovalova, N.V., Sivisay, T., Slaughterbeck, C.R., Smith, S.C., Smith, K.A., Smith, B.I., Sodt, A.J., Stewart, N.N., Stumpf, K.R., Sunkin, S.M., Sutram, M., Tam, A., Teemer, C.D., Thaller, C., Thompson, C.L., Varnam, L.R., Visel, A., Whitlock, R.M., Wohnoutka, P.E., Wolkey, C.K., Wong, V.Y., Wood, M., Yaylaoglu, M.B., Young, R.C., Youngstrom, B.L., Yuan, X.F., Zhang, B., Zwingman, T.A., Jones, A.R., 2007. Genome-wide atlas of gene expression in the adult mouse brain. *Nature* 445, 168-176.

Lepeta, K., Lourenco, M.V., Schweitzer, B.C., Martino Adami, P.V., Banerjee, P., Catuara-Solarz, S., de La Fuente Revenga, M., Guillem, A.M., Haidar, M., Ijomone, O.M., Nadorp, B., Qi, L., Perera, N.D., Refsgaard, L.K., Reid, K.M., Sabbar, M., Sahoo, A., Schaefer, N., Sheean, R.K., Suska, A., Verma, R., Vicidomini, C., Wright, D., Zhang, X.D., Seidenbecher, C., 2016. Synaptopathies: synaptic dysfunction in neurological disorders - A review from students to students. *J Neurochem* 138, 785-805.

Levi, S., Logan, S.M., Tovar, K.R., Craig, A.M., 2004. Gephyrin is critical for glycine receptor clustering but not for the formation of functional GABAergic synapses in hippocampal neurons. *J Neurosci* 24, 207-217.

Li, Y., Pawlik, B., Elcioglu, N., Aglan, M., Kayserili, H., Yigit, G., Percin, F., Goodman, F., Nurnberg, G., Cenani, A., Urquhart, J., Chung, B.D., Ismail, S., Amr, K., Aslanger, A.D., Becker, C., Netzer, C., Scambler, P., Eyaid, W., Hamamy, H., Clayton-Smith, J., Hennekam, R., Nurnberg, P., Herz, J., Temtamy, S.A., Wollnik, B., 2010. LRP4 mutations alter Wnt/beta-catenin signaling and cause limb and kidney malformations in Cenani-Lenz syndrome. *Am J Hum Genet* 86, 696-706.

Li, Z., Hilgenberg, L.G., O'Dowd, D.K., Smith, M.A., 1999. Formation of functional synaptic connections between cultured cortical neurons from agrin-deficient mice. *J Neurobiol* 39, 547-557.

Li, Z., Massengill, J.L., O'Dowd, D.K., Smith, M.A., 1997. Agrin gene expression in mouse somatosensory cortical neurons during development in vivo and in cell culture. *Neuroscience* 79, 191-201.

Li, Z., Okamoto, K., Hayashi, Y., Sheng, M., 2004. The importance of dendritic mitochondria in the morphogenesis and plasticity of spines and synapses. *Cell* 119, 873-887.

Lin, W., Burgess, R.W., Dominguez, B., Pfaff, S.L., Sanes, J.R., Lee, K.-F., 2001. Distinct roles of nerve and muscle in postsynaptic differentiation of the neuromuscular synapse. *Nature* 410, 1057.

Lohmann, C., Bonhoeffer, T., 2008. A role for local calcium signaling in rapid synaptic partner selection by dendritic filopodia. *Neuron* 59, 253-260.

Luscher, C., Nicoll, R.A., Malenka, R.C., Muller, D., 2000. Synaptic plasticity and dynamic modulation of the postsynaptic membrane. *Nat Neurosci* 3, 545-550.

Mantych, K.B., Ferreira, A., 2001. Agrin differentially regulates the rates of axonal and dendritic elongation in cultured hippocampal neurons. *J Neurosci* 21, 6802-6809.

Marques, M.J., Conchello, J.A., Lichtman, J.W., 2000. From plaque to pretzel: fold formation and acetylcholine receptor loss at the developing neuromuscular junction. *J Neurosci* 20, 3663-3675.

Marrs, G.S., Green, S.H., Dailey, M.E., 2001. Rapid formation and remodeling of postsynaptic densities in developing dendrites. *Nat Neurosci* 4, 1006-1013.

Mascarenhas, J.B., Ruegg, M.A., Sasaki, T., Eble, J.A., Engel, J., Stetefeld, J., 2005. Structure and laminin-binding specificity of the NtA domain expressed in eukaryotic cells. *Matrix Biol* 23, 507-513.

Matthews-Bellinger, J.A., Salpeter, M.M., 1983. Fine structural distribution of acetylcholine receptors at developing mouse neuromuscular junctions. *J Neurosci* 3, 644-657.

McCroskery, S., Bailey, A., Lin, L., Daniels, M.P., 2009. Transmembrane agrin regulates dendritic filopodia and synapse formation in mature hippocampal neuron cultures. *Neuroscience* 163, 168-179.

McCroskery, S., Chaudhry, A., Lin, L., Daniels, M.P., 2006. Transmembrane agrin regulates filopodia in rat hippocampal neurons in culture. *Mol Cell Neurosci* 33, 15-28.

McMahan, U.J., 1990. The agrin hypothesis. Cold Spring Harb Symp Quant Biol 55, 407-418.

Meier, T., Hauser, D.M., Chiquet, M., Landmann, L., Ruegg, M.A., Brenner, H.R., 1997. Neural Agrin Induces Ectopic Postsynaptic Specializations in Innervated Muscle Fibers. *J Neurosci* 17, 6534-6544.

Messeant, J., Dobbertin, A., Girard, E., Delers, P., Manuel, M., Mangione, F., Schmitt, A., Le Denmat, D., Molgo, J., Zytnicki, D., Schaeffer, L., Legay, C., Strochlic, L., 2015. MuSK frizzled-like domain is critical for mammalian neuromuscular junction formation and maintenance. *J Neurosci* 35, 4926-4941.

Metzger, D., Clifford, J., Chiba, H., Chambon, P., 1995. Conditional site-specific recombination in mammalian cells using a ligand-dependent chimeric Cre recombinase. *Proc Natl Acad Sci USA* 92, 6991-6995.

Meyer, G., Kirsch, J., Betz, H., Langosch, D., 1995. Identification of a gephyrin binding motif on the glycine receptor beta subunit. *Neuron* 15, 563-572.

Miermans, C.A., Kusters, R.P., Hoogenraad, C.C., Storm, C., 2017. Biophysical model of the role of actin remodeling on dendritic spine morphology. *PLoS One* 12, e0170113.

Miyata, S., Mori, Y., Fujiwara, T., Ikenaka, K., Matsuzaki, S., Oono, K., Katayama, T., Tohyama, M., 2005. Local protein synthesis by BDNF is potentiated in hippocampal neurons exposed to ephrins. Brain research. *Mol Brain Res* 134, 333-337.

Mosca, T.J., Luginbuhl, D.J., Wang, I.E., Luo, L., 2017. Presynaptic LRP4 promotes synapse number and function of excitatory CNS neurons. *Elife* 6.

Mukherjee, J., Kretschmannova, K., Gouzer, G., Maric, H.M., Ramsden, S., Tretter, V., Harvey, K., Davies, P.A., Triller, A., Schindelin, H., Moss, S.J., 2011. The residence time of GABA(A)Rs at inhibitory synapses is determined by direct binding of the receptor alpha1 subunit to gephyrin. *J Neurosci* 31, 14677-14687.

Nakagawa, T., Engler, J.A., Sheng, M., 2004. The dynamic turnover and functional roles of alpha-actinin in dendritic spines. *Neuropharmacol* 47, 734-745.

Neumann, F.R., Bittcher, G., Annies, M., Schumacher, B., Kröger, S., Ruegg, M.A., 2001. An alternative amino-terminus expressed in the central nervous system converts agrin to a type II transmembrane protein. *Mol Cell Neurosci* 17, 208-225.

Nikonenko, I., Boda, B., Steen, S., Knott, G., Welker, E., Muller, D., 2008. PSD-95 promotes synaptogenesis and multiinnervated spine formation through nitric oxide signaling. *J Cell Biol* 183, 1115-1127.

Nitkin, R.M., Smith, M.A., Magill, C., Fallon, J.R., Yao, Y.M., Wallace, B.G., McMahan, U.J., 1987. Identification of agrin, a synaptic organizing protein from Torpedo electric organ. *J Cell Biol* 105, 2471-2478.

Nusser, Z., Lujan, R., Laube, G., Roberts, J.D., Molnar, E., Somogyi, P., 1998. Cell type and pathway dependence of synaptic AMPA receptor number and variability in the hippocampus. *Neuron* 21, 545-559.

O'Connor, L.T., Lauterborn, J.C., Gall, C.M., Smith, M.A., 1994. Localization and alternative splicing of agrin mRNA in adult rat brain: transcripts encoding isoforms that aggregate acetylcholine receptors are not restricted to cholinergic regions. *J Neurosci* 14, 1141-1152.

O'Connor, L.T., Lauterborn, J.C., Smith, M.A., Gall, C.M., 1995. Expression of agrin mRNA is altered following seizures in adult rat brain. Brain research. *Mol Brain Res* 33, 277-287.

Okabe, S., Miwa, A., Okado, H., 2001. Spine formation and correlated assembly of presynaptic and postsynaptic molecules. *J Neurosci* 21, 6105-6114.

Okada, K., Inoue, A., Okada, M., Murata, Y., Kakuta, S., Jigami, T., Kubo, S., Shiraishi, H., Eguchi, K., Motomura, M., Akiyama, T., Iwakura, Y., Higuchi, O., Yamanashi, Y., 2006. The muscle protein Dok-7 is essential for neuromuscular synaptogenesis. *Science* 312, 1802-1805.

Ostroff, L.E., Fiala, J.C., Allwardt, B., Harris, K.M., 2002. Polyribosomes redistribute from dendritic shafts into spines with enlarged synapses during LTP in developing rat hippocampal slices. *Neuron* 35, 535-545.

Papadopoulos, T., Eulenburg, V., Reddy-Alla, S., Mansuy, I.M., Li, Y., Betz, H., 2008. Collybistin is required for both the formation and maintenance of GABAergic postsynapses in the hippocampus. *Mol Cell Neurosci* 39, 161-169.

Paradis, S., Harrar, D.B., Lin, Y., Koon, A.C., Hauser, J.L., Griffith, E.C., Zhu, L., Brass, L.F., Chen, C., Greenberg, M.E., 2007. An RNAi-based approach identifies molecules required for glutamatergic and GABAergic synapse development. *Neuron* 53, 217-232.

Parker, J.M., Guo, D., Hodges, R.S., 1986. New hydrophilicity scale derived from high-performance liquid chromatography peptide retention data: correlation of predicted surface residues with antigenicity and X-ray-derived accessible sites. *Biochemistry* 25, 5425-5432.

Petralia, R.S., Sans, N., Wang, Y.X., Wenthold, R.J., 2005. Ontogeny of postsynaptic density proteins at glutamatergic synapses. *Mol Cell Neurosci* 29, 436-452.

Petrini, E.M., Ravasenga, T., Hausrat, T.J., Iurilli, G., Olcese, U., Racine, V., Sibarita, J.B., Jacob, T.C., Moss, S.J., Benfenati, F., Medini, P., Kneussel, M., Barberis, A., 2014. Synaptic recruitment of gephyrin regulates surface GABAA receptor dynamics for the expression of inhibitory LTP. *Nat Commun* 5, 3921.

Pfeiffer, F., Graham, D., Betz, H., 1982. Purification by affinity chromatography of the glycine receptor of rat spinal cord. *J Biol Chem* 257, 9389-9393.

Pierce, J.P., van Leyen, K., McCarthy, J.B., 2000. Translocation machinery for synthesis of integral membrane and secretory proteins in dendritic spines. *Nat Neurosci* 3, 311-313.

Pohlkamp, T., Durakoglugil, M., Lane-Donovan, C., Xian, X., Johnson, E.B., Hammer, R.E., Herz, J., 2015. Lrp4 domains differentially regulate limb/brain development and synaptic plasticity. *PLoS One* 10, e0116701.

Porten, E., Seliger, B., Schneider, V.A., Woll, S., Stangel, D., Ramseger, R., Kröger, S., 2010. The process-inducing activity of transmembrane agrin requires follistatin-like domains. *J Biol Chem* 285, 3114-3125.

Prange, O., Murphy, T.H., 2001. Modular transport of postsynaptic density-95 clusters and association with stable spine precursors during early development of cortical neurons. *J Neurosci* 21, 9325-9333.

Prior, P., Schmitt, B., Grenningloh, G., Pribilla, I., Multhaup, G., Beyreuther, K., Maulet, Y., Werner, P., Langosch, D., Kirsch, J., et al., 1992. Primary structure and alternative splice variants of gephyrin, a putative glycine receptor-tubulin linker protein. Neuron 8, 1161-1170.

Qu, Z., Huganir, R.L., 1994. Comparison of innervation and agrin-induced tyrosine phosphorylation of the nicotinic acetylcholine receptor. *J Neurosci* 14, 6834-6841.

Qu, Z., Apel, E.D., Doherty, C.A., Hoffman, P.W., Merlie, J.P., Huganir, R.L., 1996. The synapse-associated protein rapsyn regulates tyrosine phosphorylation of proteins colocalized at nicotinic acetylcholine receptor clusters. *Mol Cel Neurosci* 8, 171-184.

Ramseger, R., White, R., Kröger, S., 2009. Transmembrane form agrin-induced process formation requires lipid rafts and the activation of Fyn and MAPK. *J Biol Chem* 284, 7697-7705.

Reist, N.E., Magill, C., McMahan, U.J., 1987. Agrin-like molecules at synaptic sites in normal, denervated, and damaged skeletal muscles. *J Cell Biol* 105, 2457-2469.

Remedio, L., Gribble, K.D., Lee, J.K., Kim, N., Hallock, P.T., Delestree, N., Mentis, G.Z., Froemke, R.C., Granato, M., Burden, S.J., 2016. Diverging roles for Lrp4 and Wnt signaling in neuromuscular synapse development during evolution. *Genes & Development* 30, 1058-1069.

Ruegg, M.A., Tsim, K.W., Horton, S.E., Kröger, S., Escher, G., Gensch, E.M., McMahan, U.J., 1992. The agrin gene codes for a family of basal lamina proteins that differ in function and distribution. *Neuron* 8, 691-699.

Rupp, F., Ozcelik, T., Linial, M., Peterson, K., Francke, U., Scheller, R., 1992. Structure and chromosomal localization of the mammalian agrin gene. *J Neurosci* 12, 3535-3544.

Rupp, F., Payan, D.G., Magill-Solc, C., Cowan, D.M., Scheller, R.H., 1991. Structure and expression of a rat agrin. *Neuron* 6, 811-823.

Sabre, L., Evoli, A., Punga, A.R., 2019. Cognitive dysfunction in mice with passively induced MuSK antibody seropositive myasthenia gravis. *J Neurol Sci* 399, 15-21.

Sakmann, B., Brenner, H.R., 1978. Change in synaptic channel gating during neuromuscular development. *Nature* 276, 401-402.

Samuel, M.A., Valdez, G., Tapia, J.C., Lichtman, J.W., Sanes, J.R., 2012. Agrin and synaptic laminin are required to maintain adult neuromuscular junctions. *PLoS One* 7, e46663.

Savtchenko, L.P., Rusakov, D.A., 2007. The optimal height of the synaptic cleft. *Proc Natl Acad Sci USA* 104, 1823-1828.

Schick, A., 2018. Overexpression of transmembrane-agrin in the murine central nervous system, Dissertation, LMU München. LMU Munich, Munich.

Schindelin, J., Arganda-Carreras, I., Frise, E., Kaynig, V., Longair, M., Pietzsch, T., Preibisch, S., Rueden, C., Saalfeld, S., Schmid, B., Tinevez, J.Y., White, D.J., Hartenstein, V., Eliceiri, K., Tomancak, P., Cardona, A., 2012. Fiji: an open-source platform for biological-image analysis. *Nature methods* 9, 676-682.

Schnell, E., Sizemore, M., Karimzadegan, S., Chen, L., Bredt, D.S., Nicoll, R.A., 2002. Direct interactions between PSD-95 and stargazin control synaptic AMPA receptor number. *Proc Natl Acad Sci USA* 99, 13902-13907.

Schrader, N., Kim, E.Y., Winking, J., Paulukat, J., Schindelin, H., Schwarz, G., 2004. Biochemical characterization of the high affinity binding between the glycine receptor and gephyrin. *J Biol Chem* 279, 18733-18741.

Schwenk, F., Kuhn, R., Angrand, P.O., Rajewsky, K., Stewart, A.F., 1998. Temporally and spatially regulated somatic mutagenesis in mice. *Nucleic Acids Res* 26, 1427-1432.

Scotton, P., Bleckmann, D., Stebler, M., Sciandra, F., Brancaccio, A., Meier, T., Stetefeld, J., Ruegg, M.A., 2006. Activation of muscle-specific receptor tyrosine kinase and binding to dystroglycan are regulated by alternative mRNA splicing of agrin. *J Biol Chem* 281, 36835-36845.

Serpinskaya, A.S., Feng, G., Sanes, J.R., Craig, A.M., 1999. Synapse formation by hippocampal neurons from agrin-deficient mice. *Dev Biol* 205, 65-78.

Setou, M., Nakagawa, T., Seog, D.H., Hirokawa, N., 2000. Kinesin superfamily motor protein KIF17 and mLin-10 in NMDA receptor-containing vesicle transport. *Science* 288, 1796-1802.

Shapira, M., Zhai, R.G., Dresbach, T., Bresler, T., Torres, V.I., Gundelfinger, E.D., Ziv, N.E., Garner, C.C., 2003. Unitary assembly of presynaptic active zones from Piccolo-Bassoon transport vesicles. *Neuron* 38, 237-252.

Sharma, K., Fong, D.K., Craig, A.M., 2006. Postsynaptic protein mobility in dendritic spines: long-term regulation by synaptic NMDA receptor activation. *Mol Cell Neurosci* 31, 702-712.

Singh, S., Narang, A.S., Mahato, R.I., 2011. Subcellular fate and off-target effects of siRNA, shRNA, and miRNA. *Pharmaceutical Res* 28, 2996-3015.

Sjostrom, P.J., Rancz, E.A., Roth, A., Hausser, M., 2008. Dendritic excitability and synaptic plasticity. *Physiol Rev* 88, 769-840.

Smith, M.A., Magill-Solc, C., Rupp, F., Yao, Y.M., Schilling, J.W., Snow, P., McMahan, U.J., 1992. Isolation and characterization of a cDNA that encodes an agrin homolog in the marine ray. *Mol Cell Neurosci* 3, 406-417.

Spacek, J., Harris, K.M., 1997. Three-dimensional organization of smooth endoplasmic reticulum in hippocampal CA1 dendrites and dendritic spines of the immature and mature rat. *J Neurosci* 17, 190-203.

Steiner, E., Enzmann, G.U., Lyck, R., Lin, S., Ruegg, M.A., Kröger, S., Engelhardt, B., 2014. The heparan sulfate proteoglycan agrin contributes to barrier properties of mouse brain endothelial cells by stabilizing adherens junctions. *Cell Tissue Res* 358, 465-479.

Steward, O., Schuman, E.M., 2001. Protein synthesis at synaptic sites on dendrites. *Annu Rev Neurosci* 24, 299-325.

Sudhof, T.C., 2018. Towards an Understanding of Synapse Formation. Neuron 100, 276-293.

Sun, X.D., Li, L., Liu, F., Huang, Z.H., Bean, J.C., Jiao, H.F., Barik, A., Kim, S.M., Wu, H., Shen, C., Tian, Y., Lin, T.W., Bates, R., Sathyamurthy, A., Chen, Y.J., Yin, D.M., Xiong, L., Lin, H.P., Hu, J.X., Li, B.M., Gao, T.M., Xiong, W.C., Mei, L., 2016. Lrp4 in astrocytes modulates glutamatergic transmission. *Nat Neurosci* 19, 1010-1018.

Sutton, M.A., Schuman, E.M., 2006. Dendritic protein synthesis, synaptic plasticity, and memory. *Cell* 127, 49-58.

Takeichi, M., Abe, K., 2005. Synaptic contact dynamics controlled by cadherin and catenins. *Trends Cell Biol* 15, 216-221.

Tian, Q.B., Suzuki, T., Yamauchi, T., Sakagami, H., Yoshimura, Y., Miyazawa, S., Nakayama, K., Saitoh, F., Zhang, J.P., Lu, Y., Kondo, H., Endo, S., 2006. Interaction of LDL receptor-related protein 4 (LRP4) with postsynaptic scaffold proteins via its C-terminal PDZ domain-binding motif, and its regulation by Ca/calmodulin-dependent protein kinase II. *Eur J Neurosci* 23, 2864-2876.

Tiffany, A.M., Manganas, L.N., Kim, E., Hsueh, Y.P., Sheng, M., Trimmer, J.S., 2000. PSD-95 and SAP97 exhibit distinct mechanisms for regulating K(+) channel surface expression and clustering. *J Cell Biol* 148, 147-158.

Till, J.H., Becerra, M., Watty, A., Lu, Y., Ma, Y., Neubert, T.A., Burden, S.J., Hubbard, S.R., 2002. Crystal structure of the MuSK tyrosine kinase: insights into receptor autoregulation. *Structure* 10, 1187-1196.

Tintignac, L.A., Brenner, H.R., Ruegg, M.A., 2015. Mechanisms Regulating Neuromuscular Junction Development and Function and Causes of Muscle Wasting. Physiol Rev 95, 809-852.

Trachtenberg, J.T., Chen, B.E., Knott, G.W., Feng, G., Sanes, J.R., Welker, E., Svoboda, K., 2002. Long-term in vivo imaging of experience-dependent synaptic plasticity in adult cortex. *Nature* 420, 788-794.

Tretter, V., Jacob, T.C., Mukherjee, J., Fritschy, J.M., Pangalos, M.N., Moss, S.J., 2008. The clustering of GABA(A) receptor subtypes at inhibitory synapses is facilitated via the direct binding of receptor alpha 2 subunits to gephyrin. *J Neurosci* 28, 1356-1365.

Tretter, V., Kerschner, B., Milenkovic, I., Ramsden, S.L., Ramerstorfer, J., Saiepour, L., Maric, H.M., Moss, S.J., Schindelin, H., Harvey, R.J., Sieghart, W., Harvey, K., 2011. Molecular basis of the gamma-aminobutyric acid A receptor alpha3 subunit interaction with the clustering protein gephyrin. *J Biol Chem* 286, 37702-37711.

Tsen, G., Halfter, W., Kröger, S., Cole, G.J., 1995. Agrin is a heparan sulfate proteoglycan. *J Biol Chem* 270, 3392-3399.

Tsim, K.W., Ruegg, M.A., Escher, G., Kröger, S., McMahan, U.J., 1992. cDNA that encodes active agrin. *Neuron* 8, 677-689.

Tyagarajan, S.K., Ghosh, H., Yevenes, G.E., Nikonenko, I., Ebeling, C., Schwerdel, C., Sidler, C., Zeilhofer, H.U., Gerrits, B., Muller, D., Fritschy, J.M., 2011. Regulation of GABAergic synapse formation and plasticity by GSK3beta-dependent phosphorylation of gephyrin. *Proc Natl Acad Sci USA* 108, 379-384.

van Zundert, B., Yoshii, A., Constantine-Paton, M., 2004. Receptor compartmentalization and trafficking at glutamate synapses: a developmental proposal. *Trends Neurosci* 27, 428-437.

Waites, C.L., Craig, A.M., Garner, C.C., 2005. Mechanisms of vertebrate synaptogenesis. *Annu Rev Neurosci* 28, 251-274.

Wallace, B.G., Qu, Z., Huganir, R.L., 1991. Agrin induces phosphorylation of the nicotinic acetylcholine receptor. *Neuron* 6, 869-878.

Washbourne, P., Bennett, J.E., McAllister, A.K., 2002. Rapid recruitment of NMDA receptor transport packets to nascent synapses. *Nat Neurosci* 5, 751-759.

Weatherbee, S.D., Anderson, K.V., Niswander, L.A., 2006. LDL-receptor-related protein 4 is crucial for formation of the neuromuscular junction. *Development* 133, 4993-5000.

Wierenga, C.J., 2017. Live imaging of inhibitory axons: Synapse formation as a dynamic trial-and-error process. *Brain Res Bull* 129, 43-49.

Wierenga, C.J., Becker, N., Bonhoeffer, T., 2008. GABAergic synapses are formed without the involvement of dendritic protrusions. *Nat Neurosci* 11, 1044-1052.

Winzen, U., Cole, G.J., Halfter, W., 2003. Agrin is a chimeric proteoglycan with the attachment sites for heparan sulfate/chondroitin sulfate located in two multiple serine-glycine clusters. *J Biol Chem* 278, 30106-30114.

Woods, G.F., Oh, W.C., Boudewyn, L.C., Mikula, S.K., Zito, K., 2011. Loss of PSD-95 enrichment is not a prerequisite for spine retraction. *J Neurosci* 31, 12129-12138.

Xu, H.T., Pan, F., Yang, G., Gan, W.B., 2007. Choice of cranial window type for in vivo imaging affects dendritic spine turnover in the cortex. *Nat Neurosci* 10, 549-551.

Yao, I., Iida, J., Nishimura, W., Hata, Y., 2003. Synaptic localization of SAPAP1, a synaptic membrane-associated protein. *Genes Cells* 8, 121-129.

Yuste, R., Bonhoeffer, T., 2004. Genesis of dendritic spines: insights from ultrastructural and imaging studies. *Nat Rev Neurosci* 5, 24-34.

Zambrowicz, B.P., Imamoto, A., Fiering, S., Herzenberg, L.A., Kerr, W.G., Soriano, P., 1997. Disruption of overlapping transcripts in the ROSA beta geo 26 gene trap strain leads to widespread expression of beta-galactosidase in mouse embryos and hematopoietic cells. *Proc Natl Acad Sci USA* 94, 3789-3794.

Zhai, R.G., Vardinon-Friedman, H., Cases-Langhoff, C., Becker, B., Gundelfinger, E.D., Ziv, N.E., Garner, C.C., 2001. Assembling the presynaptic active zone: a characterization of an active one precursor vesicle. *Neuron* 29, 131-143.

Zhang, B., Luo, S., Wang, Q., Suzuki, T., Xiong, W.C., Mei, L., 2008. LRP4 serves as a coreceptor of agrin. *Neuron* 60, 285-297.

Zhang, W., Coldefy, A.S., Hubbard, S.R., Burden, S.J., 2011. Agrin binds to the N-terminal region of Lrp4 protein and stimulates association between Lrp4 and the first immunoglobulin-like domain in muscle-specific kinase (MuSK). *J Biol Chem* 286, 40624-40630.

Ziv, N.E., Garner, C.C., 2001. Principles of glutamatergic synapse formation: seeing the forest for the trees. *Curr Opin Neurobiol* 11, 536-543.

Ziv, N.E., Smith, S.J., 1996. Evidence for a role of dendritic filopodia in synaptogenesis and spine formation. Neuron 17, 91-102.

Zong, Y., Zhang, B., Gu, S., Lee, K., Zhou, J., Yao, G., Figueiredo, D., Perry, K., Mei, L., Jin, R., 2012. Structural basis of agrin-LRP4-MuSK signaling. *Genes & Development* 26, 247-258.

Zuo, Y., Yang, G., Kwon, E., Gan, W.B., 2005. Long-term sensory deprivation prevents dendritic spine loss in primary somatosensory cortex. *Nature* 436, 261-265.

Annexes

List of abbreviations

nAChRs	: nicotinic acetylcholine receptors
AMPAR	: α-amino-3-hydroxy-5-methyl-4-isoxazolepropionic acid receptor
bp	: basepairs
BLASTp	: basic local alignment search tool for protein
BSA	: bovine serum albumin
CAG	: chicken-beta-actin
CamKIIa	: Calcium/Calmodulin dependent protein kinase II alpha
cDNA	: complementary deoxyribonucleic acid
CMV	: cytomegalovirus
DAPI	: 4',6-diamidino-2-phenylindole
DIV	: day in *vitro*
E	: embryonic day
GABA	: γ-aminobutyric acid
GFP	: green fluorescent protein
HA	: human influenza hemagglutinin
HEK	: human embryonic kidney
HSPG	: heparan sulfate proteoglycan
ICC	: immunocytochemistry
IHC	: immunohistochemistry
IRES	: internal ribosome entry site
kD	: kilo Daltons
Lrp4	: low-density lipoprotein receptor-related protein 4
mEPSCs	: miniature excitatory postsynaptic currents
mIPSCs	: miniature inhibitory postsynaptic currents
MuSK	: muscle-specific tyrosine kinase
NMJ	: neuromuscular junction
NMDAR	: N-Methyl-D-aspartat receptor
PDL	: poly-D-lysine
PFA	: paraformaldehyde
PSD-95	: postsynaptic density protein-95
qRT-PCR	: quantitative real time polymerase chain reaction
RFP	: red fluorescent protein

RT : room temperature

SEM : standard error of the mean

TM-agrin : transmembrane-form of agrin

WB : Western blotting

List of publications

Handara, G., Hetsch, F.J.A., Juttner, R., Schick, A., Haupt, C., Rathjen, F.G., Kröger, S., (2019). The role of agrin, Lrp4 and MuSK during dendritic arborization and synaptogenesis in cultured embryonic CNS neurons. *Dev Biol*. 1;445(1):54-67

Handara G and Kröger S. (2019) Alternative splicing and the intracellular domain mediate TM-agrin's ability to differentially regulate the density of excitatory and inhibitory synapse-like specializations in developing CNS neurons. *Neuroscience*, in press.